

Departamento de Bioquímica y Biología Molecular

Programa de doctorado 030E: Bioquímica Clínico-Médica e Inmunología. 2ª Edición

UNIVERSIDAD DE VALENCIA

ROLE OF IRS2 IN OBESITY AND ADIPOGENESIS

Tesis Doctoral con mención Internacional presentada por

Veronica Moreno Viedma

Directora: Dra. Deborah Jane Burks

Tutora: Dra. María Teresa Barber Sanchis

Valencia, 2013

UNIVERSIDAD DE VALENCIA

Departamento de Bioquímica y Biología Molecular
Programa de doctorado 030E: Bioquímica Clínico-Médica e Inmunología. 2ª Edición

ROLE OF IRS2 IN OBESITY AND ADIPOGENESIS

Trabajo original presentado para optar al título de Doctor con mención Internacional por la Universidad de Valencia.

Valencia, 2013

Firmado: **Verónica Moreno Viedma**

PRINCIPE FELIPE
CENTRO DE INVESTIGACION

La doctora **Deborah Jane Burks**, jefa del laboratorio de Neuroendocrinología Molecular en el Centro de Investigación Príncipe Felipe

CERTIFICA

Que la presente memoria titulada ROLE OF IRS2 IN OBESITY AND ADIPOGENESIS ha sido realizada por la Licenciada en Farmacia Verónica Moreno Viedma bajo mi dirección, en el Laboratorio de Neuroendocrinología Molecular del Centro de Investigación Príncipe Felipe y autorizo su presentación para que sea calificada como tesis doctoral y obtener así el TITULO DE DOCTOR CON MENCIÓN INTERNACIONAL.

Firmado: **Deborah Burks**

Valencia Abril 2013

La doctora **María Teresa Barber Sanchis**, catedrática del Departamento de Bioquímica y Biología Molecular en la Facultad de Farmacia de la Universidad de Valencia.

CERTIFICA

Que la presente memoria titulada ROLE OF IRS2 IN OBESITY AND ADIPOGENESIS ha sido realizada por la Licenciada en Farmacia Verónica Moreno Viedma bajo mi tutela académica, en el Laboratorio de Neuroendocrinología Molecular del Centro de Investigación Príncipe Felipe y autorizo su presentación para que sea calificada como tesis doctoral y obtener así el TITULO DE DOCTOR CON MENCIÓN INTERNACIONAL.

Firmado: **María Teresa Barber Sanchis**

Valencia Abril 2013

La investigación desarrollada en esta tesis doctoral ha sido llevada a cabo en el Centro de Investigación Príncipe Felipe (CIPF, Valencia, España) y en el Christian Doppler-Laboratory for Cardiometabolic Immunotherapy & Clinical Division of Endocrinology and Metabolism, Department of Medicine III, Medical University of Vienna. (Viena, Austria).

Este trabajo se ha realizado con el apoyo económico de los proyectos de investigación:

SAF2008-00011

SAF2011-28331

Veronica Moreno Viedma ha disfrutado de un contrato predoctoral del Centro de Investigación Biomédica en Red de Diabetes y Enfermedades Metabólicas Asociadas (CIBERDEM) constituido a iniciativa del Instituto de Salud Carlos III (Ministerio de Economía y Competitividad)

ACKNOWLEDGMENTS

I would like to express my gratitude for my supervisor Dr Deborah Burks for her invaluable support, guidance and knowledge over the years, you have been more than a boss. También agradecer a los profesores Teresa Barber y Joaquín Timoneda del Departamento de Bioquímica de la Facultad de Farmacia por su ayuda con los tramites de la Universidad y por iniciarme en el mundo de la ciencia, siempre os voy a llevar en mi corazón.

I would like to acknowledge the people from the lab I-23 at CIPF. In particular Inma, she had helped me in everything that I have asked her. I would like to specially mention Arantxa, she had always been my right hand, she had taken care of my cells better than me. Thanks for helping me with everything, not only science

I´m very grateful for my colleagues in Vienna of Thomas Stulnig ´s Lab: Max, Bianca, Angelika… you´ve really supported me and I enjoyed working with you.

Gracias a Mª Carmen y Carol por cuando todo empezaba y ahora que todo está terminando, me habéis ayudado en todo. Pilarica, gracias por tus piruletas que me sacaban la sonrisa. Beth, siempre subiéndome el ánimo incluso mejor que mi abuela. Imelda, gracias por tus bromas y "grupos" que hacían que nos pegáramos unas risas tan necesitadas en momentos de desesperación.

Gracias a TODO el servicio de Citómica del CIPF, porque creo que me llevo el premio de horas invertidas. Paco y Dom, gracias por consejillos, risas y alcahueteos varios que hacían los días mucho más llevaderos, Guada, ¡molas mucho! y Ali, gracias a ti por todo, porque todo empezó de tu mano y no me has soltado hasta el final, eres una tía incansable y luchadora a la que admiro.

Chuchi y Rubia, mis dos pilares, dentro pero sobretodo fuera del CIPF, sin vosotras todo hubiera sido mucho más difícil. Gracias por estar junto a mí, frenarme y calmarme cuando lo he necesitado, me habéis enseñado mucho y voy a estar siempre agradecida al CIPF por haberos conocido. Miss Talogo Mary, my sister, I would also thanks for your wise advise, everywhere and everytime you're willing to help me and you are especially ready to enjoy with me.

Mi familia, que habéis sufrido la tesis más que yo, por fin, ¡lo hemos conseguido! Pensabais ¿preguntamos o no como va?, ese miedo a que saltara con alguna borderia lo habéis llevado como lo que sois, las personas más admirables que tengo a mi lado, ¡GRACIAS por vuestro apoyo, por estar a mi lado y por aguantarme!

And finally, Daniel, there are no words to thank you all these years, without you I don't think this day would ever have come to an end. Because of you I knew how to fight for my dreams and because of you I witness more happiness. We are a team, we are a family…*Okan mi fa si ololu femi, Mo ni ife re.*

Todo parece imposible hasta que se hace…

Nelson Rolihlahla Mandela ,Madiba

(Mvezo, Sudáfrica, 18 de julio de 1918)

TABLE OF CONTENTS

FIGURE INDEX

TABLE INDEX

ABBREVIATIONS

ADN *(Adn)*	adipsin
AKT/PKB	thymoma viral proto-oncogene 1, protein kinase B
APC	adipocyte progenitors cells
APS	SH2B adaptor protein 2
AT	adipose tissue
ATM	adipose tissue macrophages
BAD	BCL2-associated agonist of cell death
BAT	brown adipose tissue
BMI	Body mass index
BSA	bovine serum albumin
BSP	bone sialoprotein
cAMP	Cyclic adenosine monophosphate
CBL	casitas B-lineage lymphoma
CCR2	MCP1 receptor
CD31	cluster of differentiation 31 / Platelet endothelial cell adhesion molecule (PECAM1)
CD34	cluster of differentiation molecule 34 / Glycoprotein with cell-cell adhesion functions that mediate the attachment of stroma cells
CD44	hyaluronic acid receptor
CD45 (*Prpcr*) / LCA	cluster of differentiation molecule 45 / Protein tyrosine phosphatase receptor type C / leukocyte common antigen
CDK4	Cyclin-dependent kinase 4
C/EBP	CCAAT-enhancer-binding proteins
CRP	C-reactive protein
CNS	central nervous system
CVD	Cardiovascular disease
DAPI	4,6-diamidino-2-phenylindole dihydrochloride

DM	Diabetes mellitus
DMEM	dulbecco's modified eagle medium
DSPP	dentin sialophosphoprotein
FABP4 / aP2 *(Fabp4*)	fatty acid binding protein 4
FACS	fluorescent activated cell sorting
FASN *(Fasn)*	fatty acid synthase
FBS	Fetal Bovine Serum from Sigma
FcBS	Fetal Clone III Bovine Serum from HyClone
FFA	Free fatty acids
FGFβ	recombinant Human Fibroblast Growth Factor- basic
FPG	fasting plasma glucose
GAB1	growth factor receptor bound protein 2associated protein 1
GLUT *(Slc2a)*	glucose transporter
GRB2	growth factor receptor bound protein 2
GSK3β (*Gsk3b*)	glycogen synthase kinase 3 beta
HA	hydroxyapatite
hADS	Human adipose-derived stem cells
HIF1α (*Hif1a*):	hypoxia inducible factor-1alpha
HSL	Hormone sensitive lipase
IGF1/2	insulin-like growth factor 1 / 2
IGF1R (*Igf1r*)	insulin-like growth factor receptor
IGT	Impaired glucose tolerance
IKKβ	I-kappa-β kinase
IL (*Il*)	interleukin
IR (*Insr*)	insulin receptor
IRR	insulin receptor-related receptor
IRS *(Irs)*	insulin receptor substrate

***Irs2*$^{-/-}$**	*Irs2*-deficient mouse
JNK	c-Jun NH2-terminal kinase
KRLB	kinase regulatory loop binding
LPL	lipoprotein lipase
LH	luteinizing hormone
MAPK	mitogen-activated protein kinase
MCSF	macrophage colony-stimulating factor
MEPE	matrix extracellular phosphoglycoprotein
mRNA	messenger RNA
MSC	mesenchymal stem cell
mTOR	mammalian target of rapamycin serine/threonine kinase
NAFDL	nonalcoholic fatty liver disease
NCK	non-catalytic region of tyrosine kinase adaptor protein
NPXY	asparagine proline unspecified tyrosine motif
OPN (*Spp1*)	osteopontin
PBS	phosphate-Buffered Saline
PDK	phosphoinositide-dependent kinase
PDX	pancreatic duodenal homeobox
PGC1α (*Ppargc1a*)	Peroxisome proliferator-activated receptor gamma coactivator 1 alpha
PH	pleckstrin homology
pH3	phospho Histone 3 (Serine 10)
PI	propidium iodide
PI3K	phosphatidylinositol 3 kinase
PKC θ	protein kinase C θ
PKC z/l	protein kinase C isoforms z and l
PPARγ *(Pparg)*	peroxisome proliferator activated receptor-γ

PTB	phosphotyrosine-binding domain
PTEN	phosphatase and tensin homologue deleted on chromosome ten
PTP1b	protein-tyrosine phosphatase 1B
RGD	arginine-glycine-aspartic acid cell binding sequence
RNA	ribonucleic acid
RT-PCR	quantitative Real-Time Polymerase Chain Reaction
RT	room temperature
T1D / T2D	Type 1 / 2 Diabetes Mellitus
Ter119 / Ly76	Erythroid cell marker
TG	triglyceride
Th 1/2	T helper type 1 /2 cytokine
TNFα (*Tnfa)*	Tumor necrosis factor α
SIBLING	small integrin binding ligand, N-linked glycosylation
SIRP	signal-regulatory protein
Sca1	Mouse Stem Cell Antigen
SC	subcutaneous
SH2	Src homology 2 domains
SHC	Src Homology 2 domain
SHIP 2	SH2-containing inositol phosphatase 2
SOCS	suppressor of cytokine signaling proteins
***Spp1*$^{-/-}$**	Osteopontin-deficient mouse
SRE	sterol-regulatory-elements
SREBP1c (*Srebf1*)	steroid regulatory element-binding protein 1
SVF	stroma-vascular fraction
TG	triglycerides
UCP1	uncoupling protein 1

V	visceral
VEGF A (*Vegfa*)	vascular endothelial growth factor A
VLDL	very low density lipoprotein
WAT	white adipose tissue
WC	waist circumference
WHO	World health organization
WHR	waist-hip ratio circumference
WT	wild type

CHAPTER 1

INTRODUCTION

1. INTRODUCTION

1.1. Insulin

Insulin is the most potent anabolic hormone and is essential for appropriate tissue development and growth as well as the maintenance of whole-body glucose homeostasis (Chang et al., 2004). Insulin is secreted by the β cells of the pancreatic islets of Langerhans in response to increased circulating levels of glucose and regulates glucose homeostasis by reducing hepatic glucose output via decreased gluconeogenesis and glycogenolysis and increasing the rate of glucose uptake into muscle and adipose tissue (Rinderknecht and Humbel, 1978, Burks and White, 2001)

Human insulin contains 51 amino acids (molecular weight 5700 daltons) and is structurally homologous to insulin-like growth factors 1 and 2 (IGF1 and 2) and also to the ovarian hormone, relaxin (Bell et al., 1980, Dull et al., 1984, Nussey S, 2001). It is synthesized in the β cells of the pancreatic islets. The gene for insulin codes for pre-proinsulin which is made up of a signal sequence, and the B chain, connecting (or C) peptide and A chain (Figure 1). The A and B chains are joined together by two disulfide bonds between common cysteine amino-acid residues. The C peptide is essential to the formation of these disulfide bonds and is cleaved in the Golgi apparatus leaving the joined A and B chains which form the active insulin molecule (Duckworth, 1988) The cleaved C peptide is co-secreted with insulin, a point of great clinical importance. Previously considered to have no physiological role, C peptide is now recognized to have G-protein-coupled cellular receptors and is likely to have some function in regulating blood flow and renal function (Philippe, 1991).

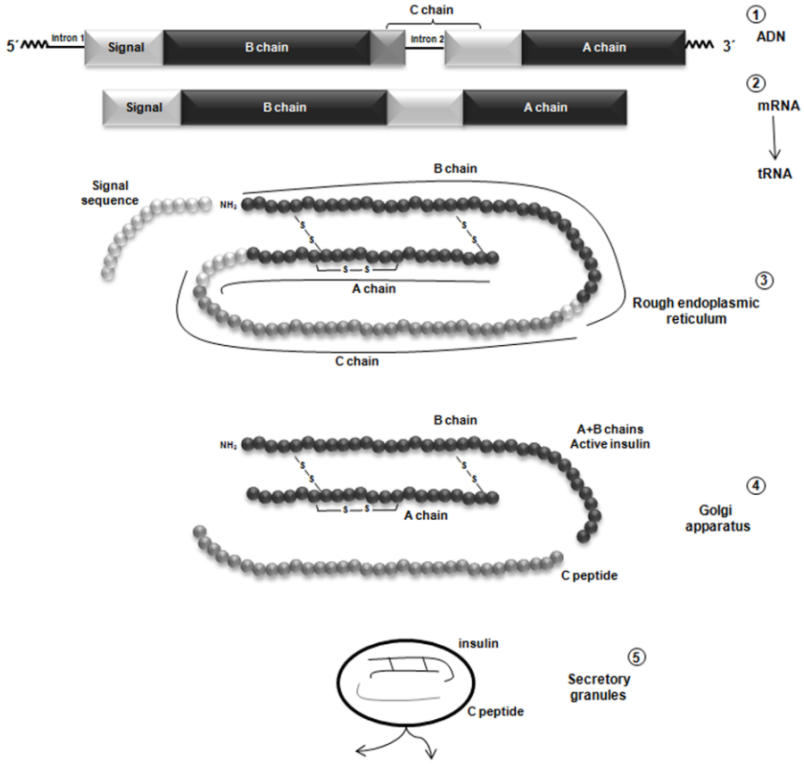

Figure 1: Synthesis of insulin.
1. Structure of the insulin gene, 2. Mature messenger RNA after exicision of the introns, 3. Structure of proinsulin after cleavage of the signal sequence from pre-proinsulin, 4. Cleavage of the C peptide leaving biologically active insulin, 5. Packaging of insulin and C-peptide in secretory granules for storage and release (Nussey S, 2001).

When β cells are appropriately stimulated, insulin is secreted by exocytosis and diffuses into the blood of islet capillaries. Insulin is secreted in pulses and has a $t_{1/2}$ in the systemic circulation of approximately 3 minutes (Rubenstein et al., 1972, Lang et al., 1979). About 50% is removed by the liver. This is known as the 'first-pass' effect (i.e. the first time insulin passes through the liver). Insulin that has escaped the liver's inactivating activity exerts important regulatory actions on peripheral tissues. C peptide is released in a 1:1 ratio with insulin and since it is not significantly removed by the liver, has a $t_{1/2}$ of 30 min. For this reason, the measurement of C-peptide has been used

as an index of insulin secretion (Rubenstein et al., 1972, Horwitz et al., 1975).

1.1.1. Physiological effects

Insulin regulates energy metabolism by stimulating cells in peripheral tissues to incorporate glucose from the blood and stimulating the storage of glycogen in the liver and muscle and lipids in adipose tissue. The ultimate effector system for regulating glucose disposal is the translocation of vesicles containing glucose transporters (GLUT) to the plasma membrane to increase the rate of cellular glucose transport (Suzuki and Kono, 1980). When insulin is absent, glucose is not taken up by body cells and the body begins to use fat as an energy source. The hyperglycemia observed in diabetes results from impairments in insulin secretion, insulin action, or a combination of both (Kahn et al., 1993, Kahn, 1998).

The action of insulin in controlling the overall flow of fuels is summarized in Table 1. In the liver, insulin promotes glycogen synthesis by stimulating glycogen synthetase and inhibiting glycogen phosphorylase although it has no direct effect on the GLUT 2 and, hence, the uptake of glucose into hepatocytes (Board et al., 1995). In contrast, insulin induces a rapid uptake of glucose in muscle and fat tissue by recruiting intracellular GLUT 4 and, thus, increasing their cell-surface expression (Klip and Pâquet, 1990). As a consequence, muscle converts glucose to glycogen. In adipose tissue, glucose is converted to fatty acids for storage as triglyceride. Insulin also stimulates the uptake of amino acids into muscle. At the same time, insulin suppresses mobilization of fuels by inhibiting the breakdown of glycogen in the liver, the release of amino acids from muscle and the release of free fatty acids from adipose tissue. This explains, in part,

why patients with Diabetes Mellitus (DM) lose weight although they have normal or increased appetite (Woods et al., 1979, Ikeda et al., 1986, Schwartz et al., 1992, Baskin et al., 1999, Burks et al., 2000).

INSULIN ACTION		
Liver	**Muscle**	**Adipose tissue**
+ glycogen synthesis	+ glucose uptake	+ glucose uptake
+ glycolysis	+ amino acid uptake	+ free fatty acid uptake
- glycogenolysis	- proteolysis	- lipolysis
- gluconeogenesis		
- ketogenesis		

Table 1: Effects of insulin on the flow of fuels in the body.
(+) stimulates and (-) inhibits.

1.1.2. Insulin receptor

Insulin action is initiated through binding and activating its cell surface receptor (IR), which consists of two α subunits and two β subunits that are disulfide linked into an α2β2 heterotetrameric complex (Pessin and Saltiel, 2000). IGF1 signals via the type 1 IGF1 receptor (IGF1R), a widely expressed cell-surface heterotetramer, highly similar to the IR, which possesses intrinsic kinase activity in its cytoplasmic domains (Favelyukis et al., 2001). Insulin binds to the extracellular α subunit of the IR/IGF1R and modifies the α subunit dimer which mediates trans-autophosphorylation between the membrane-spanning β subunits (White, 1997). This activates the intrinsic tyrosine kinase activity of the intracellular β subunit of the receptor which then leads to tyrosine phosphorylation of a variety of docking proteins.

Interestingly, unlike other receptor tyrosine kinases that bind directly to the cytoplasmic tails of downstream effectors, the IR and the IGF1R

utilize insulin receptor substrate (IRS) proteins to mediate the binding of intracellular effectors (Ullrich and Schlessinger, 1990). The activity of the IR/IGF1R is tightly regulated, as unchecked activation or inactivity would lead to profound metabolic consequences. Ligand-stimulated internalization and degradation of the IR is a common feature of most insulin-resistant, hyperinsulinemic states, including obesity and type 2 Diabetes Mellitus (T2D) (Friedman et al., 1997). A third member of the insulin receptor family is insulin receptor-related receptor (IRR). Despite similar homology, IRR is still an orphan receptor with obscure function and is expressed in few tissues (Klammt et al., 2005). The main difference compared to the IR and IGF1R is the C-terminal region which lacks at least 50 amino acids (Hanke and Mann, 2009).

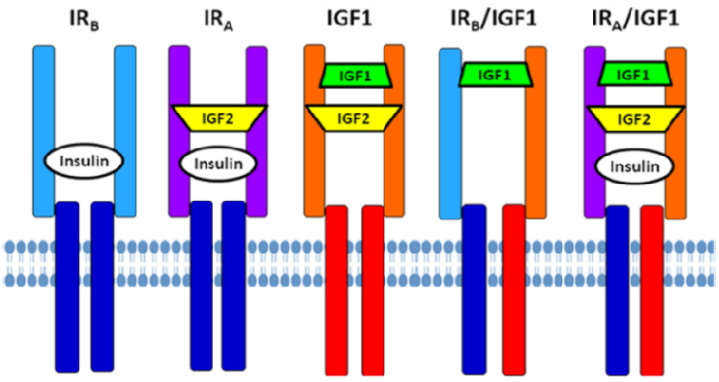

Figure 2: Structure of Receptors for insulin, IGF1, and IGF2.
Each receptor is composed of a α2β2 heterotetrameric complex. However single α-β dimers are derived from separate genes and the IR has two splice variants, IR_B and IR_A. Therefore, combinations of the single α-β dimers exist and insulin, IGF1, and IGF2 can bind to several hybrid receptors, albeit at different affinities. The α subunit is the extracellular portion of the receptor while the β subunit spans the membrane and its cytoplasmic portion interacts with IRS proteins.

1.1.3. Insulin signal transduction

Once activated, the IR phosphorylates a number of important proximal substrates on tyrosine, including members of the insulin receptor substrate family (IRS1/2/3/4), the SHC adapter protein isoforms, signal-regulatory protein (SIRP) family members, growth factor receptor bound protein 2 associated protein 1 (GAB1), Casitas B-lineage lymphoma (CBL) , and SH2B adaptor protein 2 (APS) (Pawson and Scott, 1997, White and Yenush, 1998, Nelms et al., 1999). Tyrosine phosphorylation of the IRS proteins creates recognition sites for additional effector molecules containing Src homology 2 (SH2) domains (Burks and White, 2001, Rui and White, 2003). These include the small adapter proteins growth factor receptor bound protein 2 (GRB2) and non-catalytic region of tyrosine kinase adaptor protein (NCK), the SHP2 protein tyrosine phosphatase and, most importantly, the regulatory subunit of the type 1A phosphatidylinositol 3 kinase (PI3K) (Figure 3).

Two classes of serine/threonine kinases are known to act downstream of PI3K (Coffer et al., 1998), namely the serine/threonine kinase AKT, also known as protein kinase B (PKB) or thymoma viral proto-oncogene 1, and the atypical protein kinase C isoforms z and l (PKCz/l) Each IRS protein contains a highly conserved NH2-terminal pleckstrin homology (PH) domain followed by a phosphotyrosine-binding (PTB) domain, which together couple IRS proteins to the activated insulin or IGF1 receptors (Myers et al., 1998, Yenush et al., 1996). IRS proteins contain 8–18 potential tyrosine phosphorylation sites in various amino acid sequence motifs, which bind after phosphorylation to the SH2 domains in effector proteins, including the regulatory subunit of the lipid kinase PI3K, GRB 2, NCK, and SHP2 (Myers Jr and White, 1996, Sun et al., 1995). Products of PI3K

activate a network of serine-threonine kinases implicated in the action of insulin on glucose transport, glycogen synthesis, protein synthesis, antilipolysis, and the control of hepatic gluconeogenesis (White, 2006) (see Figure 3).

Activated AKT induces glycogen synthesis, through inhibition of glycogen synthase kinase 3 beta (GSK3β), protein synthesis via mammalian target of rapamycin serine/threonine kinase (mTOR) and downstream elements (Engelman et al., 2006), and cell survival, through inhibition of several pro-apoptotic agents (BCL2-associated agonist of cell death (BAD), forkhead family transcription factors, GSK 3). PI3K and AKT play critical roles in GLUT4 translocation (Fasshauer et al., 2000). Stable expression of a constitutively active membrane-bound form of AKT in 3T3L1 adipocytes results in increased glucose transport and persistent localization of GLUT4 to the plasma membrane (Hill et al., 1999). Conversely, expression of a dominant interfering AKT mutant inhibits insulin-stimulated GLUT4 translocation.PKCz is also activated by polyphosphoinositides, which accumulate in insulin-treated cells; PKCz is, therefore, also sensitive to pharmacologic PI3K inhibitors, such as wortmannin (Fasshauer et al., 2000). Expression of PKCz or PKCl is also reported to induce GLUT4 translocation, whereas expression of a dominant-interfering PKCl inhibited GLUT4 translocation.

Insulin promotes the uptake of fatty acids and the synthesis of lipids, whilst inhibiting lipolysis (Kahn, 2001). Lipid synthesis requires an increase in the transcription factor steroid regulatory element-binding protein 1c (SREBP1c) (Shimomura et al., 2000). However, the pathway leading to changes in SREBP expression are unknown. Insulin inhibits lipid metabolism through decreasing cellular concentrations of cyclic adenosine monophosphate (cAMP) by

activating a cAMP specific phosphodiesterase in adipocytes (Kubota et al., 1999, Kahn, 2001). Insulin signaling also has growth and mitogenic effects, which are mostly mediated by the AKT cascade as well as by activation of the RAS/RAF/mitogen-activated protein (MAP) kinase (RAS/MAPK) cascade. A negative feedback signal emanating from AKT, PKCZ, p70 S6K and the MAPK cascades results in serine phosphorylation and inactivation of IRS signaling (White, 2003).

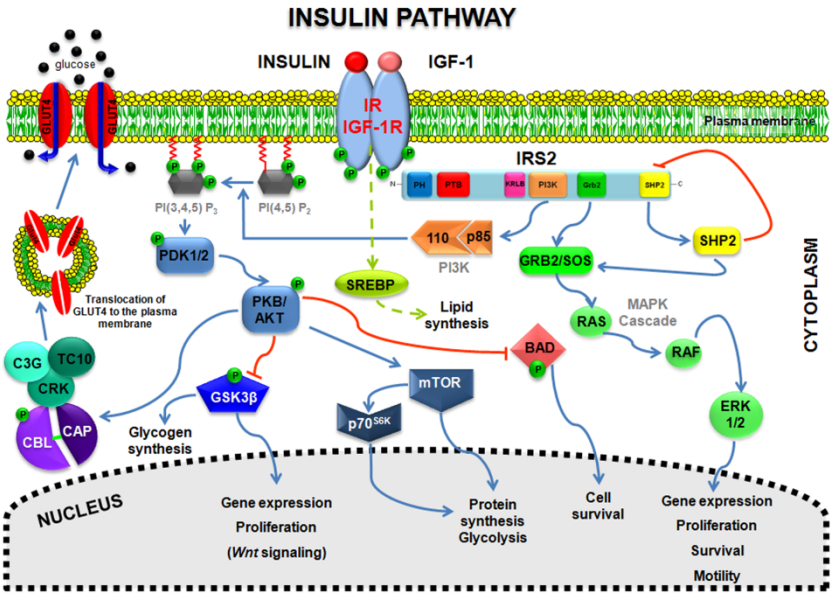

Figure 3: A simplified view of insulin/IGF1 signaling through IRS proteins.
Activation of the receptors for insulin and IGF-I results in tyrosine phosphorylation of the IRS proteins. The IRS proteins then recruit PI 3-kinase, Grb2/son of sevenless (SOS), and SHP-2. The Grb2/SOS complex mediates the activation of p21ras, thereby activating the ras/raf/mitogen-activated protein (MAP) kinase kinase (MEK)/MAP kinase cascade. SHP-2 feeds back to inhibit IRS protein phosphorylation by directly dephosphorylating the IRS protein and may transmit an independent signal to activate MAP kinase. The activation of PI 3-kinase by IRS protein recruitment results in the generation of PI-3,4-diphosphate (PI3,4P2) and PI-3,4,5-triphosphate (PI3,4,5P3). In aggregate, PI3,4P2 and PI3,4,5P3 activate a variety of downstream signaling kinases, including the mammalian target of rapamycin (mTOR), which regulates protein synthesis via PHAS/p70 S6 kinase (p70S6k). These lipids also activate phosphoinositide-dependent kinase (PDK) isoforms. The PDKs (PDK1, PDK2) activate protein kinase B (PKB or AKT), which mediates glucose transport in concert with the atypical PKC isoforms. AKT also regulates glycogen synthase kinase 3 (GSK-3) in glycogen synthesis, and a variety of regulators of cell survival. (White, 2002).

1.1.4. Insulin Receptor Substrates

The Insulin Receptor Substrate (IRS) proteins are a family of cytoplasmic adaptor proteins that were first identified based on their role in insulin signaling. At least 11 intracellular substrates of the IR/IGF1R have been identified and at least four of these belong to the IRS family of proteins (Taniguchi et al., 2006). The first family member to be identified, IRS 1, was initially characterized as a 185kD phosphoprotein that was detected in anti-phosphotyrosine immunoblots in response to insulin stimulation (White et al., 1985). IRS 2 was discovered as an alternative insulin receptor substrate, initially named 4PS, in insulin-stimulated cells derived from from *Irs1*$^{-/-}$ mice (Patti et al., 1995, Sun et al., 1995).

IRS 1 appears to be ubiquitously expressed. IRS 2 was identified as a component of the interleukin 4 (IL4) signaling pathway, but it is now known to be expressed in nearly all cells and tissues (Boura-Halfon and Zick, 2009). IRS 3 is predominantly expressed in adipose tissue, and it was purified and cloned from rat adipose tissue (Lavan et al., 1997). However, IRS3 has not been detected in humans (Björnholm et al., 2002). IRS 4 was purified and cloned from HEK293 cells, where it is the major IRS protein. IRS 4 is expressed predominantly in the pituitary, thymus, and brain (Fantin et al., 1999).

Despite their significant structural homology (Figure 4), it is clear from the genotypes of knockout mice that the IRS proteins have non-redundant physiological functions. *Irs1*$^{-/-}$ mice are born small and remain so throughout their lives, implicating a role for this IRS protein in somatic growth regulation (White, 1997, Withers et al., 1998). A similar contribution of the IRS homolog Chico to the regulation of cell size and growth in Drosophila has been observed (Böhni et al., 1999). Mice deficient for *Irs1* develop insulin resistance but do not progress

to diabetes because they maintain normal pancreatic β-cell numbers. *Irs2*$^{-/-}$ mice are normal in size but have brain defects, the result of a 50% decrease in neuronal proliferation. In contrast to *Irs1*$^{-/-}$ mice, IRS2-deficient mice develop early-onset diabetes due to a combination of peripheral insulin resistance and a loss of β-cell function (Withers et al., 1998, Burks and White, 2001). *Irs2*$^{-/-}$ females are also infertile, which together with evidence from insulin-signaling in Drosophila and *C. elegans*, supports a conserved mechanism for integrating reproduction and metabolism (Burks et al., 2000). *Irs4*$^{-/-}$ mice are phenotypically normal, with only mild growth, reproductive and insulin sensitivity defects (Mardilovich et al., 2009). Thus, IRS1/IRS2 are not redundant and appear to regulate unique signals in various tissues, whereas in certain tissues two IRS proteins might reinforce each other as in the case of IRS1/IRS3 in adipocytes (White, 2002). A summary of phenotypes resulting from deletion of IRS proteins is presented in Table 2.

Genotype	Body weight	Fasting glucose	Insulin resistance	Glucose tolerance	β cell mass	Life expectancy	Other abnormalities
Irs1$^{-/-}$	-50%	Normal	Hyperinsulinemia	normal	2 fold	>1,5 years	decreased leptin
Irs2$^{-/-}$	-10%	-	6-8 weeks 10-12 weeks	impaired	-50%	10 weeks(♂) 6-12 months (♀)	increased leptin ♀ obesity and infertility
Irs3$^{-/-}$	normal	Normal	normal	normal	¿?	¿?	-
Irs4$^{-/-}$	-10%	Slight decrease	normal	normal	¿?	¿?	reduced infertility

Table 2: Murine phenotypes produced by IRS protein deficiency (Burks and White, 2001).

1.1.4.1. Structure and isoforms

Alignment of the amino acid sequences of the IRS proteins reveals important similarities and differences (Figure 4). Mammalian IRS1,2,3, and IRS4, and the Drosophila ortholog Chico contain an NH2-terminal PH domain adjacent to a phosphotyrosine-binding domain (Burks et

al., 1998). The PH domain possibly directs IRS proteins to the membrane in proximity to the IR/IGF1R and the PTB domain binds to phosphotyrosine 960 located in a NPXY (Asparagine-Proline-Unspecified-Tyrosine) motif of the juxtamembrane region of the IR/IGF1R (Biddinger and Kahn, 2006) but hindrance of these interactions by serine/threonine phosphorylation negatively affects insulin signalling (Voliovitch et al., 1995). The structures of these domains are remarkably similar, and both facilitate recruitment of IRS proteins to the activated insulin and IGF-1 receptors. Deletion of both domains almost completely prevents tyrosine phosphorylation, even when insulin receptors are expressed at high levels (Burks et al., 1997). PH domains can be exchanged among IRS proteins without noticeable loss of bioactivity, but chimeric IRS proteins composed of heterologous PH domains that are known to bind phospholipids are not phosphorylated by the insulin receptor (Burks et al., 1997). The center and C-terminus contain up to 20 potential tyrosine phosphorylation sites that after phosphorylation by the IR/IGF1R, bind to intracellular adaptor molecules that contain Src-homology-2 (SH2) domains, such as the p85 regulatory subunit of PI3K or GRB2. Serine/Threonine phosphorylation adjacent to tyrosine phosphorylation sites impedes binding of the SH2 domains of IRS proteins, thus inhibiting insulin signalling (Boura-Halfon and Zick, 2009). More distantly related IRS family members IRS 5 and IRS 6, also known as DOK4 and DOK5 (Cai et al., 2003, Favre et al., 2003), share homology in their N-termini, but have truncated C-termini (Figure 4).

IRS2 contains a unique region of undefined structure that binds to the phosphorylated regulatory loop of the insulin receptor kinase called the kinase regulatory loop-binding (KRLB) domain (Sawka-Verhelle et al., 1997). Phosphorylation of tyrosine residues in the KRLB domain

by the insulin receptor inhibits IRS2 binding to the receptor, suggesting a novel mechanism regulating the interaction of the insulin receptor and IRS2 that might distinguish the signal of IRS2 from IRS1. There are also multiple amino acid sequence differences between IRS1 and IRS2 that might create unique interaction sites for other partner proteins to fine-tune the biologic signals (Derek LeRoith MD, 2003).

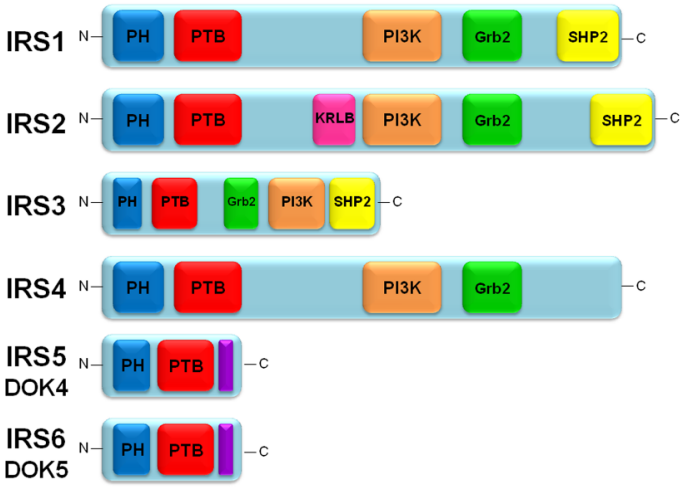

Figure 4: Structure of IRS protein family.
Interaction domains of the IRS proteins are indicated. PH (blue), pleckstrin homology domain; PTB (red), phosphotyrosine binding domain; KRLB (pink), kinase regulatory loop binding domain; PI3K (orange), region containing multiple PI3K binding motifs; Grb-2 (green), Grb-2 binding site; SHP-2 (yellow), SHP-2 binding site. IRS-5 and IRS-6 contain unique regions in their C termini (purple). IRS2 contains a unique KRLB (Kinase Regulatory-Loop Binding, pink) domain which serves as a negative regulatory element to control the extent of tyrosine phosphoylation of IRS2. Figure (Mardilovich et al., 2009).

1.1.4.2. *Irs2*-deficient mouse model

The crucial role of IRS proteins in insulin action has been demonstrated using transgenic knockout mouse models. A compelling molecular link to diabetes emerged from the finding that loss of the IRS2 branch of the insulin/IGF signaling system in mice impairs the

capacity of the pancreatic β-cells to compensate for insulin resistance (Burks and White, 2001). Targeted disruption of the *Irs2* gene was first reported by the laboratory of Morris White (Withers et al., 1998). *Irs2* deficiency causes peripheral insulin resistance due to defective insulin action but it also prevents β cell compensation. Histological analysis revealed that, as early as 4 weeks, β cell mass is reduced by 17% compared with wild-type, in marked contrast to the 85% increase in β cell mass in *Irs1*$^{-/-}$ islets (Withers et al., 1998, Burks and White, 2001). *Irs2*$^{-/-}$ mice develop hyperinsulinemia as young adults, and males usually die by 12 weeks of age whereas diabetes in females progresses less rapidly and many live until around 24 weeks of age (Burks et al., 2000). As the disease progresses, pancreatic islet size invariably decreases and β cell function fails.

Irs2$^{-/-}$ mice also display profound peripheral insulin resistance, particularly at the hepatic level (White, 1997, Withers et al., 1998, Previs et al., 2000). More recent studies with conditional knockout models have confirmed the importance of IRS2 signals for maintaining hepatic insulin sensitivity (Dong et al., 2006). *Irs2*$^{-/-}$ mice also display dysregulated lipolysis characteristic of insulin resistance (Garcia-Barrado et al., 2011). Thus, the *Irs2*-deficient model provides proof-of-concept that a single gene mutation can induce both peripheral insulin resistance and the β cell deficiency typical of T2D (Brady, 2004). In contrast, *Irs1*$^{-/-}$ mice never develop diabetes because they display lifelong, compensatory hyperinsulinemia (White, 2002, White, 2006). The progression of *Irs2*$^{-/-}$ mice toward diabetes is retarded or prevented by modifying elements of the insulin/IGF-signaling cascade that promote compensatory β cell function, including downregulation of protein tyrosine phosphatase PTP1b or the transcription factor Foxo1; or upregulation of AKT or pancreatic duodenal homeobox 1 (PDX1). Transgenic upregulation of *Irs2* in pancreatic β cell also

prevents diabetes in *Irs2*$^{-/-}$ mice, obese mice, and streptozotocin-induced diabetic mice by promoting sufficient and sustained compensatory insulin secretion (Lin et al., 2004).

Irs2 null mice also display a dysregulation of appetite at the hypothalamic level (Bruning et al., 2000, Lin et al., 2004). Furthermore, increased food intake is further complicated by abnormalities in fuel storage; *Irs2*$^{-/-}$ mice weigh 20% more and store twice as much body fat as age-matched controls (Burks et al., 2000). Interestingly, the development of peripheral insulin resistance could be uncoupled from increased fat mass, suggesting that the reduction in hypothalamic IRS2 mediated signalling affected insulin sensitivity in other tissues (Kubota et al., 2004, Taguchi et al., 2007). *Irs2*-deficiency also causes elevated leptin levels and central nervous system (CNS) resistance to leptin (Burks et al., 2000), suggesting crosstalk between leptin and insulin signaling in regulating hypothalamic neuronal energy sensing and appetite. *Irs2*-deficient females are infertile due to reduced pituitary size and gonadotroph numbers, a decrease in concentrations of luteinizing hormone (LH) in plasma, a reduction in ovary size, reduced numbers of follicles, and consequent anovulation (Burks et al., 2000). Although IRS2 signaling in the CNS plays crucial roles in energy homeostasis (Choudhury et al., 2005), signaling events downstream of IRS2 in the ovary play critical roles in follicular development and ovulation by regulating key components of the cell-cycle (Neganova et al., 2007). However, the mechanisms by which reduced *Irs2* expression in the brain diminishes both central leptin sensitivity and peripheral insulin sensitivity are unclear (Brady, 2004).

1.2. Type 2 Diabetes Mellitus

1.2.1. Definition and epidemiology

Type 1 diabetes (T1D) is due primarily to autoimmune-mediated destruction of pancreatic β cell islets, resulting in absolute insulin deficiency. Its frequency is low relative to type 2 diabetes, which accounts for over 90% of cases globally (Amos et al., 1997). Type 2 diabetes (T2D) is characterized by insulin resistance and/or abnormal insulin secretion, either of which may predominate. Patients with T2D are not dependent on exogenous insulin, but may be required if control of blood glucose levels if this is not achieved with diet alone or with oral hypoglycaemic agents (Campbell, 2000). The “diabetes epidemic” particularly describes T2D, and is occuring both in developed and developing nations.

Prevalence of diabetes in adults worldwide was estimated to be 4.0% in 1995 and to rise to 5.4% by the year 2025 (King et al., 1998). It is higher in developed than in developing countries. The world prevalence of diabetes among adults (20-79 years) will be 6.4%, affecting 285 million adults, in 2010, and will increase to 7.7%, and 439 million adults by 2030 (Shaw et al., 2010). Between 2010 and 2030, there will be a 69% increase in numbers of adults with diabetes in developing countries and a 20% increase in developed countries. The countries with the largest number of people with diabetes are, and will be in the year 2025, India, China, and the U.S. In developing countries, the majority of people with diabetes are in the age range of 45-64 years. In the developed countries, the majority of people with diabetes are aged 65 years.

The Di@bet.es Study is the first national study to examine the prevalence of diabetes and impaired glucose regulation in Spain. The

results of this study indicate an increase in the prevalence of diabetes mellitus: 13.8% of the Spanish population over 18 years of age suffers from diabetes, whereas 30% present with either impaired fasting glucose or impaired glucose tolerance (Soriguer et al., 2012). Diabetes mellitus and impaired glucose regulation (IGR) were significantly associated with a greater frequency of obesity, high blood pressure, hypertriacylglycerolaemia and low HDL cholesterol (Soriguer et al., 2012, Marcuello et al., 2012).

The current criteria for the diagnosis of T2D established by the American Diabetes Association Expert Committee on Diagnosis and Classification of Diabetes Mellitus are: a random plasma glucose of ≥200mg/dl (11,1 mmol/l); or a fasting plasma glucose (FPG) of ≥126mg/dl (7,0 mmol/l); or a two-hour oral glucose tolerance test with plasma glucose ≥200 mg/dl. Abnormal FPG is ≤110mg/dl (6,1 mmol/l) and a FPG 110–126mg/dl is defined as impaired glucose tolerance, impaired fasting glucose, or prediabetes (Lieberman, 2003).

1.2.2. Inflammation and potential molecular mechanisms of insulin resistance

The ability of insulin to stimulate glucose disposal varies at least six-fold in healthy individuals, and approximately one-third of the population is resistant to insulin action. When insulin-resistant individuals cannot maintain the hyperinsulinemia needed to overcome the defect in insulin action, T2D develops, and this was the first clinical syndrome identified as insulin resistance. The combination of insulin resistance and hyperinsulinemia increases the risk of developing other diseases involved in other tissues (Reaven, 2004b, Reaven, 2004a).

Defects in insulin-receptor function are associated with insulin-resistant states such as obesity and T2D. Mutations in the IR gene have been identified in patients with genetic syndromes of extreme insulin resistance (Taylor, 1992). In other patients, insulin resistance results from a decrease in the number of insulin receptors on the cell surface (Gavin et al., 1974, Epstein et al., 1991) However, defects in downstream signalling cascades may account for insulin resistance in most T2D patients. Most if not all insulin signals are produced or modulated through tyrosine phosphorylation of IRS 1, 2, its homologs, or other scaffold proteins. Dysregulation of these IRS proteins by proinflammatory cytokines impairs glucose tolerance as a result of peripheral insulin resistance (Starr et al., 1997, Yasukawa et al., 2000, Rui et al., 2001, Yuan et al., 2001). The idea that inflammation is associated with insulin resistance has been known for a long time and is consistent with the finding that stress-induced cytokines tumor necrosis factor α (TNF-α) and interleukin 6 (IL6) cause insulin resistance, suggesting that diet, physiological stress, and obesity promote insulin resistance (Derek LeRoith MD, 2003).

TNF α via activation of their transduction pathways, are able to alter insulin signaling by inactivating IRS through serine/threonine phosphorylation (Hotamisligil et al., 1996). There are many serine/threonine kinases are involved in the inhibition of phosphorylation of insulin signaling: I-kappa-β kinase (IKKβ), c-Jun NH2-terminal kinase (JNK) and protein kinase C θ (PKC θ). JNK phosphorylates numerous cellular proteins, including IRS 1 and IRS 2, SHC, and GAB1 (Rui et al., 2001, Lee et al., 2003, Taniguchi et al., 2006, Boura-Halfon and Zick, 2009) A role for JNK during insulin action is compelling, as both IRS 1 and IRS 2 contain JNK binding motifs. Both factor pathways are activated in obesity, not only in response to adipokines, but also by increased free fatty acid

concentrations and oxidative stress. As well as its link with insulin resistance, JNK activity regulates insulin production, while selective inhibition of JNK improves insulin production in the pancreatic islets of obese mice in response to glucose (Hirosumi et al., 2002).

Ubiquitin-mediated degradation of IRS1 and IRS2 also promotes insulin resistance (Rui et al., 2002). IL6 secreted from leukocytes and adipocytes increases expression of suppressor of cytokine signaling proteins (SOCS), which are known for their ability to inhibit cytokine receptor signaling. However, SOCS1 and SOCS3 also recruit an elongin BC-based ubiquitin ligase into the IRS protein complexes to mediate ubiquitinylation. Protein or lipid phosphatases, including protein-tyrosine phosphatase 1B (PTP1B), SH2-containing inositol phosphatase 2 (SHIP2) or phosphatase and tensin homologue deleted on chromosome ten (PTEN) inhibit insulin signaling. Disruption of each gene in mice increases insulin sensitivity (White, 2003, White, 2002).

1.3. Obesity

1.3.1. Definition and epidemiology

Obesity has been classified as a 'global epidemic' by the WHO. At least 2.8 million adults die each year as a result of being overweight or obese. The WHO estimates that globally there are more than 1 billion overweight adults [Body Mass Index in kg/m^2 (BMI) > 27], 300 million of whom are obese (BMI > 30). Overweight and obesity are linked to more deaths worldwide than underweight pathologies (Wang et al., 2002, Popkin and Gordon-Larsen, 2004, Mendez et al., 2005). In adults, obesity is associated with an increased risk of diseases that

are a major cause of morbidity and mortality, 44% of the DM burden, 23% of the ischemic heart disease burden and between 7% and 41% of certain cancer burdens are attributable to overweight and obesity, (Organization, 2010, Organization, 2011, Organization, 2012, James et al., 2012). Obesity is a complex disease (Figure 5) since body weight, composition, and the storage of energy as triglyceride (TG) in adipose tissue are determined by the interaction between genetic, environmental, and psychosocial factors (Excellence, 2006). .

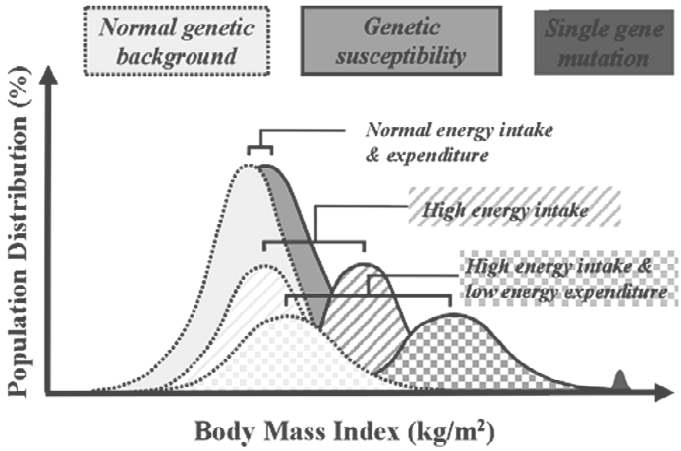

Figure 5: Population distribution of BMI.
Under conditions of normal energy intake and expenditure, subpopulations with a normal genetic background or with a genetic susceptibility to obesity have comparable body mass indices (BMI, expressed as mass in kg divided by squared height in m). When energy intake is high, the BMI distribution curve shifts to the right. This shift is more pronounced in a subpopulation with genetic susceptibility for obesity. An additional reduction in energy expenditure results in a further rise in BMI and a wider separation of the subpopulations. Patients with rare monogenic forms of obesity show a marked increase in BMI irrespectively of the environmental conditions (Hofbauer, 2002).

BMI is a simple index of weight to height ratio that is commonly used to classify overweight and obesity in adults. It is defined as a person's weight in kilograms divided by the square of his height in meters (kg/m2). The WHO define overweight as a BMI greater than or equal

to 25 and obesity with a BMI greater than or equal to 30. Fat distribution plays an important role in metabolic risk (Björntorp, 1991b, Jensen, 2008). Increased intra-abdominal/visceral fat (central or apple shaped obesity) promotes a high risk of metabolic disease, whereas increased subcutaneous fat in the thighs and hips (peripheral or pear-shaped obesity) exerts little or no risk (Figure 6). Both fat mass and distribution can be measured by body mass index (BMI) and waist-hip ratio (WHR) or waist circumference (WC).

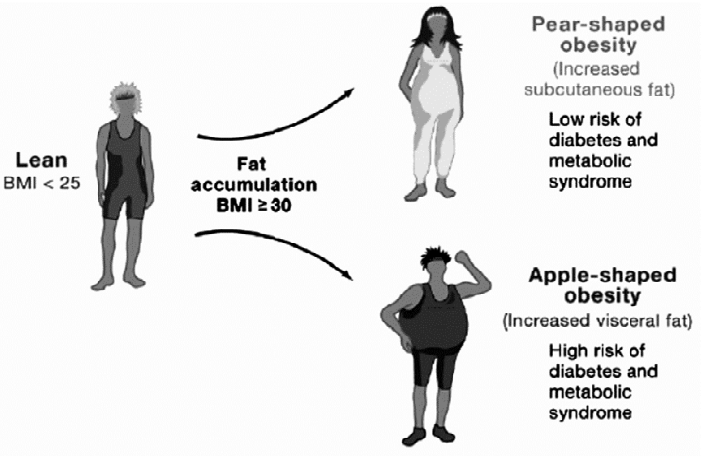

Figure 6: Fat Distribution Influences Risks Associated with Obesity in Humans. Obesity is the consequence of an excess in fat accumulation and is defined by a BMI of ≥ 30. Fat distribution can be estimated by measurements of the ratio of WHR. Obese individuals with low WHR, (subcutaneous or pear-shaped obesity) are at low risk for metabolic complications of obesity, whereas individuals with a high WHR (visceral or apple-shaped obesity) are at high risk for these complications (Gesta et al., 2007)

T2D is the most common form of diabetes in the Western world, and is strongly linked to obesity since over 80% of sufferers are obese and most disease models point to obesity as an important cause of T2D, because of its association with skeletal muscle insulin resistance and pancreatic β cell failure (Lin et al., 2004). Adipose tissue not only serves to store energy but is also the body's largest endocrine organ,

secreting hormones, cytokines, and proteins that affect the function of cells and tissues throughout the body (Gesta et al., 2007).

The CNS influences energy balance and body weight through three mechanisms (Spiegelman and Flier, 2001): (1) effects on behaviour, including feeding and physical activity; (2) effects on autonomic nervous system activity, which regulates energy expenditure and other aspects of metabolism; and (3) effects on the neuroendocrine system, including secretion of hormones such as growth hormone, thyroid, cortisol, insulin, and sex steroids.

1.3.2. Adipose Tissue

All animal species, from *C. elegans* to Homo sapiens have developed a mechanism for storing excess energy in the form of fat for future needs. In most species, fat storage occurs in a mesodermal tissue (Gesta et al., 2007). Adipose tissue (AT) has been historically considered as an inert tissue, providing a site for passive fat accumulation, insulation against heat loss and mechanical and/or structural support. However, newly recognized endocrine, paracrine and autocrine activities of AT have forced a re-evaluation of this static view of AT biology. Research of the last two decades has demonstrated the importance of white adipose tissue (WAT) metabolism and WAT-derived factors in the development of obesity and systemic insulin resistance. WAT secretes bioactive molecules, generally termed adipokines ,that modulate fat storage, adipogenesis, energy metabolism, and food intake (Zulet et al., 2012).

When the intake of energy chronically exceeds energy expenditure, the excess energy is stored in the form of triglycerides (TG) in adipocytes. Increased AT mass may be produced by an increase in

cell size, cell number, or both since adipose cells are variable in size, reflecting principally the amount of stored TG (Björntorp, 1974, Johnson et al., 1978, Björntorp et al., 1982). Mild obesity mainly reflects an increased adipose cell size (hypertrophic obesity) while more severe obesity also involves an increased fat cell number (hyperplastic obesity). The reversible response to obesity treatment may be related to the plasticity of AT. Studies in humans and other models of obesity indicate that an increase in cell size (adipocyte hypertrophy) often precedes increases in cell number (adipocyte hyperplasia). The development of hyperplastic adipose tissue is associated with the most severe forms of obesity and has the poorest prognosis for treatment (Hausman et al., 2001).

1.3.2.1. Types of adipose tissue

The AT of mammals is classified into 2 types: white and brown adipose tissue. Both share many metabolic characteristics but WAT mainly stores excess energy for subsequent metabolic demand whereas BAT functions as an energy-dissipating organ (Cannon et al., 1982, Cinti, 2001b, Cannon and Nedergaard, 2004, Cinti, 2005). WAT is found as subcutaneous (SC) and visceral (V) depots. Classically, the V depot was considered to be more metabolically active as it released factors can be delivered to the portal venous system and, thus, can directly impact liver metabolism (Björntorp, 1990). In humans, WAT is dispersed throughout the body with major intra-abdominal depots around the omentum, intestines, and perirenal areas, as well as in SC depots in the buttocks, thighs, and abdomen (Figure 7). WAT can be found in many other areas, including in the retro-orbital space, on the face and extremities, and within the bone marrow. Some AT is responsive to sex hormones, such as adipose tissue in the breasts and thighs (Cinti, 2001a).

The developmental patterns of BAT and WAT are distinct. BAT emerges earlier than WAT during fetal development. Morphologically, BAT can be distinguished from WAT by multilocular lipid inclusions, rich vascularization, and abundant mitochondrial density (Cinti, 2001b). BAT responds to cold-induced energy loss through the expression of uncoupling protein 1 (UCP 1) found in the mitochondria membrane that allows dissipation of the proton electrochemical gradient generated by respiration in the form of heat (Nicholls and Locke, 1984). With the exception of UCP 1, which is generally accepted as the defining marker of brown fat, most other differentially expressed genes show only relative differences between the two types of adipose cells. These include among others the fatty acid activated transcription factor PPARα and the peroxisome proliferator-activated receptor gamma coactivator 1 alpha (PGC 1α) as well as factors involved in mitochondrial biogenesis and function (Gesta et al., 2006). Leptin, the nuclear corepressor RIP140, and the matrix protein fibrillin-1 are more enriched in WAT than BAT. At the cellular level, both BAT and WAT appear to originate from MSC (Gesta et al., 2007, Powelka et al., 2006).

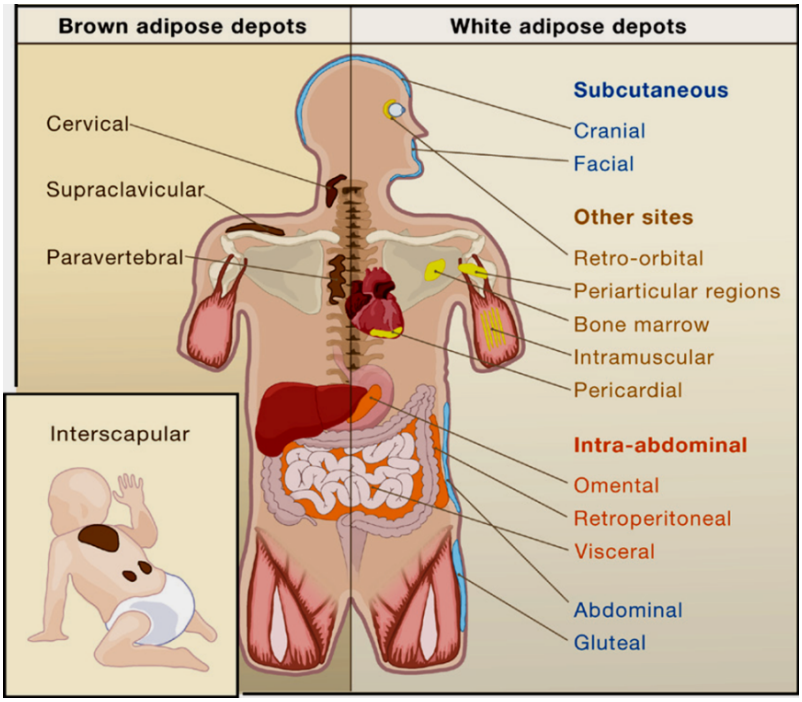

Figure 7: Types of AT and distribution in the human body.
In humans, depots of WAT are found all over the body, with SC and V depots representing the main compartments for fat storage. BAT is abundant at birth and still present in adulthood but to a lesser extent (Gesta et al., 2007).

The distribution of WAT not only varies considerably between species but also between individuals of the same species. In humans, variations of WAT distribution have gained considerable interest due to their association with metabolic disorders. There are two major theories about why these different fat distributions are differentially linked to metabolic complications. The first is based on anatomy and the fact that V fat drains its products (FFA and various adipokines) into the portal circulation where they can act preferentially on the liver to affect metabolism (Björntorp, 1990). The second reflects cell biology and is based on the concept that fat cells in different depots have different properties causing them to be linked to a greater or

lesser development of metabolic disorders (Lafontan and Berlan, 2003). Depot-specific variations in gene expression and adipose tissue function appear to be intrinsic. Thus, isolated cloned human preadipocytes from SC adipose tissue exhibit a greater ability to differentiate in culture than those from V depots (Hauner and Entenmann, 1991, van Harmelen et al., 2004). These differences are conserved over multiple cell generations and are associated with different patterns of gene expression, suggesting that these adipose depots could result in part from different precursor cells (Tchkonia et al., 2002, Tchkonia et al., 2005, Tchkonia et al., 2006, Tchkonia et al., 2007).

Sensitivity of AT to insulin is also depot-dependent. Lipogenesis is the pathway of TG synthesis and is promoted by insulin via activation of lipoprotein lipase (LPL) and by adenosine, the autocrine regulator (Mauriege et al., 1990, Bouchard and Perusse, 1993, Bouchard, 1997). Insulin acts as a potent lipogenic agent, both by promoting lipid synthesis (LPL activity, glucose transport and TG synthesis) and by reducing catecholamine sensitivity via down regulation of β adrenergic receptors (Engfeldt et al., 1988). Adipocytes isolated from V fat depots have reduced (via decreased β 1 and β 2 receptor expression) lipolytic response to catecholamines when compared to SC abdominal adipocytes (increased β 1 and β 2 and decreased α 2 receptor expression). SC abdominal fat cells have a higher affinity for insulin and are more sensitive than V fat cells (Bouchard et al., 1993). There are marked differences between AT origen, particularly in women, in LPL expression (SC < V) and in the sensitivity of AT to insulin stimulated increases in LPL activity (Fried et al., 1993). There are also important depot-specific differences exist in replication, adipogenesis and apoptosis. Adipose depots appear to possess differing proportions of preadipocyte populations with differing capacities for

replication and apoptosis. Human preadipocytes and adipocytes from the V depot display greater rates of apoptosis than cells from SC depots of the same subject. Human V adipocytes are also more susceptible to apoptosis induced by TNF α (Henry et al., 2006).

1.3.2.2. Developmental Origen of Adipose Tissue

The prevailing developmental model suggests that mesoderm/ mesenchymal stem cells (MSC) give rise to bone, muscle, WAT, and BAT in response to appropriate developmental cues (Wassermann, 1965). The formation of the mesoderm begins with the migration of a layer of cells between the primitive endoderm and ectoderm. This layer spreads along the anteroposterior and dorsoventral axes of the developing embryo giving rise to the axial, intermediate, lateral plate, and paraxial mesoderm. MSC were initially identified in postnatal human bone marrow and are capable of differentiating into adipocytes, osteoblasts, chondrocytes, myoblasts, and connective tissue (Grigoriadis et al., 1988, Pittenger et al., 1999, Zuk et al., 2001). Although the exact number of intermediate stages between a MSC and a mature adipocyte is uncertain, it is believed that the MSC gives rise to a common early precursor (preadipocyte), which in turn develops into committed white and brown preadipocytes that under appropriate stimulatory conditions differentiate into mature adipocytes of different types (Figure 8). However, as none of these precursor cells possesses any unique morphological characteristics or definitive gene expression markers, it is not clear if separate preadipocytes for BAT and WAT exist or if there are different white preadipocytes for different white adipose depots (Gesta et al., 2007). Recent studies suggest that WAT and BAT may actually derive from distinct precursor populations. Skeletal muscle progenitor cells can give rise to either muscle cells or brown fat cells, but not white fat cells and the decision

of this precursor to become muscle or BAT is controlled by the transcription factor PRDM16 (Seale et al., 2007, Seale et al., 2008). Expression of PRDM16 causes Myf5 expressing muscle precursors to commit to becoming brown fat cells, whereas reduction of PRDM16 expression by shRNA targeting induces the myogenic differentiation program (Seale et al., 2008). The discovery that muscle and BAT share common progenitor cells may also help to explain the functional dimorphism of adipose tissues, with WAT acting primarily to storage lipid and BAT serving to metabolize lipids to produce heat. Although the WAT and BAT are superficially similar in that they both contain lipid droplets, they appear to arise from divergent developmental programs (Won Park et al., 2008)

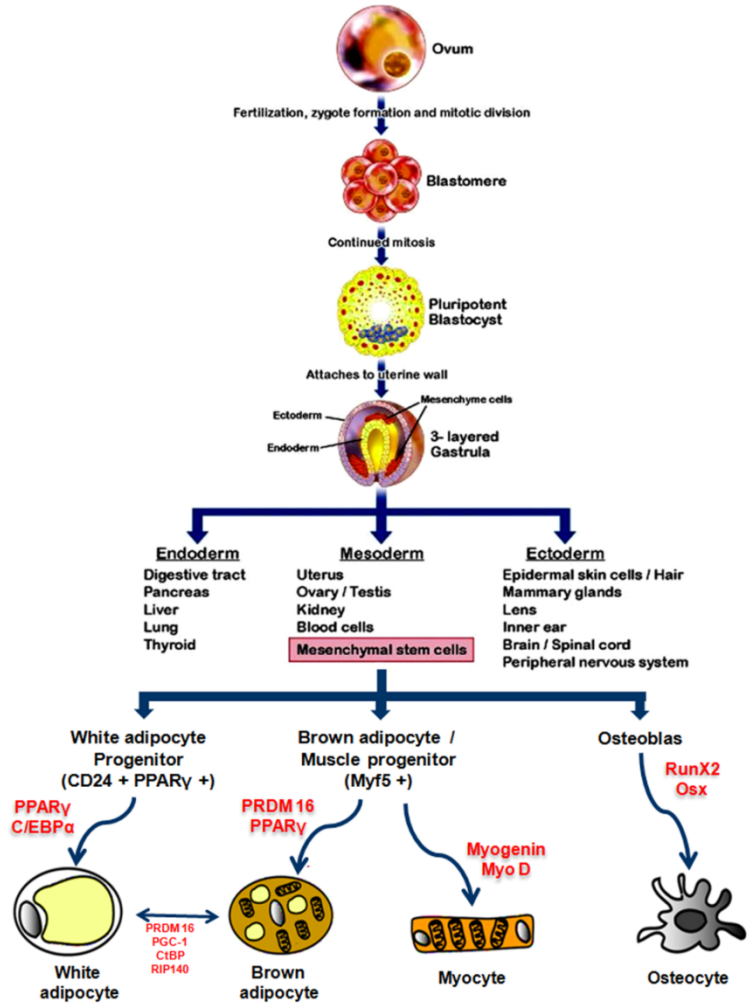

Figure 8: Development of AT from Mesoderm Lineage.
Mesenchymal stem cells are precursors of bone, muscle, and fat cells. WAT differentiation is driven by the transcription factors PPARγ and C/EBPs, giving rise to TG storing WAT. Brown fat cells share precursors (Myf5+) with muscle cells but not with white adipocytes. Adapted figure from American College of Cardiology and (Won Park et al., 2008).

1.3.2.3. Function and metabolism of adipose tissue

The main role of WAT is the storage of TG during energy consumption and release of fatty acids (FA) when energy expenditure exceeds energy intake (Figure 9). As de novo lipogenesis from glucose or other precursors is reduced in human AT, most of the substrate for storage is obtained from circulating lipids, either in the form of lipoprotein particles or complexed with albumin (Henry et al., 2006). This regulation is achieved through endocrine, paracrine and autocrine signals that allow the adipocyte to regulate the metabolism of other fat cells or cells located in brain, liver, muscle or pancreas. Adipocytes and AT are actively involved in metabolic processes such as angiogenesis, adipogenesis, extracellular matrix dissolution and reformation, steroid metabolism, immune response and hemostasis (Vázquez-Vela et al., 2008).

The adipocyte has developed a system for the control of the storage and release of FA. The following proteins involved in lipogenesis program have an impact on insulin sensitivity and circulating lipid levels:

- ✓ Lipoprotein lipase (LPL) catalyzes the release of FA from circulating lipoproteins. LPL activity is greater in SC WAT compared to V WAT (Fried et al., 1993).
- ✓ Fatty acid transporters: The uptake of long chain FA (LCFA) into adipocytes is a saturable process and at least a portion of FFA diffusion is protein mediated (Stahl, 2004). Several proteins are involved including plasma membrane fatty acid-binding protein (FABP), fatty acid transport protein (FATP) and fatty acid translocase (FAT).
- ✓ Fatty acid-binding proteins (FABP): Subsequent to diffusion and transport, cytosolic FFA bind to FABPs. FABPs increase the

solubility of FFAs, augment FFA uptake by increasing the FFA concentration gradient and serve to direct intracellular FFAs to specific fates (Haunerland and Spener, 2004). Nine members of the FABP subfamily of lipid-binding proteins have been identified (Glatz and Storch, 2001).

- ✓ Phosphoenolpyruvate carboxykinase (PEPCK): Efficient storage of FA requires esterification to TG. The backbone for TG formation is provided by glycerol-3-phosphate (G3P), arising from glucose uptake into the cell during the fed state. The key enzyme in the glyceroneogenesis pathway is the cytosolic PEPCK (Reshef et al., 2003, Beale et al., 2003).
- ✓ Perilipin: properly stored TG does not exist as lipid micelles. Rather, the lipid droplet is coated by members of the family of lipid droplet-associated proteins (Londos et al., 1999, Tansey et al., 2004). In adipocytes, this role is filled by the perilipin family of lipid-binding proteins, including perilipin, adipophilyn and TIP47. Alternative splicing of the perilipin gene results in two products, perilipin A and B; perilipin A is the hormone sensitive form (Greenberg et al., 1993).
- ✓ Hormone-sensitive lipase (HSL): Stoed TG are hydrolyzed by HSL to generate FFA when needed. Three isoforms of HSL have been identified (Holm, 2003, Yeaman, 2004).
- ✓ Glucose transporters (GLUT): WAT represents a secondary site for glucose utilization. Glucose transport into adipocytes is mediated by two members of the family: GLUT1 and GLUT4. GLUT1 is constitutively expressed and predominately localized to the plasma membrane and is primarily responsible for basal transport. Meanwhile, GLUT4 is responsible for insulin-stimulated increases in cellular transport in cardiac and skeletal muscle and adipocytes, rapidly translocating from intracellular pools to the cell surface (Yokomori et al., 1999, Uldry and Thorens, 2004)

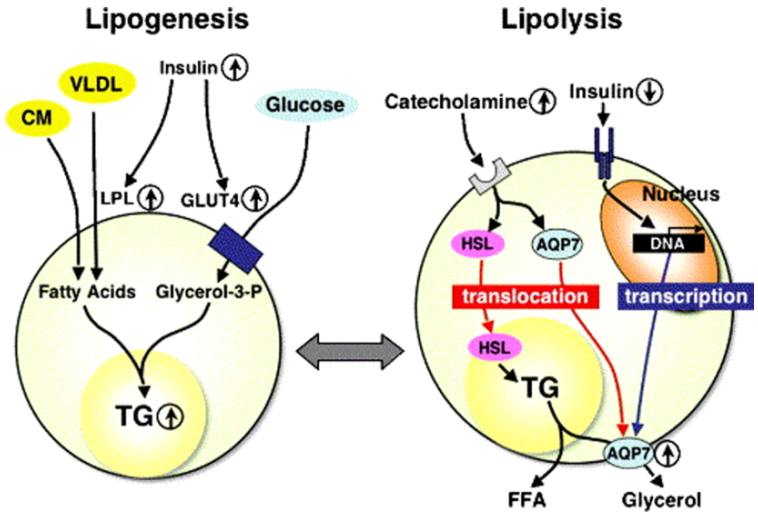

Figure 9: Regulation of lipogenesis and lipolysis in adipocytes.
Under lipogenic conditions, insulin stimulates translocation of GLUT4 to the plasma membrane. Intracellular glucose is converted to G3P. Insulin also activates LPL located on the cell surface of the vascular endothelium. Activated LPL removes fatty acids from intestine-derived chylomicron (CM) and liver-derived very low density lipoprotein (VLDL), and then fatty acids are incorporated into adipocytes. Under lipolytic conditions, catecholamines stimulate adrenergic receptors to translocate HSL, a key enzyme hydrolyzing TG to FFA and glycerol, to the lipid droplets. FFA and glycerol are released into the bloodstream and utilized for thermogenesis and gluconeogenesis, respectively (Hibuse et al., 2006).

1.3.2.4. Control of Adipose tissue: cell size vs number

Hyperplasia (increase of cell number) and hypertrophy (cell size increase) are two possible mechanisms for increasing AT mass (Hirsch and Batchelor, 1976). Radio-tracing studies of human AT suggest that adipocyte number may be determined early in life (Spalding et al., 2008), providing a possible basis for the concept of a fixed individual body weight. AT adipocytes are remarkably variable in size, reflecting principally the amount of stored TG. Fat cell size reflects the integrated effect of a number of factors affecting cellular lipid metabolism. Adipocyte volume has been correlated with lipolytic activity in human WAT (Björntorp, 1974, Mauriege et al., 1990).

Adipocyte size correlates positively with insulin resistance and IL6/TNFα secretion. In addition, severely obese individuals with a healthy metabolic profile have smaller adipocytes than obese individuals with altered metabolism (O'Connell et al., 2010). The mechanism underlying this phenomenon is poorly understood but the hypothesis suggests that as an adipocyte increases in size it eventually reaches a state where it can no longer store lipids. This causes an 'overflow' of FA into ectopic sites such as the liver and muscle, promoting insulin resistance. Individuals with a low adipocyte endowment or impaired lipid storage may be more susceptible to obesity related diseases than individuals with superior lipid storage potential (Henry et al., 2012).

1.3.2.5. The role of inflammation and adipokines in metabolic diseases

Obesity is associated with a state of chronic low-grade inflammation such as elevated serum concentrations of C reactive protein (CRP) and inflammatory cytokines produced by immune cells located within the AT (Rajala and Scherer, 2003, Pickup et al., 1997). The number of macrophages present in WAT strongly correlates with obesity and adipose tissue macrophages (ATM) are considered as a critical factor for the development of obesity-induced insulin resistance and the progression to T2D (Falcão-Pires et al., 2012, Rupnick et al., 2002, Maury and Brichard, 2010, Trayhurn and Wood, 2004). Moreover, AT itself is a source of inflammation: increased TNFα and IL6 expression are implicated in both whole-body and local insulin resistance (Pittas et al., 2004, Ofei et al., 1996, Bastard et al., 2002).

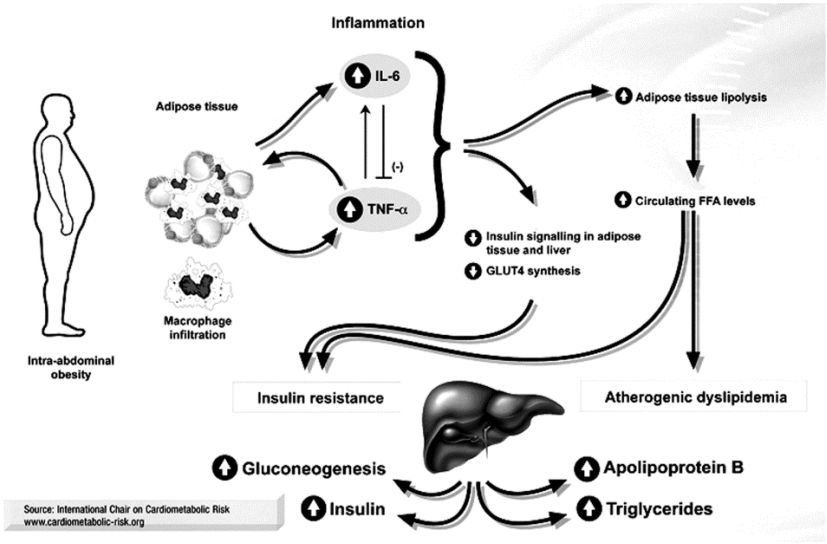

Figure 10: Relationship between obesity, inflammation and insulin resistance. Different pathways through which adipokines generated by an expanding adipose tissue can contribute to the development of the metabolic complications associated with abdominal obesity such as insulin resistance and atherogenic dyslipidemia. Figure adapted from the International Chair on Cardiometabolic Risk.

Adipokines are factors that are produced and secreted by AT and induce responses in various tissues through binding to specific receptors (Calle and Fernandez, 2012). Some adipokines such as adiponectin or lepitn are exclusively produced by the adipose tissue whereas others like TNF α or IL6 can be secreted by diverse cell types in different organs (Antuna-Puente et al., 2008, Kiefer et al., 2010, Zeyda et al., 2011). Obesity is associated with altered expression of the following adipokines:

- ✓ LEPTIN is the product of the the *ob* gene (Zhang et al., 1994). Leptin is secreted mainly by SC fat (Montague et al., 1997). Plasma leptin and mRNA expression in AT are directly related to obesity severity, as an increase of fat mass is associated with an increase of leptin (Considine and Caro, 1997). Leptin activates its

receptors (gen *db*) in hypothalamus, inhibiting food intake and promoting energy expenditure (Vaisse et al., 1996, Friedman and Halaas, 1998). Additionally, leptin is associated with inflammation since it can modulate TNFα production and macrophage activation (Kiguchi et al., 2009). Insulin resistance characterizes states of severe leptin deficiency or resistance, such as *ob/ob* or *db/db* mice, or genetic models of lipoatrophic diabetes. (Kahn, 2001, Adilson Guilherme, 2008).

- ✓ ADIPONECTIN, also called Acrp30 or adipoQ (gen *Adipoq*), is a fat cell derived peptide that, in contrast to other adipokines, is downregulated in obese patients with insulin resistance or T2D (Hu et al., 1996). Acute treatment of mice with this adipokines decreases insulin resistance, decreases plasma FFAs and the TG content of muscle and liver, and increases expression of genes involved in FA oxidation and energy expenditure (Kahn, 2001). A genome-wide scan in humans mapped a susceptibility locus for type 2 DM and metabolic syndrome to chromosome 3q27 in a region near the adiponectin gene (Kahn, 2001, Adilson Guilherme, 2008).
- ✓ RESISTIN: Initial studies suggested that resistin might cause insulin resistance, as levels were increased in obese mice and reduced by anti-diabetic drugs of the TZD class (Steppan et al., 2001). However, studies of resistin in humans have failed to reveal a clear relationship with obesity and T2D and more recent studies suggest a role for this factor in inflammation. Resistin can directly injure endothelium not only by inducing synthesis and secretion of endothelin 1 by endothelial cells, but also by altering vascular cell adhesion molecule (VCAM1) and monocyte chemoattractant protein 1 (MCP 1) expression (Calabro et al., 2004)..

- ✓ RETINOL BINDING PROTEIN (RBP) 4: RBP4 levels are elevated in insulin-resistant mice and humans with obesity and type 2 DM. Transgenic overexpression of human RBP4 or injection of recombinant RBP4 in normal mice causes insulin resistance. Conversely, genetic deletion of *Rbp4* enhances insulin sensitivity (Qin Yang, 2005).
- ✓ Tumor Necrosis Factor (TNFα) is a proinflammatory cytokine produced by numerous cells, but mainly macrophages and lymphocytes. Adipocytes also produce TNFα in rodents, and to a lesser extent in humans (Hotamisligil et al., 1993). TNFα is increased in fat of obese rodents and humans, and has been shown to produce serine phosphorylation of IRS, resulting in reduced insulin receptor kinase activity and insulin resistance (Hotamisligil et al., 1996).
- ✓ Interleukin 6 (IL6) is a cytokine produced by several cells (fibroblasts, endothelial cells, monocytes) and by AT, which is increased in obesity. Capacity to secrete IL6 is six times higher in V than in SC adipose tissue (Fried et al., 1998, Fain et al., 2004). Several studies suggest that IL6 could be implicated in insulin resistance and its complications (Bastard et al., 2000, Bastard et al., 2002) . One of its major actions is control of the hepatic production of inflammatory proteins such as CRP. There is a positive relationship between IL6 levels in AT and circulating CRP levels which is an important cardiovascular risk factor.
- ✓ MONOCYTE CHEMOATTRACTANT PROTEIN 1 (MCP1) is secreted in large amounts by hypertrophied adipocytes where it functions as a chemoattractant that enhances macrophage infiltration into adipose tissue in obese mice and humans (Sartipy and Loskutoff, 2003, Weisberg et al., 2003, Cancello et al., 2005). Consistent with this role of MCP1, AT of lean subjects usually consists of approximately 5–10% macrophages, whereas

in obese patients, macrophage content in adipose tissue can be as high as 50% of the total number of cells. Thus, the increased production of MCP1 by larger adipocytes might contribute to a pro-inflammatory state (Adilson Guilherme, 2008).

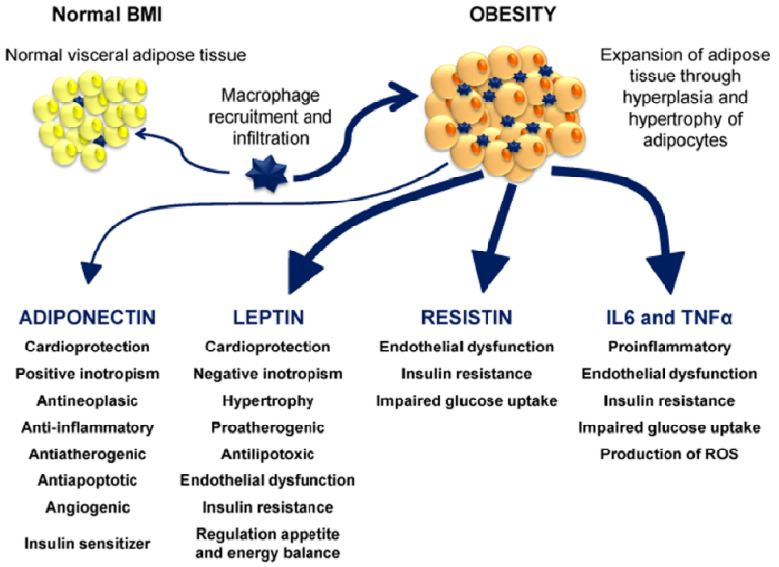

Figure 11: Contribution of adipokines to obesity and metabolic syndrome.
The schematic overview summarizes the action of some adipokines in peripheral and central metabolic processes. Macrophage-infiltration of the expanding AT is crucial in the inflammatory response modulation, but their interaction with endothelial cells and adipocytes is also fundamental. ROS: reactive oxygen species. Figure modified from (Falcão-Pires et al., 2012).

1.4. Adipocyte Progenitors Cells

Studies of the last decade have demonstrated that a pool of adipocyte progenitors (APC) remains present in AT during adult life (Rodeheffer et al., 2008, Tang et al., 2008) and reside in the stroma vascular component (SVF), which also contains immune cells and endothelial cells. Expansion of WAT during normal development and in obesity is

the result of an increase in size and number of adipocytes. As the proliferation of mature adipocytes *in vivo* is very limited, this pool of APC is responsible for the renewal of adipocytes and the potential of this tissue to expand in response to chronic energy overload (Dani and Billon, 2012).

1.4.1. Identification and phenotype of APC

Considerable controversy exists regarding the specific makers expressed by preadipocyte and thus, the only definitive criteria that identifies preadipocytes is their subsequent ability to differentiate to cells that express adipocyte markers and accumulate lipid. It is also important to realize that even cell lines considered good models of WAT do not express all WAT markers. For example, mouse preadipocytes line 3T3L1 produce little, if any, leptin compared to normal white adipocytes (Gesta et al., 2007).

APC have been detected in the proximity of WAT vasculature. Using FACS to analyze the expression of cell surface and stem cell markers, two cell populations were isolated: one CD24+ (lin-:CD29+:CD34+:Sca-1+:CD24+) and one CD24-. Transplantation of this CD24+ population into the fat depots of A-Zip lipodystrophic mice (lipoatrophic diabetic phenotype) led to the development of fat depots with normal adipocyte morphology (Rodeheffer et al., 2008). However, the CD24- and CD34- populations failed to reconstitute WAT after transplantation into A-ZIP mice, suggesting that CD24+ populations are the true source of white APC in vivo (Won Park et al., 2008).

APC isolated from different depots display different characteristics in terms of proliferation, differentiation, and gene expression profiles. The cellular and molecular mechanisms underlying these fat depot

dependent differences are currently unknown. However, several observations suggest that developmental mechanisms contribute to regional variation in function. Consequently, studies on the origins of APC could verify that adipocytes derived from different developmental origins or cellular sources are functionally different (Gesta et al., 2006, Tchkonia et al., 2007, Dani and Billon, 2012).

1.4.2. Molecular regulation of adipogenesis

Adipogenesis is the process by which preadipocytes mature into adipocytes. The transition from preadipocyte to adipocyte involves four stages: growth arrest, clonal expansion, early differentiation, and terminal differentiation (Gregoire et al., 1998). These stages are orchestrated by a cascade of transcription factors (Spiegelman and Flier, 1996). Initial growth arrest coincides with the expression of the transcription factors peroxisome proliferator activated receptor γ (PPARγ) and CCAAT/ enhancer binding protein α (C/EBPα). The induction of these two proteins is characterized by a second, permanent period of growth arrest followed by expression of the fully differentiated phenotype (Figure 12).

PPARγ is a member of the nuclear-receptor superfamily, and is both necessary and sufficient for adipogenesis (Tontonoz et al., 1994b, Tontonoz et al., 1994a). Thus, it has been called the master regulator of adipogenesis. Most pro-adipogenic factors active PPARγ expression or activity. Indeed, the pro-adipogenic C/EBPs and Kruppel-like factors (KLFs) have all been shown to induce at least one of the two *Pparγ* promoters. By contrast, anti-adipogenic GATA factors function in part by repressing PPARγ expression (Rosen and MacDougald, 2006). PPARγ exists as two isoforms (γ1 and γ2) formed by alternative splicing and differing in their N-termini. PPARγ2

is expressed at high levels in adipose tissue, while levels of PPARγ1 can be found in many other tissues. This receptor is induced very early in adipose cell differentiation, and is present at higher levels in preadipocytes than other fibroblastic cells (Zhu et al., 1995, Fajas et al., 1997). The adipogenic activity of PPARγ, like the well established 3T3-L1 and 3T3-F442A preadipocyte cell lines, is markedly enhanced by presence of insulin (Spiegelman and Flier, 1996). Roles for PPARγ in energy homeostasis have been extensible studied following the discovery that PPARγ ligands decrease blood glucose of patients with T2D (Yki-Järvinen, 2004, Rangwala and Lazar, 2004) (Figure 12).

PPARγ is not the only transcription factor that is significantly elevated in adipocyte differentiation. C/EBP α, β and δ are all markedly induced during differentiation in culture (Cao et al., 1991). C/EBPβ and C/EBPδ are induced early during the differentiation upon hormonal stimulation and this is followed by the induction of PPARγ and C/EBPα, since both C/EBPβ and C/EBPδ play a role in the initiation of the adipogenic program (Wu et al., 1996). Ectopic expression of C/EBPβ promotes adipogenesis in both pre-adipocytes and fibroblasts by inducing the expression of PPARγ. C/EBPα, like PPARγ, directly binds to many fat cell–specific genes and it is increased late in the process of adipogenesis. Precocious expression of C/EBPα can accelerate the endogenous differentiation program of preadipocytes, while antisense mRNA blocks the differentiation markedly. The genetic disruption of C/EBPα causes a major reduction in the lipid content of the fat tissue; however, fat cell differentiation apparently still occurs (Spiegelman and Flier, 1996, Wu et al., 1999). C/EBPα may also play a role in glucose homeostasis and appears to regulate insulin sensitivity during adipogenesis (Rosen and Spiegelman, 2000, Gerin et al., 2006).

ADD1/SREBP1 was cloned as a factor from fat cells that bound to E box sequence motifs (Tontonoz et al., 1993, Kim et al., 1995) and as a liver component that bound to sterol-regulatory-elements (SREs) in cholesterol regulatory genes (Brown and Goldstein, 1997). ADD1/SREBP1 is induced during adipogenesis and is further regulated by fasting and refeeding in vivo. The induction during refeeding represents regulation by insulin because insulin modulates ADD1/SREBP1 expression in cultured adipocytes (Kim and Spiegelman, 1996). ADD1/SREBP1 regulates a variety of genes linked to fatty acid and TG metabolism. ADD1/SREBP1 is able to activate PPAR -mediated transcription, which suggests that ADD1/SREBP1 is also involved in the production of an endogenous PPAR ligand (Rosen and Spiegelman, 2000).

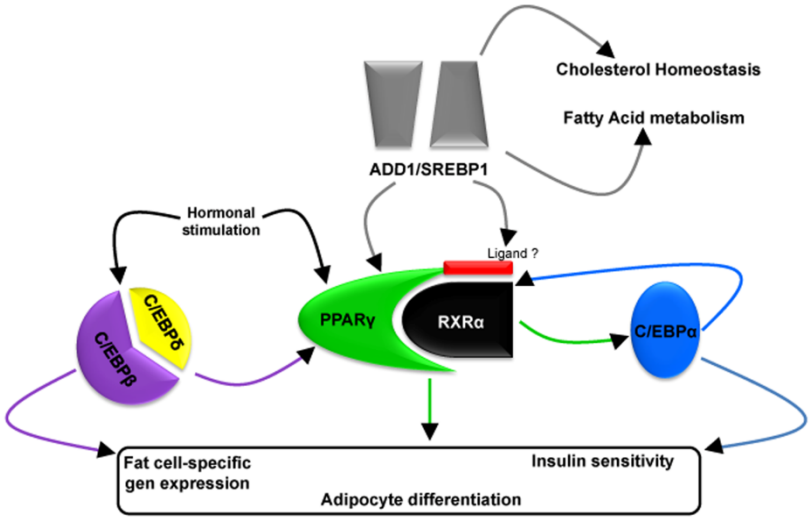

Figure 12: Transcription factors involved in adipocyte differentiation.
The transcriptional control of adipogenesis involves the activation of a variety of transcription factors. These proteins are expressed in a cascade in which C/EBPβ and C/EBPδ induce the expression of PPARγ , which in turn activates C/EBPα. C/EBPα feeds back on PPARγ to maintain the differentiated state. ADD1/SREBP1, in addition to regulating genes important in fatty acid metabolism, can activate PPAR by inducing its expression as well as by promoting the production of an endogenous PPAR ligand. Adapted from (Rosen and Spiegelman, 2000).

1.4.3. Insulin and IGF1 in adipogenesis

Efficient differentiation of APC to adipocytes requires insulin (Hauner et al., 1989, Litthauer and Serrero, 1992). In the early stages of adipogenesis, insulin functions predominantly through IGF1 receptor signalling. Fibroblasts and brown pre-adipocytes from mice that lack insulin receptors are deficient in adipogenesis (Blüher et al., 2002). The loss of individual IRS proteins inhibits adipogenesis in brown adipocytes, with an order of importance of IRS1>IRS3>IRS2>IRS4 (Tseng et al., 2004). Combined deletion of *Irs1* and *Irs3* induce significant lipoatrophy, although brown-adipose tissue is relatively unaffected (Laustsen et al., 2002).

1.5. Osteopontin

Osteopontin (OPN, gene *Spp1*), also called secreted phosphoprotein-1 and sialoprotein-1, is a multifunctional protein expressed in activated macrophages and T cells, osteoclasts, hepatocytes, smooth muscle, endothelial, and epithelial cells. OPN was originally classified as a T helper type 1 (Th1) cytokine that is involved in physiological and pathological mineralization in bone and kidney, cell survival, inflammation, and tumor biology (Mazzali et al., 2002, Kiefer, 2010, Kiefer et al., 2010). OPN can exist as a soluble cytokine or a mineralized matrix-associated molecule. The OPN gene consists of 7 exons, of which exon 1 is non-coding (Craig and Denhardt, 1991, Hijiya et al., 1994). Similarities in gene location and exon structure, but not amino acid sequence have led to the proposal that OPN is a member of a family of proteins termed the small integrin binding ligand, N-linked glycosylation (SIBLING) family. Other members of this family include bone sialoprotein (BSP), dentin matrix protein 1

(DMP1), dentin sialophosphoprotein (DSPP), and matrix extracellular phosphoglycoprotein (MEPE) (Fisher et al., 2001, Kazanecki, 2007).

1.5.1. Structure and functions

OPN is a negatively-charged acidic hydrophilic protein of approximately 300 amino acid residues, and is secreted into all body fluids (Mazzali et al., 2002). The OPN cDNA from various mammalian species exhibits a high degree of sequence homology. The molecule undergoes post-translational modification, and is phosphorylated and glycosylated (Sørensen et al., 1995, Jono et al., 2000). OPN has an arginine-glycine-aspartic acid (RGD) cell binding sequence, a calcium binding site and two heparin binding domains. Alternate splice forms, different alleles, and polymorphisms of OPN have been reported, however the significance of these changes with regard to OPN's function have not been elucidated.

Cells may bind OPN via multiple integrin receptors including the vitronectin receptor ($\alpha v\beta 3$) as well as various $\beta 1$ and $\beta 5$ integrins. OPN does not bind the standard form of CD44 (hyaluronic acid receptor) but does bind various isoforms of CD44. The interaction of CD44 and OPN has been implicated in migration of macrophages and tumor cell lines. A feedback loop may also exist as many researchers have shown that OPN increased expression of CD44, primarily using cancer cell lines such as the breast cancer cell line 21NT (Khan et al., 2005), liver carcinoma cell line HepG2 (Gao et al., 2003), melanoma cells (Samanna et al., 2006) or macrophages. OPN may be cleaved by thrombin, resulting in the exposure of additional cryptic binding sites as well as the production of functional chemotactic fragments (Kazanecki et al., 2007). Osteopontin's function in many tissues is to promote adhesion and facilitate migration of a variety of cell types

through interaction with the integrin and CD44 variants; it is also a cytokine that activates many signaling pathways and supports cell survival.

In bone, OPN is one of the more abundant non-collagenous proteins in bone and is localized to cell-matrix and matrix-matrix interfaces. OPN is expressed by all the major bone-specific cell types: osteoblasts, osteoclasts and osteocytes (Merry et al., 1993). The major role for OPN is in stress-induced bone remodeling, with most studies focusing on stresses that induce bone resorption by osteoclasts. In addition to its effects on the cells in bone, OPN is also a regulator of crystal growth, including hydroxyapatite (HA) the crystal of bone (Shapses et al., 2003).

In kidney and urine, OPN protein has been shown to be a component of kidney stones and its expression is upregulated in the diseased state (Xie et al., 2001). OPN promotes accumulation of macrophages, and may play a role in macrophage-mediated renal injury. However, OPN has some renoprotective actions in renal injury, such as increasing tolerance to acute ischemia, inhibiting inducible nitric oxide synthase and suppressing nitric oxide synthesis, reducing cell peroxide levels and promoting the survival of cells exposed to hypoxia, decreasing cell apoptosis and participating in the regeneration of cells. In addition, OPN is associated with renal stones, but whether it acts as a promoter or inhibitor of stone formation is controversial (Xie et al., 2001).

In immune response and inflammation, OPN induces the expression of a variety of proinflammatory cytokines and chemokines in peripheral blood mononuclear cells (O'Regan et al., 2000). Moreover, it functions in cell migration, particularly of monocytes/macrophages, and stimulates expression of matrix metalloproteases to induce matrix

degradation and facilitate cell motility. In a mouse model of systemic lupus, OPN produced by T cells stimulated IgM and IgG production by B cells. OPN expression is increased in response to cellular injury, attracting and supporting the infiltration of macrophages and T lymphocytes into sites of injury and inflammation (Wang et al., 2005, Wang and Denhardt, 2008). OPN is chemotactic for many cell types including macrophages, dendritic cells, and T cells; it enhances B lymphocyte immunoglobulin production and proliferation. In inflammatory situations it stimulates both pro- and anti-inflammatory processes, which on balance can be either beneficial or injurious depending on what the cell is receiving. OPN influences cell-mediated immunity and has been shown to have Th1 cytokine functions. OPN deficiency is linked to a reduced Th1 immune response in infectious diseases, autoimmunity and delayed type hypersensitivity. OPN's role in the central nervous system and in stress responses has also emerged as an important aspect related to its cytoprotective and immune functions (Wang and Denhardt, 2008). OPN plays a role in various inflammatory disorders, such as rheumatoid arthritis and atherosclerosis, in diabetic macro- and microvascular diseases and hepatic inflammation. Hepatic OPN expression is upregulated in obesity and in various models of liver injury where OPN is localized to macrophages and Kupffer cells. Furthermore, OPN is involved in the pathogenesis of non-alcoholic fatty liver disease (NAFLD), which is strongly associated with visceral obesity (Gómez-Ambrosi et al., 2007, Kiefer et al., 2011, Zeyda et al., 2011).

1.5.2. Role of OPN in Diabetes and Obesity

OPN plasma concentrations are elevated in morbidly obese patients but data are conflicting in murine models of obesity (Zeyda et al., 2011, Kiefer et al., 2011). Adipose tissue macrophages (ATM)

infiltrating into obese adipose tissue from the circulation are a key source of inflammation in obesity and provide a causal link between obesity and the development of adipose tissue insulin resistance. Macrophage recruitment during inflammatory processes is dependent on the expression of OPN (Ashkar et al., 2000). Consistent with this notion, OPN expression in obese adipose tissue colocalized with macrophages and that OPN mRNA is highly expressed in macrophages isolated from the SVF (Nomiyama et al., 2007). Although OPN is expressed in proliferating fibroblasts, earlier reports documenting decreased OPN mRNA levels in differentiated adipocytes as compared with preadipocytes (Senger et al., 1983, Dorheim et al., 1993). Interestingly, OPN has previously been characterized as a PPARγ target gene in macrophages, and overexpression of PPARγ or ligand treatment with a thiazolidinedione suppresses OPN transcription (Wang et al., 2005, Wang and Denhardt, 2008).

OPN is rapidly expressed after cellular activation, and it is abundantly secreted by activated macrophages but not resting macrophages or monocytes. The MAPK kinase kinase 1/c-Jun N-terminal kinase (JNK)1/activator protein, which is also strongly activated upon obesity, is activated by OPN in a myeloma cell line (Philip and Kundu, 2003, Rangaswami et al., 2006). Importantly, JNK is readily phosphorylated by OPN treatment in adipocytes. OPN inhibits adipocyte insulin sensitivity of differentiating or fully mature adipocytes (Hotamisligil, 2006, Weisberg et al., 2003, Nomiyama et al., 2007). Moreover, inflammatory signaling can be induced in adipocytes by OPN. Hence, adipocytes express functional receptors for OPN. Therefore, OPN could contribute to adipose tissue insulin resistance in obesity by a direct action on adipocytes in addition to its role in macrophage migration (Zeyda et al., 2011)..

Hepatic levels of OPN are upregulated in obesity, and hepatic OPN levels correlate with liver TG content (Sahai et al., 2004b, Sahai et al., 2004a, Kiefer et al., 2008, Bertola et al., 2009). Within the liver, OPN is predominantly produced in inflammatory cells but also hepatocytes. Antibody-mediated OPN neutralisation was shown to protect against high-fat diet-induced hepatic macrophage infiltration and D-galactosamine- induced inflammatory liver injury. However, a functional role of OPN in obesity-associated hepatic steatosis and liver insulin sensitivity still remains unclear (Nomiyama et al., 2007, Kiefer et al., 2011) .

1.5.3. OPN knockout model

Loss of osteopontin *(Spp1$^{-/-}$)* prevents high-fat diet-induced hepatic steatosis and inflammation in mice, and markedly improves insulin signalling and insulin sensitivity in the liver, thereby improving hepatic glucose and lipid homeostasis (Nomiyama et al., 2007, Kiefer et al., 2010, Kiefer et al., 2011). *Spp1$^{-/-}$* mice are protected from obesity induced hepatic steatosis. Reduced hepatic TG synthesis underlies this absence of steatosis. Indeed, V WAT weight is increased in obese *Spp1$^{-/-}$* mice indicating that OPN deficiency facilitates fat storage in adipose tissue, thereby preventing its ectopic accumulation in the liver. Decreased inflammatory alterations in V WAT of obese *Spp1$^{-/-}$* mice could contribute to the improvement of metabolic parameters. Moreover, decreased steatosis in obese *Spp1$^{-/-}$* mice was paralleled by improved whole-body insulin sensitivity due to reduction in hepatic insulin resistance and glucose production. Phosphorylation of IRS2 and AKT is enhanced in liver of OPN deficient mice (Kiefer et al., 2011).

Macrophages are the major source of obesity associated inflammatory cytokine production in liver and adipose tissue. Loss of OPN is also associated with downregulated hepatic gene expression of MCP1, a chemokine that promotes hepatic macrophage infiltration and steatosis (Kanda et al., 2006, Obstfeld et al., 2010, Kiefer et al., 2011). Since OPN and MCP1 cooperate in monocyte chemotaxis, abrogation of inflammatory cell migration is likely to account for reduced abundance of macrophages in livers from obese *Spp1*$^{-/-}$ mice (Kiefer et al., 2011).

The observation that OPN is primarily expressed by macrophages in obese adipose tissue combined with the important autocrine role of OPN in macrophage function suggest a model in which endogenous OPN amplifies macrophage recruitment in the early stages of obesity (Giachelli et al., 1998). Ex vivo experiments demonstrate increased macrophage chemotaxis toward the SVF isolated from obese mice, indicating that the continued recruitment of macrophages within the SVF may further exacerbate macrophage infiltration. In contrast, migration toward the SVF was substantially decreased in obese *Spp1*$^{-/-}$ mice (Nomiyama et al., 2007). Decreased ATM accumulation in OPN-deficient mice is associated with increased insulin sensitivity: *Spp1*$^{-/-}$ mice developed less obesity-associated hyperinsulinemia, cleared glucose more rapidly following an intraperitoneal glucose challenge, and exhibited an enhanced insulin response after an intraperitoneal injection of insulin. Increased insulin sensitivity associated with OPN deficiency was unlikely a result of altered adipokine secretion, since plasma levels of 3 adipokines implicated in insulin resistance (adiponectin, resistin, and leptin) were not significantly different in *Spp1*$^{-/-}$ mice. Macrophages present in adipose tissue directly interfere with insulin signaling and insulin-stimulated glucose uptake in adipocytes by decreasing GLUT4 and IRS 1

expression, leading to a decrease in Akt phosphorylation and impaired insulin-stimulated GLUT4 translocation to the plasma membrane (Nomiyama et al., 2007).

CHAPTER 2

MATERIALS AND METHODS

2. MATERIALS AND METHODS

2.1. Animals

Mice were maintained in an enclosed, pathogen-free facility with a controlled photoperiod of 12h light and 12h dark per day at 23ºC with free access to food and water. All studies involving rodents were approved by animal welfare committee of the Principe Felipe Research Center (CV-46007, CIPF, Valencia). Animal experimentation was conducted according to the regulations of the Spanish and European law (RD 1201/2005, B.O.E. 252, 10th October 2005 and European Convention 1-2-3 18th March 1986). For this study, only female mice were used. *Irs2*-deficient (*Irs2*$^{-/-}$) mice were produced and maintained on a C57BL/6 background as described (Withers et al., 1998). Wild-type (WT) mice of the same genetic background were employed as controls. *Irs2*$^{-/-}$ were identified by genotyping using a published PCR strategy (Withers et al., 1998)

The mice used during the collaboration in Vienna were produced and maintained on a C57BL/6J WT. B6.Cg-Spp1tm1Blh/J (referred to as OPN knockouts or *Spp1*$^{-/-}$) mice were purchased from Charles River Laboratories (Sulzfeld, Germany). All mice were housed in a specific pathogen-free facility with a 12 h light/ dark cycle. Mice had free access to food and water. The protocol was approved by the local ethics committee for animal studies and the Austrian Federal Ministry for Science and Research and complied fully with the guidelines on accommodation and care of animals formulated by the European Convention for the Protection of Vertebrate Animals Used for Experimental and Other Scientific Purposes. Animals were fasted for 12-16 h.

Females of 12-16 weeks were used in all experiments. Animals were sacrificed by decapitation and blood was collected to measure glucose and hormones.

2.2. Tissue collection

Upon sacrifice, visceral (V) WAT was excised from the abdominal cavity and subcutaneous (SC) WAT was excised from the inguinal skin-folds. Tissue samples were weighed and were frozen in liquid nitrogen for protein and gene expression studies. For histological analysis, WAT was fixed in 4% paraformaldehyde.

2.3. Glucose and hormones measurements

Blood glucose was determined upon decapitation of mice using a glucometer (Ascensia ELITE®, Bayer HealthCare). Collected blood was centrifuged (13200rpm 20 minutes 4ºC) and serum was frozen for hormone analysis. Insulin levels were determined by Ultrasensitive Mouse Insulin ELISA (Mercodia®). Leptin, Adiponectin and Resistin were estimated by Luminex® technology using the Millipore commercial kit MILLIPLEX™ Multi-Analyte Profiling (MAP). MAP technology performs a variety of immunoassays on the surface of fluorescent-coded beads known as microspheres, which are then read in a compact analyzer. Using flow cytometry-based bead isolation, two lasers and high-speed digital-signal processors, the analyzer reads signals on each individual microsphere particle. The multiple conjugated beads permit the measurement of various hormones from a sample of 10µL of serum.

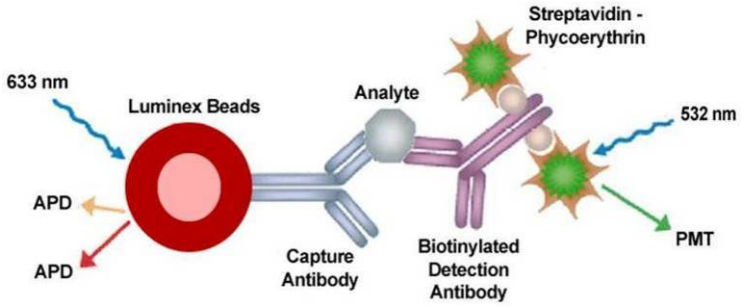

Figure 13: Scheme of the Luminex® technology.
The method is based on the use of 2 different wavelengths for detection of antigen-antibody reactions. The 633nm laser distinguishes the color of the bead and the type of analyte detected. The second laser at 522nm permits quantification by indirect measuring of the Streptavidin-Phycoerythrin conjugate.

2.4. Histological analysis of WAT depots

Fat tissue was fixed overnight by immersion in 4% paraformaldehyde, washed, dehydrated in ethanol and embedded in paraffin as described (Cinti, 2001b) using the Spin Tissue Processor (Myr; STP 120-2, El Vendrell, Spain). The processor consists of a metal wire chamber and 12 buckets which are set up in a circle. The plastic cassettes which contain the fat are placed into the chamber and covered with a lid. 3µm sections were cut using a microtome (Microm/Thermo Scientific; HM 340E, Walldorf, Germany) and placed on 25 x 75 x 1mm polylysine slides (VWR International, Leuven, Belgium). For assessment of V and SC WAT architecture and structure, sections were stained with hematoxylin and eosin. Tissue sections were first placed in xylene for 15 min to remove the paraffin, then hydrated in decreasing concentrations of ethanol (96% and 70%) for 5 min each, then rinsed in distilled H_2O for 5 min. Slides were then immersed in Harris Hematoxylin solution (Sigma) for 1 min and washed with water for 5 min before being rinsed 10 times in 1% hydrochloric acid/70% ethanol. Tissue sections were rinsed in water for 5 min and subsequently stained in Eosin Y Solution (Sigma) for 10

min. After a 5 min rinse in water, tissue sections were dehydrated in increasing concentrations of ethanol (70% and 96%) for 5 min each and finally cleared in xylene for 10 min. Samples were allowed to dry and then were mounted using Entellan (Merck #107961, Darmstadt, Germany) and covered with a 24 x 60mm coverslip (Menzel-Glaser, Braunschweig, Germany). Images of stained WAT sections were captured using a Leica DM microscope and the Leica Application Suite (v 2.4.0 RI) imaging software. The diameter of the adipocyte was measured with ImageJ (v 1.43u, NIH, USA), a public domain Java image processing and analysis program. At least 40 cells were measured from each image. V and SC depots were analyzed from 12 mice of each genotype.

2.5. Analysis of mRNA expression by Real Time Polymerase Chain Reaction (RT-PCR)

To isolate RNA, frozen tissue or cell samples were homogenized in TRIzol® reagent (Invitrogen/Life Technologies, Carlsbad, CA, USA) and processed based on manufacturer's instructions. RNA quality was assessed using the 280/260 nm absorbance ratio which provides an assessment of RNA integrity and 280/230 nm absorbance ratio which indicates the contamination of the sample with salts or organic compounds. RNA concentrations were quantified using a ND-1000 Nanodrop Spectrophotometer (v3.7, Thermo Scientific, Wilmington, DE, USA) and RNA was stored at -80ºC until used for cDNA synthesis.

Total RNA (1µg) was treated with DNase I and transcribed into cDNA using Superscript II and random hexamer primers (Invitrogen). The samples were incubated for 50min at 42ºC, 15min at 70ºC to inactivate the enzyme. Quantitative PCR was performed using Step

One Plus Real Time PCR System (Applied Biosystems) with the TaqMan probes (Applied Biosystems) summarized in Table 3. The RT-PCR reaction contained: 12.5µL TaqMan® Universal PCR Master Mix 2x (Applied Biosystems), 1.25µL primer mix (Applied Biosystem) 1µL cDNA (sample) and 10.25µL MilliQ water. The comparative threshold cycle (CT) method was used to calculate the relative expression (Livak and Schmittgen, 2001) and Stem One ™ Software v 2.1. was used to analyze the data. The cycling conditions were as followed: an initial step called Holding stage for the reaction initiation (50ºC for 2 min and 95ºC for 10 min) followed by 40 cycles of the Cycling Stage (95ºC for 15 sec and 60ºC for 1 min). Each reaction was performed in duplicate and the value of the gene of interest was normalized to the expression of Ubiquitin C. A negative control (MilliQ water) was included for each gene and data were analyzed by the comparative Ct method ($2^{-\Delta\Delta Ct}$).

Gene	Name	Assay ID
Ubc	Ubiquitin C	Mm01201237_m1
Spp1	OPN, secreted phosphoprotein 1	Mm00436767_m1
Irs1	Insulin receptor substrate 1	Mm01278327_m1
Irs2	Insulin receptor substrate 2	Mm03038438_m1
Irs3	Insulin receptor substrate 3	Mm01207023_m1
Insr	Insulin receptor	Mm01211875_m1
Gsk3β	Glycogen synthase kinase 3 beta	Mm00444911_m1
Slc2a4	Glucose transporter member 4 (GLUT4)	Mm00436615_m1
Pparg	Peroxisome proliferator activated receptor gamma	Mm01184322_m1
Fabp4	Fatty acid binding protein 4	Mm00445878_m1
Adn	Complement factor D, adipsin (ADN)	Mm01143935_g1
Fasn	Fatty acid synthase	Mm00662319_m1
Ppargc1a	Peroxisome proliferative activated receptor gamma coactivator 1 alpha (PGC1)	Mm00447183_m1
Srebf1	Sterol regulatory element binding transcription factor 1	Mm01138344_m1
Dgat1	Diacylglycerol O-acyltransferase 1	Mm00515643_m1
Dgat2	Diacylglycerol O-acyltransferase 2	Mm01273905_m1
Adipoq	Adiponectin	Mm00456425_m1
Rbp4	Retinol binding protein 4	Mm00803266_m1
Retn	Resistin	Mm00445641_m1
Hif1a	Hypoxia inducible factor 1	Mm00468869_m1
Vegfa	vascular endothelial growth factor A	Mm01281447_m1
Ccl2	Chemokine (C-C motif) ligand 2, monocyte chemotactic protein-1 (MCP1)	Mm00441242_m1
Emr1	EGF-like module-containing mucin-like hormone receptor-like 1, F4/80	Mm00802530_m1
Tnf	Tumor necrosis factor alpha	Mm00443258_m1
Il6	Interleukin 6	Mm00446190_m1
Ptprc	Protein tyrosine phosphatase receptor type C (CD45)	Mm01293575_m1
Cd3e	CD3 antigen epsilon polypeptide	Mm01179194_m1
Cd8a	CD8 antigen alpha chain	Mm01182108_m1

Table 3: Summary of primers used in mRNA expression studies.
The complete name of the gene and the Applied Biosystem reference number are provided.

2.6. Preparation of Stromal-Vascular Fraction (SVF) from mouse WAT

SC-WAT tissue was obtained from inguinal skin-fold and V-WAT was obtained from the abdomen of female mice. Tissue was minced with scissors and then digested in adipocyte isolation buffer Krebs Ringer containing: $NaHCO_3$ 24mM, HEPES 10mM, Bovine Serum Albumin (BSA) 2.5% (Sigma 7906), Collagenase 1mg/mL (GIBCO CAT Nº 17104-019 1.362 PZU/mg), Dispase 1mg/mL (GIBCO Cat No. 17105-041 1.7 units /mg), Desoxirribonuclease 1 0,25mg/mL (Sigma DN25), 1% v/v of Penicillin /Streptomycin (Gibco Cat.Nº 15140-122) and 0,005mg/mL Amphotericin B (Sigma 9528). Subsequently, samples were incubated in 3 mL of buffer Krebs Ringer/g WAT for 40-60 min at 37 ºC in a shaker bath. The digested tissue was passed through a nylon screen and rinsed several times with PBS/2,5% BSA/antibiotics to remove the collagenase. The suspension was centrifuged at 300xg for 10 minutes and the pellet was resuspended in complete Dulbecco's Modified Eagle high glucose Medium (DMEM, Gibco 41966) supplemented with 10% (v/v) of Fetal Clone III Bovine Serum (FcBS) (HyClone SH30109.03) and Penicillin/ Streptomycin 1% (Gibco Cat.Nº 15140-122). This suspension was filtered through a 100μ cell-strainer and centrifuged again at 300xg for 10 minutes. The pellet was resuspended and filtered first through a 70μ cell strainer and subsequently through a 40μ cell strainer. The resulting cells were counted and $1x10^5$ cells were seeded in $60cm^2$ plates or sorted by Fluorescent Activated Cell Sorting Analysis (FACS) to obtain the specific APC population.

2.7. Fluorescent Activated Cells Sorting (FACS) Isolation of APC

To isolate the APC population from the stroma vascular fraction (SVF) of WAT, a FACS enrichment strategy was developed based on published methods (Rodeheffer et al., 2008). The High Speed Cell Sorter MoFlo (Beckman Coulter, CA, USA) is equipped with 3 lasers (488nm, 351nm y 635nm), two detectors for the light forward (FS) and side (SS) scatter and eight photomultipliers for fluorescence detection. This optical configuration allows a selection procedure based on staining of five antibodies specific to certain cell populations (Table 4). Each antibody was tittered and the corresponding isotype was analyzed to minimize possible false positive.

Conjugated Primary Antibody	Manufacturer	Cell population	Quantity (µg/10^6 cells)	λ_{em} (nm)
Sca1 FITC	eBioscience 11-5981	Stem cell	0.25	530 ± 40
CD31 PE	eBioscience 12-0311	Endothelial cells	0.4	580 ± 40
Ter119 PE Cy5	eBioscience 15-5921	Erythroid cells	0.25	670 ± 30
CD34 Alexa 647	eBioscience 51-0341	Stroma cells	1.5	670 ± 20
CD45 PE Cy7	eBioscience 25-0451	Hematopoietic cells	0.125	> 740
DAPI	Sigma D8417	dead cells	1µg/µL	405

Table 4: Fluorescent-conjugated primary antibodies utilized for APC isolation.

Cells isolated from SVF were incubated with the antibodies for 1h at 4ºC. Just prior to FACS, DAPI was added to each sample in order to identify and eliminate dead cells. First, the endothelial, erythroid and hematopoietic cells were depleted from the SVF by staining for CD31, Ter119 and CD45 antigens, thereby generating a lineage-negative (Lin-) population. Subsequently, the Lin- population was further sorted based on CD34 and stem cell antigen 1 (Sca1), two cell-surface proteins expressed on stem cell populations from different tissues (Spangrude et al., 1988, Zuk et al., 2002, Rodeheffer et al., 2008). The sorting criterion was based on the double staining for CD34 antigen and Sca1. From the live cell population (DAPI-), two populations were recovered: CD34-/Sca1- and CD34+/Sca1+. Double negative population was frozen and double positive population was seeded in 60mm^2 cell culture plates and fresh medium with βFGF was added as described above. All the data were processed by Summit V4.3 software (Beckman Coulter, CA, USA).

2.8. Magnetic Cell Sorting Analysis (MACS®)

To isolate the APC from *Spp1*$^{-/-}$ and WT mice, indirect Magnetic Cell Sorting (MACS®) technology was used since these experiments were performed at the University of Vienna with different tools. This two-step procedure is summarized in Figure 14.
Cells from the SVF were first labeled with a similar set of antibodies as employed for FACS analysis. CD45, CD31 and Ter119 were incubated for 1h at 4ºC. Subsequently, the cells were incubated with a primary rat IgG antibody coupled to magnetic beads (Goat Anti-Rat IgG Microbeads, Miltenyi Biotec 130-048-502). The cell suspension was passed through a MACS® column, which is placed in the magnetic field of MACS Separator. The magnetic labeled (CD45, CD31 and Ter119) positive cells were retained within the first column.

The unlabelled cells which flowed through the column were then labeled with the second set of primary rat IgG antibodies (CD34 and Sca1) for 1h at 4ºC. After removing the column from the magnetic field, the magnetically retained cells were eluted to obtain the positively-selected cell fraction (CD45- CD31- Ter119- CD34+ and Sca1+).

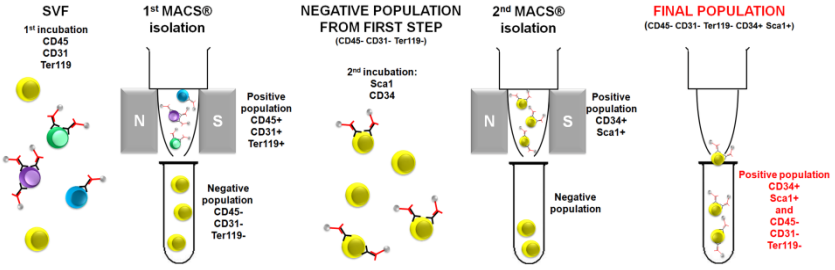

Figure 14: MACS® strategy used for APC isolation from V and SC-WAT from WT and *Spp1*$^{-/-}$.
Cells were first incubated with CD45, CD31 and Ter119 antibodies and the negative population was collected for further incubation with Sca1 and CD34. Then, the positive population was retained in the magnetic field to isolate and establish the APC culture.

2.9. Routine culture of primary APC

Mouse APCs were cultured at 37ºC and 5% CO_2. The cell culture medium was Dulbecco's Modified Eagle high glucose Medium (DMEM, Gibco 41966) supplemented with 10% (v/v) of Fetal Clone III Bovine Serum (FcBS) (HyClone SH30109.03), Penicillin / Streptomycin 1% (Gibco Cat.Nº 15140-122). To passage the cells, the medium was removed and the cells were washed with PBS without calcium and magnesium (Gibco). The cells were incubated with incubation with 0.25% trypsin / 0.02% EDTA (Gibco 25200) for 5 min at 37ºC and gently shaken to detach the cells. The trypsin/EDTA was neutralized by complete medium (DMEM/10% FBS). The suspension was then centrifuged at 200xg for 4 min. The supernatant was removed and the pellet containing the cells was resuspended in the

growth medium and seeded at $2x10^4$ cells/cm^2. For normal condition growth, the medium was supplemented with 10 ng/ml recombinant basic Human Fibroblast Growth Factor (FGFβ or FGF-2, Gibco, PHG0026) to maintain their self renewal capacity and inhibit differentiation (Rodeheffer et al., 2008, Dani and Billon, 2012).

2.10. Proliferation studies: cell growth curves and doubling time determination

$5x10^4$ of the isolated APCs were seeded in 100 mm culture plates. Every day during 5 days one plate was trypsinized and counted to establish the growth kinetics of each experimental group. The doubling time was calculated with the online tool (http://www.doubling-time.com/compute.php).

2.11. Differentiation of APC cultures

To assess the adipogenic potential of APC, cells were seeded so as to reach confluence in 3 days, based on their growth properties. On day 0 of the differentiation protocol, cells were switched from growth to adipogenic medium: advanced DMEM/F12 (Gibco 12634) with 5% heat-inactivated (56ºC for 30min) FBS (Sigma F7524) with different factors: insulin (INS, Roche), dexamethasone (DXM, Sigma) and Isobutilmethylxantine (IBMX, Sigma). The concentrations and duration of treatment are summarized in Figure 15. Samples were taken during the time-course of differentiation to analyse differentiation markers by immunostaining, Western blotting, or RT-PCR.

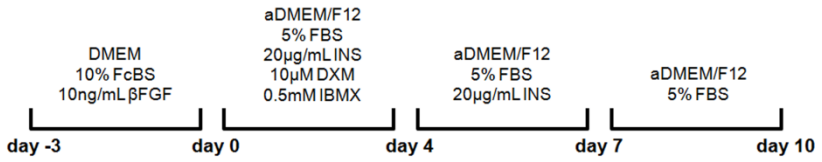

Figure 15: Adipocyte differentiation scheme.
Cells were plated to reach confluence after 3 days and then the adipocyte differentiation medium was used for 10 days until lipids droplets were detected inside the cells.

2.12. Flow Cytometry analysis of APC

The flow cytometry experiments were performed with a Cytomics FC500 MCL flow cytometer (Beckman Coulter, CA, USA) equipped with two lasers (488nm and 635nm), two detectors for the light forward (FS) and side (SS) scatter and five photomultipliers for fluorescence detection.

To detect the fluorescence emission from BODIPY, anti-Sca1 FITC, and annexin V FITC, the FL1 (525±20nm) channel in logarithmic amplification was used. For BODIPY measures FL1 was also used in linear amplification. For propidium iodide measure, FL3 (620±20nm) was used in logarithmic amplification for apoptotic assays and to exclude the dead cells and in linear amplification for cell cycle and cell proliferation studies.

2.12.1. Cell-cycle analysis by Hypotonic Propidium Iodide staining

To assess the cell cycle, APC cells were stained with propidium iodide (PI), a nucleic acid probe which identifies DNA and RNA. Upon binding to nucleic acids, the PI fluorescence emission can be detected by flow cytometry. Since the binding is proportional to the amount of nucleic acid in the sample, different amounts of DNA can be

distinguished at distinct cell cycle phases (Figure 16). For DNA staining, cells were suspended in a hypotonic solution of PI (trisodium citrate 1mg/mL, Triton X-100 0.1 % (v/v), PI 50µg/mL and ribonuclease A (RNase A) 100µg/mL) and incubated at 4 ºC in the dark. At least $1x10^4$ cells from each sample were assessed with the cytometer. The PI emission was detected in the FL3 (620±20 nm) channel and the cellular aggregates were excluded from analysis. The histograms were generated with the WimMDI® program and the FL3 histogram gated for single cells was analyzed with Cylchred® program obtaining the percentage of cells in each phase of the cell cycle.

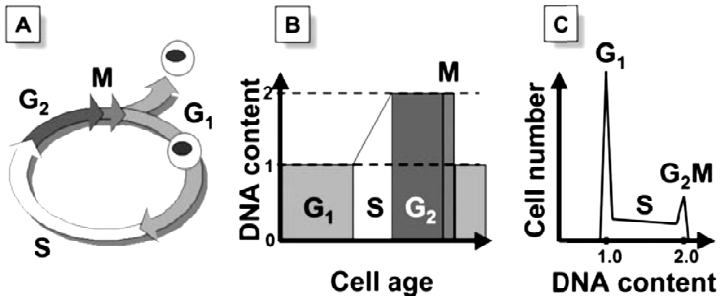

Figure 16: Schematic representation of cellular DNA content changes during cell cycle progression.
DNA replication during cell cycle is discontinuous, occurring exclusively during S phase. As a result, the post-replicative G_2-phase cells have twice higher cellular DNA content compared to the G1 cell (B). (Darzynkiewicz et al., 2010).

2.12.2. Apoptosis Assay: Annexin V staining

Highly fluorescent Annexin V conjugates provide quick and reliable detection methods for studying the externalization of phosphatidylserine, an indicator of intermediate stages of apoptosis (Koopman et al., 1994, Zhang et al., 1997). A total of $1x10^5$ cells were suspended in 100µL of binding buffer containing 10mM HEPES, 140mM NaCl and 2,5mM CaCl2 adjusted at pH 7,4. Subsequently, 5µL of Annexin V-FITC (Immunostep, Spain) was added and

incubated for 15 minutes at room temperature in the dark. 1µL of PI solution (1mg/mL) was added for 5 min. The cells were analyzed with the 525nm channel to detect the emission of Annexin V-FITC and the 620nm channel for the PI emission. All the data were processed by Summit V4.3 software (Beckman Coulter, USA). For the analysis, three different groups were identified: (i) live cells (double negative for Annexin V-FITC and PI, (ii) early apoptotic cells (positive for Annexin V-FITC and negative for PI), and (iii) dead/necrotic cells (positive for PI).

2.12.3. Sca1-FITC Staining

Fresh APC cells were gently trypsinized and transferred to flow cytometry tubes. The cells were carefully centrifuged at 100xg for 5 min and resuspended into 100µL of PBS containing 0.25µg/10^6 cells Sca1 antibody for 1 hour at room temperature in the dark. Then were washed with PBS and resuspended in 500µL of PBS containing 2.5µg/mL of PI 5 min before flow cytometry analysis. All data were processed by Summit V4.3 Build 2445 software (Dako Colorado, Inc.).

2.12.4. BODIPY™ 493/503 Staining

Detection of cellular lipid droplets with BODIPY 493/503 dye (Molecular Probes, D3922) is more specific for than staining with other dyes such as nile red (Gocze and Freeman, 1994, Listenberger and Brown, 2007). Due to its low molecular weight (262 daltons), the diffusion of BODIPY 493/503 dye across membranes is relatively fast diffusion. A stock solution of The BODIPY 493/503 was prepared at 1mg/ml in DMSO. The working solution was freshly prepared and incubated (1ng/ml) in suspension of APC cells for 30min at 37ºC. Then, 5µg/mL of PI was added to each tube for 5 min before flow cytometry analysis. The side scatter (SS) parameter was used to

detect changes in the cell granularity and the green fluorescence (525nm) of BODIPY to measure the intracellular lipid droplets formation (see Figure 17).

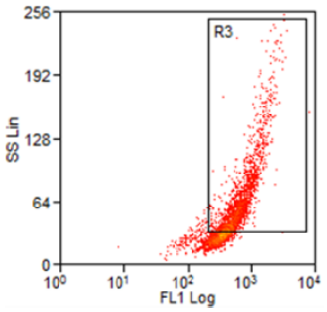

Figure 17: Analysis of positive BODIPY cells.

2.13. Indirect Immunofluorescence analysis

After cell sorting, the isolated population was plated using a CytoSpin 4 Cytocentrifuge (Thermo Scientific). To this end, $5x10^3$ isolated cells directly from the sorter were resuspended in 100µL of DMEM + 10% FcBS and processed with CytoSpin to attach the cells into polylysine slides. The cells were centrifuged and fixed with 10% formalin solution (Sigma) for 15 min in the dark. After that the slides were washed 3 times with PBS/Ca^{+2}/Mg^{+2} at pH 7.4 and then the slides were incubated in blocking solution containing PBS/Ca^{+2}/Mg^{+2} pH 7.4, 10% Horse Serum (HS) (Sigma) for 1h at RT. Primary antibody was incubated as detailed (Table 5) for 1h at RT, washed 3 times with PBS/Ca^{+2}/Mg^{+2} pH 7.4 and the nuclei stained with 4,6-diamidino-2-phenylindole dihydrochloride (DAPI) at a concentration of 1µg/mL for 5 min at RT (Table 5). The DAPI solution was removed by aspiration and washed twice for 5 min in distilled H_2O. Each slide was covered with a coverslip with one drop of Dako Fluorescent Mounting Medium (Barcelona, Spain).

Alternatively, APC were grown in 24-well plate with glass coverslips. Before the cells were stained, the culture medium was aspirated from the wells and the cells were washed in PBS/Ca^{+2}/Mg^{+2} pH 7.4, incubated in 10% formalin solution (Sigma) for 15 min in the dark, washed 3 times with PBS/Ca^{+2}/Mg^{+2} pH 7.4 and then cells were incubated in 500µL of blocking solution containing PBS/Ca^{+2}/Mg^{+2} pH 7.4, 10% Horse Serum (HS) (Sigma) and 0.05% Tween-20 (Sigma) for 1h at RT. The blocking solution was aspired and cells were incubated in each antibody, diluted in the blocking solution, for 2h at room temperature (Table 5). Afterwards, the cells were washed three times with PBS/Ca^{+2}/Mg^{+2}, and incubated with the secondary antibody diluted in the blocking solution for 1h at RT (Invitrogen). Then, cells were washed 3 times with PBS/Ca^{+2}/Mg^{+2}, the nuclei was counterstained with DAPI (1µg/ml of DAPI in MilliQ H_2O) and incubated for 5 min at RT (Table 5). The DAPI solution was removed by aspiration and stained cells were washed twice for 5 min in distilled H_2O.

For BODIPY staining, APC were grown in 24-well plate with glass coverslips. Before the cells were stained, the culture medium was aspirated from the wells and the cells were washed in PBS/Ca^{+2}/Mg^{+2} pH 7.4, incubated in 10% formalin solution (Sigma) for 15 min in the dark, washed 3 times with PBS/Ca^{+2}/Mg^{+2} pH 7.4 and then cells were incubated in 500µl of BODIPY staining containing PBS/Ca^{+2}/Mg^{+2} pH 7.4, and 0.5 µg/ml BODIPY 493/503 (Molecular Probes) for 1h at RT. Then, cells were washed 3 times with PBS/Ca^{+2}/Mg^{+2}, the nuclei was counterstained with DAPI (1µg/ml of DAPI in MilliQ H_2O) and incubated for 5 min at RT (Table 5). The DAPI solution was removed by aspiration and stained cells were washed twice for 5 min in distilled H_2O (Table 5).

Each coverslip was placed on the top of a glass slide with Dako Fluorescent Mounting Medium (Barcelona, Spain). Images were captured using a Leica DM 6000B fluorescent microscope attached to Leica Application Suite (v 2.8.1) imaging software. Three different cell cultures were used for each immunostaining and representative pictures are show for each antibody.

For In-Cell analysis, APC were cultured and processed for immunostaining in 24 well plates (Costar 3524. Corning Incorporated NY 14831) as described above (Table 5). The images were acquired and quantified with the In Cell Analyzer 1000 system (GE Healthcare). This system is a high content image analysis instrument with ability to capture cell images and quantify different cell parameters. 30 images per well were acquired and nuclei staining of both Ki67 and pH3 were analyzed.

Primary Antibody	**Dilution**	**Commercial source**	**Incubation conditions**
Ki67	1/500	Abcam 5580	2h RT
Phospho Histone H3 Serine 10-Alexa 647	1/200	Cell Signaling 9716S	2h RT
BODIPY	0.5µg/mL in PBS	Molecular Probes D3922	1h RT
Sencondary Antibody	**Dilution**	**Commercial source**	**Incubation conditions**
Goat Anti Rabbit Alexa 488	1/500	Invitrogen A11070	1h RT

Table 5: Primary antibodies used for immunofluorescence.

2.14. Western blotting

Samples were lysed in a buffer containing: 50mM HEPES, 150mM NaCl , 10% glycerol, 1% triton-X-100, pH 7.5. The appropriate protease/phosphatase inhibitors were added to the lysis buffer immediately before use: 1mM sodium orthovanadate (Na_3VO_4), 50mM sodium fluoride (NaF) and 1x Complete protease cocktail inhibitor (Roche Diagnostics, Mannheim, Germany). Tissue samples were homogenized (PT-MR 1600E, Kinematica Inc., Littau, Switzerland) in ice-cold lysis buffer at a concentration of 50mg tissue per 1ml of lysis buffer. The homogenate was cleared by centrifugation at 13200xg for 20 min. The lipid layer was removed from the top and the supernatant transfered to a clean eppendorf tube to discard pellet of debris and insoluble material. The protein concentration was estimated using the BCA Protein Assay Kit (Thermo Scientific, Rockford, IL, USA). Standards were prepared from 2mg/ml Bovine serum albumin (BSA) with serial dilutions until 0.125mg/mL. Colorimetric analysis was performed in a 96-well plate using a Multiskan FC Microplate Photometer (Thermo Scientific, Finland).

Laemmli 6x loading buffer, containing 9% sodium dodecyl sulphate (SDS, Sigma-Aldrich), 60% Glycerol (Sigma-Aldrich), 10% β-Mercaptoethanol (Sigma-Aldrich), 0.03% bromophenol blue(Biorad) and 0.375M Tris-HCl pH 6.8 was added to extracts at a 1:1 volume. Samples were denatured by heating for 2 min at 100^{o}C. 50µg of protein were loaded per lane and resolved under reducing and denaturing conditions by SDS-polyacrylamide gel electrophoresis (Sambrook and Russell, 1989, Schägger, 2006)

Polyvinylidene fluoride (PVDF) membranes were pre-activated by incubating in 100% methanol for 5 min, and then thoroughly rinsed in the transfer buffer before beginning the transference. Resolved

proteins were transferred from SDS-PAGE gels to PVDF membranes at 350mA for 1h30min-2h at 4ºC. Following transfer, non-specific binding of proteins to the PVDF membranes was blocked by incubating in blocking solution containing 5% BSA in 1xTBST (Tris-Buffered Saline-Tween 20) composed for 50mM Tris-HCl pH7.5, 150mM NaCl and 0.05% Tween-20, for 1h at room temperature on a see-saw rocker plate. Primary antibodies (Table 6 for technical details) were diluted in 3% BSA solution and incubated on a see-saw rocker. After the incubation, the primary antibody was removed and the PVDF membrane was washed 3 times for 10 min in 1x TBST on a see-saw rocker plate. The appropriate horseradish peroxidase-conjugated (HRP) secondary antibody (Thermo-Scientific) was diluted in blocking solution and incubated with the PVDF membrane for 1h at room temperature. The secondary antibody was then removed and the PVDF membrane was washed in 1xTBST 3 times for 10 min per wash on a see-saw rocker plate. Reactive bands were revealed on X-ray film CURIX RP2 Plus (AGFA), using Pierce Enhanced Chemiluminescent (ECL) Western Blotting Substrate reagents (Thermo Scientific #32106).

Primary Antibody	Dilution	Manufacturer	Incubation Conditions
C/EBPα	1/200	Santa Cruz 61	14h-4ºC
GLUT4	1/1000	Millipore 07-1404	14h-4ºC
HSL	1/500	Santa Cruz 74489	14h-4ºC
IGF1R	1/500	Santa Cruz 713	14h-4ºC
IRβ	1/1000	Santa Cruz 711	14h-4ºC
IRS1	1/1000	Cell Signaling 23825	14h-4ºC
IRS1	1/1000	Lab. Made PH	14h-4ºC
IRS2	1/1000	Millipore MAB515	14h-4ºC
IRS2	1/500	Santa Cruz 8299	14h-4ºC
IRS3	1/500	Lab. Made 299	14h-4ºC
ObR	1/200	Santa Cruz 8391	14h-4ºC
PDGFRβ	1/500	Santa Cruz 432	14h-4ºC
PPARγ	1/2000	Santa Cruz 7273	14h-4ºC
β ACTIN	1/10000	Sigma A1978	1h- RT

Table 6: Primary antibodies used in western blot analysis.

2.15. Statistical Analysis

All data presented were obtained from at least three independent experiments and are expressed as the mean ± SEM. Paired Student's *t* test was performed to compare genotypes.

CHAPTER 3

HYPOTHESIS AND OBJECTIVES

3. HYPOTHESIS AND OBJECTIVES

Defects in insulin signaling are implicated in obesity and T2D. Deletion of *Irs2* in mice causes insulin resistance and progressive beta cell failure, culminating in diabetes. Reduced expression of *Irs2* has been observed in islets of patients with T2D, suggesting a direct link between failed insulin signalling and human metabolic disease. Female *Irs2*$^{-/-}$ animals develop moderate obesity and display resistance to catecholamines and leptin. However, the precise role of IRS2 in adipose tissue and obesity-related inflammation has not yet been defined. Thus, the I*rs2* knockout model was used to address the following objectives:

1. Characterize WAT of female *Irs2*$^{-/-}$ mice by assessing markers of inflammation, adipocyte function, and insulin signal transduction.

2. Isolate and characterize APCs of WAT to determine whether IRS2 plays a role in the development, proliferation and differentiation of adipocyte progenitors.

3. Assess the potential physiological relationship between IRS2 signaling and the cytokine OPN though the study WAT from female *Irs2*$^{-/-}$ and *Spp1*$^{-/-}$ mice.

CHAPTER 4

RESULTS

4. RESULTS

4.1. *Irs2*$^{-/-}$ females mice display increased adiposity

4.1.1. Analysis of glucose and insulin levels

Consistent with published results, *Irs2*$^{-/-}$ females displayed slightly elevated blood glucose levels and pronounced hyperinsulinemia (Figure 18). Male *Irs2*-deficient mice develop hyperglycemia earlier than females and progress rapidly to severe diabetes (Garcia-Barrado et al., 2011). All females used in this study were 8-12 weeks of age and although the fasting glucose levels in *Irs2*$^{-/-}$ were higher than in WT (WT 85.6±2.69 mg/dl vs *Irs2*$^{-/-}$ 95.6±2.34), none presented hyperglycemia (fasting glucose > 120 mg/dl) which facilitated the study of *Irs2*-deficiency in the absence of diabetic complications. The presence of hyperinsulinemia in these mice is due to insulin resistance in peripheral tissues, mainly liver and muscle (Withers et al., 1998).

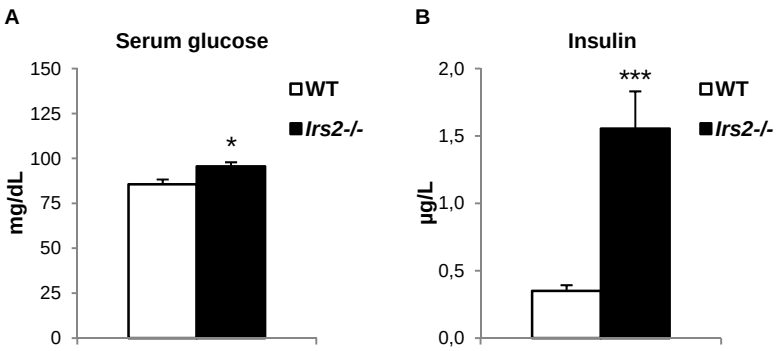

Figure 18: Glucose and insulin levels of female WT and *Irs2*$^{-/-}$ mice.
Female mice (8-12 weeks of age) were fasted for 14-16 hours. **A)**. Glucose was measured by Ascensia ELITE® glucometer. **B**) Insulin was estimated by ELISA. Results are expressed as mean ± SEM. * p<0.05, ** p<0.01, and *** p<0.001. For glucose measurements, n= 20 mice per genotype. For serum insulin levels, N=10 mice per genotype.

4.1.2. Characterization of body weight and WAT depts

As reported, female *Irs2*-deficient mice weighed more than controls (Figure 19). Increased body weight was associated with increased accumulation of WAT in both visceral (V) and subcutaneous (SC) depots (% of total body weight).

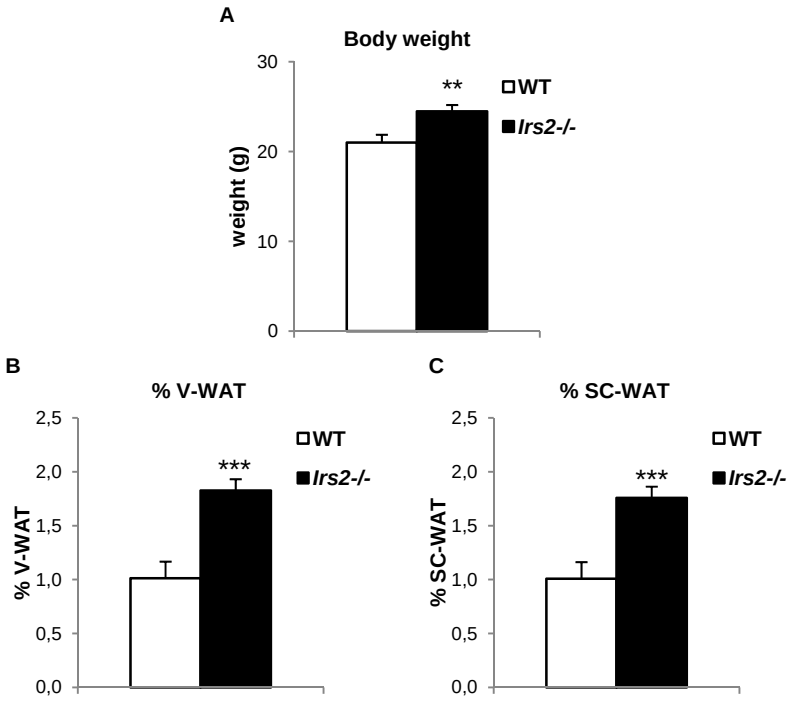

Figure 19: Analysis of adipose depots.
A) Total body weight. **B**) Visceral white adipose depots (V-WAT) were weighed and compared to total body weight. **C)** Sub-cutaneous white adipose (SC-WAT) depots were weighed and compared to total body weight. Results are expressed as mean ± SEM. * p<0.05, ** p<0.01, and *** p<0.001. N=20 mice of each genotype.

4.1.3. Morphological assessment of WAT

The increase of WAT present in the *Irs2*$^{-/-}$ female mice could be due to an increase in the size of adipocytes (hypertrophy) as a result of more stored triglycerides or to an increase in the number of adipocytes (hyperplasia). To distinguish between these possibilities, histological sections of V-WAT and SC-WAT were stained with hematoxylin and eosin and examined. The histological analysis of the V-WAT and SC-WAT revealed no apparent differences in the average diameter of adipocytes between *Irs2*-deficient and control mice (Figure 20), suggesting that enhanced adipocyte size does not account for the increased fat mass in this model.

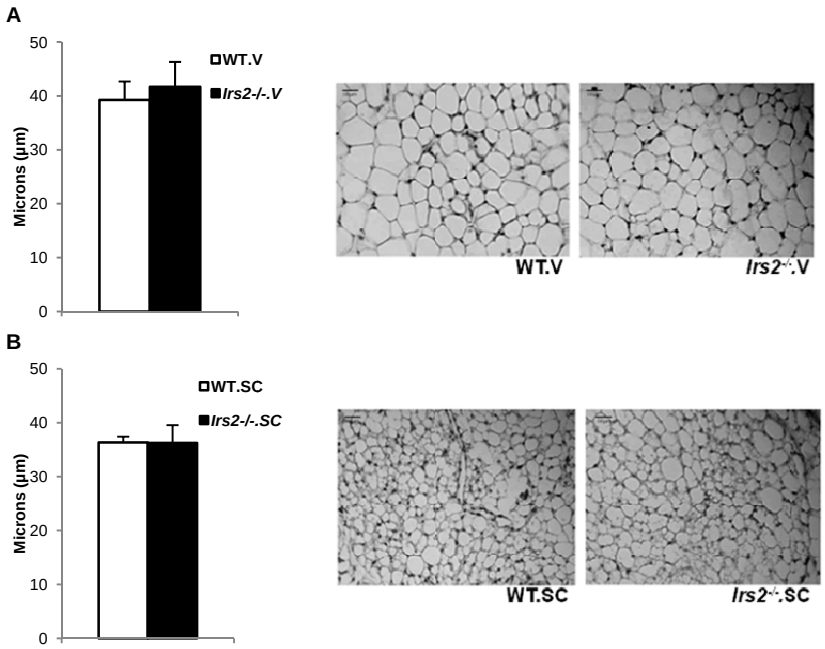

Figure 20: Analysis of V and SC adipocyte size in WT and *Irs2*$^{-/-}$ mice.
Hematoxylin and eosin staining of WAT sections was used to measure diameter of adipocytes from V-WAT **(A)** and SC-WAT **(C)** by the ImageJ program. Results were expressed as mean ± SEM and paired *t* test was used to assess differences between WT and *Irs2*$^{-/-}$. * p<0.05, ** p<0.01, and *** p<0.001. N=12 mice for each genotype. Representative images were captured using a 20x objective. The scale bar represents 50µm.

4.2. *Irs2*-deficiency is associated with enhanced expression of cytokines and markers of inflammation

Obesity is associated with low-grade chronic inflammation attributed to the dysregulated production and release of cytokines and adipokines (Barbosa-da-Silva et al., 2012). Consistent with published results (Burks et al., 2000), leptin levels of *Irs2*-deficient females were elevated (Figure 21). Serum adiponectin levels were enhanced approximately 2-fold as compared with WT control females. However, a reduction in serum resistin was observed in *Irs2*$^{-/-}$ females. The role of resistin in obesity remains controversial (Schwartz and Lazar, 2011) but some studies suggest that this cytokine activates the anti-inflammatory mediator SOCS3 in rodent WAT (Steppan et al., 2001, Steppan et al., 2005). SOCS3 is known to decrease insulin signaling in adipose and other tissues.

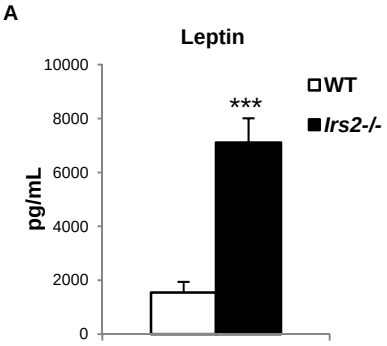

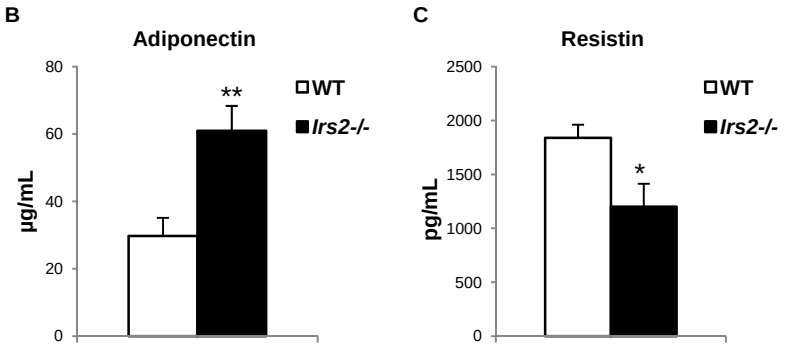

Figure 21: Adipokines serum levels in WT and *Irs2*$^{-/-}$ mice.
A, B, C) Serum was obtained from blood samples and adipokines were measure with Luminex® technology. Results were expressed as mean ± SEM. * p<0.05, ** p<0.01 and *** p<0.001. N=8 mice of each genotype.

To confirm the results obtained by measuring hormones in serum with Luminex®, RT-PCR was used to assess the mRNA expression of various adipokines in V and SC WAT. All results were normalized to the expression in V-WAT of WT mice (100% of expression). As observed in serum, adiponectin expression (*Adipoq*) was up-regulated in V and SC WAT of *Irs2*$^{-/-}$ when the expression is compared with WT V-WAT (Figure 22). Resistin was decreased in *Irs2*$^{-/-}$, confirming the results obtained from serum samples. It was not possible to measure some obesity-associated molecules with Luminex® technology because the serum values were near the lower limits of detection. Thus, Retinol Binding Protein 4 (*Rbp4*), Interleukin 6 (*IL6*), Tumor necrosis factor α (*Tnfα*), and Monocyte Chemotactic Protein 1 (*Mcp1*) were assessed by RT-PCR. RBP4, expressed mainly by adipocytes, was increased in *Irs2*$^{-/-}$ V-WAT but reduced in *Irs2*$^{-/-}$ SC-WAT (Figure 22).

Adipocytes express low levels of MCP1 but the adipose tissue of obese humans contains increased numbers of macrophages, and once activated, these macrophages are responsible for the expression of cytokines such as TNFα, IL6, and MCP1 (Vykoukal and Davies,

2011). The expression of IL6 was greater in V-WAT and SC-WAT of *Irs2*-deficient mice than in WT controls (Figure 22). IL6 impairs insulin signaling in the liver and adipocytes by inducing ubiquitin-mediated degradation of insulin receptor substrate through SOCS 1 and 3 (Kristiansen and Mandrup-Poulsen, 2005). The expression of TNFα is also up-regulated in V-WAT but not SC-WAT of *Irs2*-deficient females. However, it should be noted that the expression of TNFα is drastically higher in SC-WAT than V-WAT in animals of both genotypes (Figure 22). This may reflect contamination with lymph nodes in the SC samples. In adipose tissue, TNFα is mostly secreted by macrophages in the stroma vascular fraction (SVF) and circulating TNFα and adipose tissue TNFα gene expression are increased in insulin resistance (Kern et al., 2001). MCP1 is a chemoattractant that plays an important role in the recruitment of macrophages to the adipose tissue (Sartipy and Loskutoff, 2003, Kanda et al., 2006). Obesity is associated with increased plasma levels of MCP1 and overexpression in adipose tissue (Di Gregorio et al., 2005). MCP1 was increased in V-WAT of *Irs2*$^{-/-}$ mice but the expression was equivalent between genotypes in SC-VAT. Mice lacking MCP1 receptor (CCR2) have decreased adipose tissue macrophage infiltration and improved metabolic function (Weisberg et al., 2003, Kanda et al., 2006).

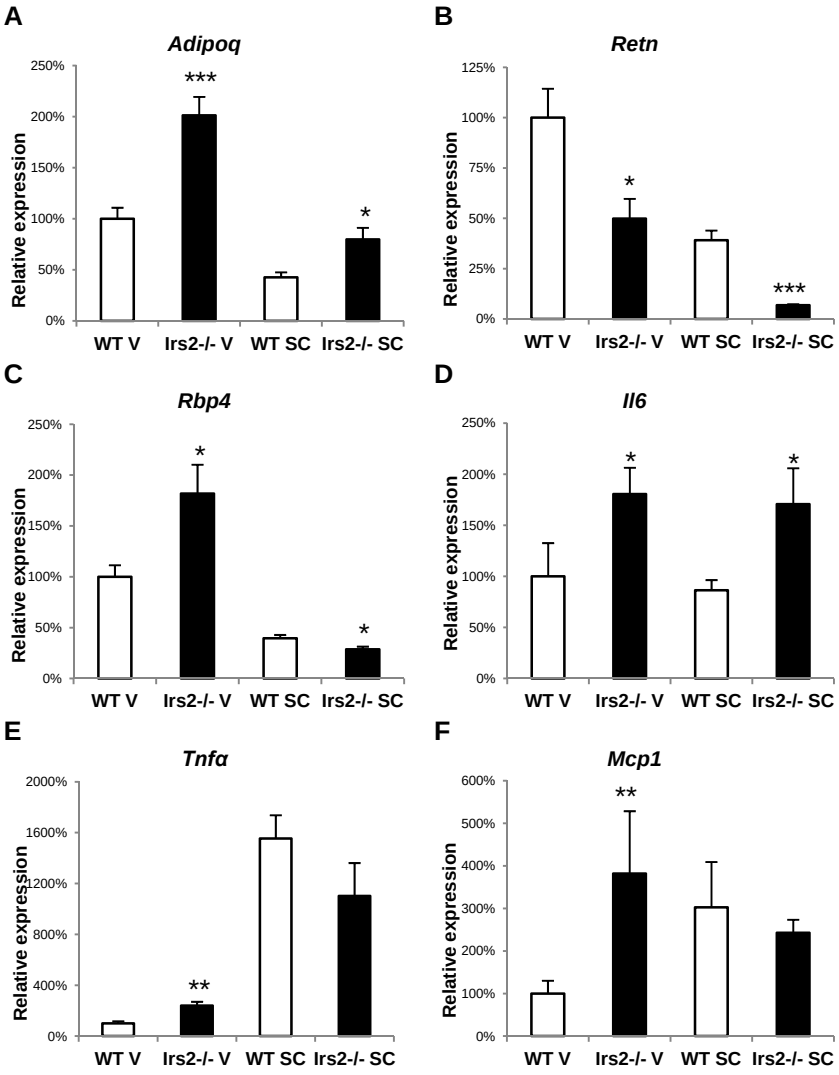

Figure 22: Gene expression studies of adipokines in WAT from WT and *Irs2*$^{-/-}$. Total RNA was extracted from V and SC-WAT with Trizol®. RT-PCR was performed using TaqMan probes for the indicated genes. Each reaction was performed in duplicate and the value of the gene of interest was normalized to the expression of Ubiquitin C. Data was analyzed by the comparative Ct method ($2^{-\Delta\Delta Ct}$) (Livak and Schmittgen, 2001). Results are expressed as mean ± SEM. * $p<0.05$, ** $p<0.01$ and *** $p<0.001$. For data presentation, V-WAT of WT mice was considered as 100%. N= 5 mice of each genotype. Relative gene expression of Adiponectin (**A**), Resistin (**B**), Retinol Binding Protein 4 (**C**), Interluekin 6 (**D**), Tumor necrosis factor α (**E**) and Monocyte Chemotactic Protein 1 (**F**) are shown in the graphs.

Osteopontin (*Spp1*, OPN) is a multifunctional protein expressed in activated macrophages and T cells that may also play an important role in the inflammatory process in WAT (Mazzali et al., 2002, Standal et al., 2004). OPN is a T helper type 1 (Th1) cytokine and has been shown to be involved in monocyte/macrophage migration and activation (Zeyda et al., 2011). In the *Irs2* knockout model, no differences were detected in the expression of OPN in either source of WAT (Figure 23). Another macrophage marker implicated in obesity-related adipose inflammation is the glycoprotein F4/80 (*Emr1*). This marker was up-regulated in V-WAT of *Irs2*-deficient females but not in SC-WAT (Figure 23), perhaps reflecting the fact that macrophage infiltration occurs to a larger extent in visceral fat.

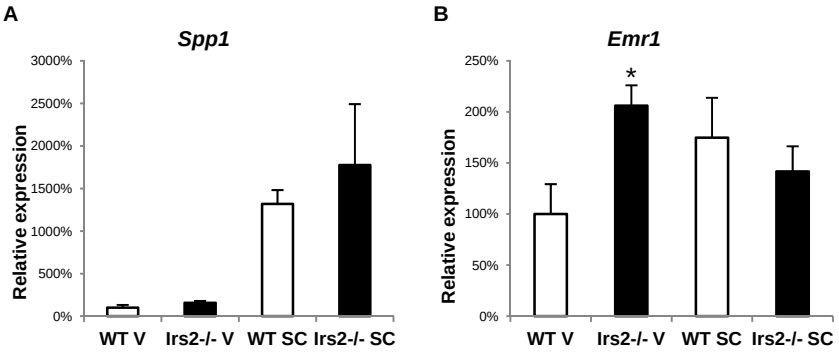

Figure 23: Gene expression studies of osteopontin and F4/80 in WAT from WT and *Irs2*$^{-/-}$.
Total RNA was extracted from V and SC-WAT with Trizol®. RT-PCR was performed using TaqMan probes for the indicated genes. Each reaction was performed in duplicate and the value of the gene of interest was normalized to the expression of Ubiquitin C. Data were analyzed by the comparative Ct method ($2^{-\Delta\Delta Ct}$) (Livak and Schmittgen, 2001). Results are expressed as mean ± SEM. * p<0.05, ** p<0.01 and *** p<0.001. For data presentation, V-WAT of WT mice was considered as 100%. N= 5 mice of each genotype. Relative gene expression of osteopontin (**A**) and F4/80 (**B**) are shown in the graphs.

Another mechanism involved in obesity-induced inflammation is the presence of lymphocytes and leukocytes in WAT, chiefly cytotoxic T lymphocytes. CD45 (*Ptprc*), also called leukocyte common antigen, was increased in V-WAT of *Irs2*-deficient mice but no differences were

observed between genotypes with respect to SC-WAT (Figure 24). CD3 together with the T-cell receptor alpha/beta and gamma/delta heterodimers forms the T-cell receptor-CD3 complex (Alarcon et al., 1988, Blumberg et al., 1990). The expression of CD3 was similar between WAT of WT and *Irs2*$^{-/-}$. CD8 is a transmembrane glycoprotein that serves as a co-receptor for the T cell receptor (Gao and Jakobsen, 2000). The expression of this marker was enhanced in V-WAT, but not SC-WAT, from *Irs2*$^{-/-}$ when compared to control mice.

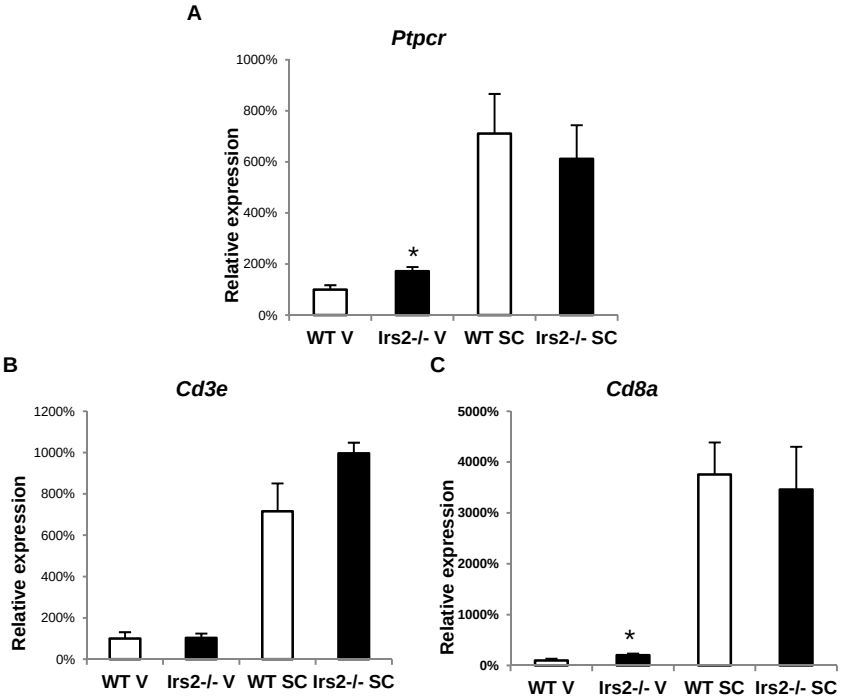

Figure 24: Gene expression studies of lymphocytes markers in WAT of WT and *Irs2*$^{-/-}$.
Total RNA was extracted from V and SC-WAT with Trizol®. RT-PCR was performed using TaqMan probes for the indicated genes. Each reaction was performed in duplicate and the value of the gene of interest was normalized to the expression of Ubiquitin C. Data was analyzed by the comparative Ct method ($2^{-\Delta\Delta Ct}$) (Livak and Schmittgen, 2001). Results are expressed as mean ± SEM. * p<0.05, ** p<0.01 and *** p<0.001. For data presentation, V-WAT of WT mice was considered as 100%. N=5 mice of each genotype. Relative gene expression of leukocyte marker CD45 (**A**), CD3 (**B**), and CD8 (**C**) are shown in the graphs.

4.3. Markers of hypoxia are up-regulated in WAT of *Irs2*$^{-/-}$ females

Hypoxia is a pathogenic state whereby the surrounding tissue is devoid of an adequate supply of oxygen (Semenza, 2000, Hosogai et al., 2007). Local hypoxia is observed in WAT of obese mice and human subjects. It has been proposed (Kabon et al., 2004, Pasarica et al., 2009, Wood et al., 2009) that hypoxia may occur as a result of adipocyte hypertrophy which reduces the O_2 supply from the vasculature, thereby triggering an inflammatory response associated with expression of the transcription factor hypoxic inducible factor-1 (*Hif1α*) and Vascular endothelial growth factor A (*Vegfa*). Thus, hypoxia-induced inflammation represents a potential underlying cause of ATM infiltration in WAT (Finucane et al., 2012). Consistent with this, the expression of *Hif1a* was significantly up-regulated in V-WAT of *Irs2*-deficient mice. *Vegfa* expression was augmented in both V-WAT and SC-WAT when compared to WT control samples (Figure 25).

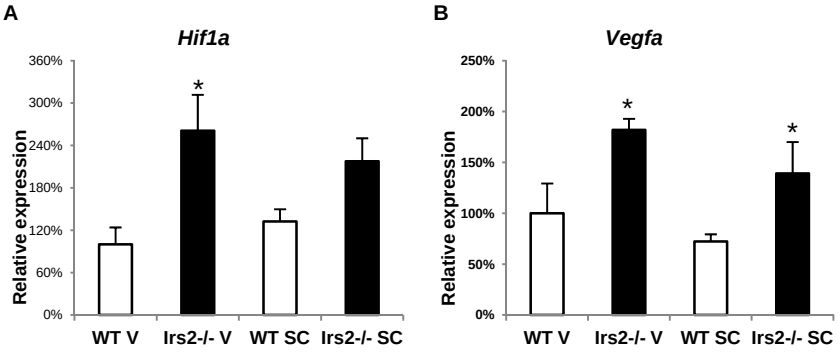

Figure 25: Gene expression studies of hypoxia markers in WT and *Irs2*$^{-/-}$ WAT.
Total RNA was extracted from V and SC-WAT with Trizol®. RT-PCR was performed using TaqMan probes for the indicated genes. Each reaction was performed in duplicate and the value of the gene of interest was normalized to the expression of Ubiquitin C. Data was analyzed by the comparative Ct method ($2^{-\Delta\Delta Ct}$) (Livak and Schmittgen, 2001). Results are expressed as mean ± SEM. * $p<0.05$, ** $p<0.01$ and *** $p<0.001$. For data presentation, V-WAT of WT mice was considered as 100%. N=5 mice of each genotype. Relative gene expression of Hypoxic inducible factor α (**A**) and vascular endothelial growth factor A (**B**) are presented in the graphs.

4.4. Expression of insulin signaling genes

Inflammatory events decrease the sensitivity to insulin in obese patients (Zeyda et al., 2011, Kiefer et al., 2010, Hotamisligil, 2003, Hotamisligil, 2006). Elevated serum concentrations of proinflammatory impairs insulin-signaling and thus, decreases insulin sensitivity in many tissues, including WAT (Belkina and Denis, 2010). Given the presence of moderate obesity and insulin resistance in the *Irs2* model, RT-PCR analysis of some components of the insulin pathway was performed from both WAT sources. *Irs1* and *Irs3* were increased in V-WAT but not SC-WAT of *Irs2*$^{-/-}$ mice as compared to WT controls (Figure 26). However, the expression of *Insr* (IRβ) was equivalent between V and SC-WAT of both experimental groups. The expression of glycogen synthase kinase 3 (GSK3β), a negative regulator of insulin signaling (Cross et al., 1995, Sharfi and Eldar-Finkelman, 2008, Boura-Halfon and Zick, 2009), was enhanced in both WAT depots of *Irs2*-deficient mice (Figure 26).

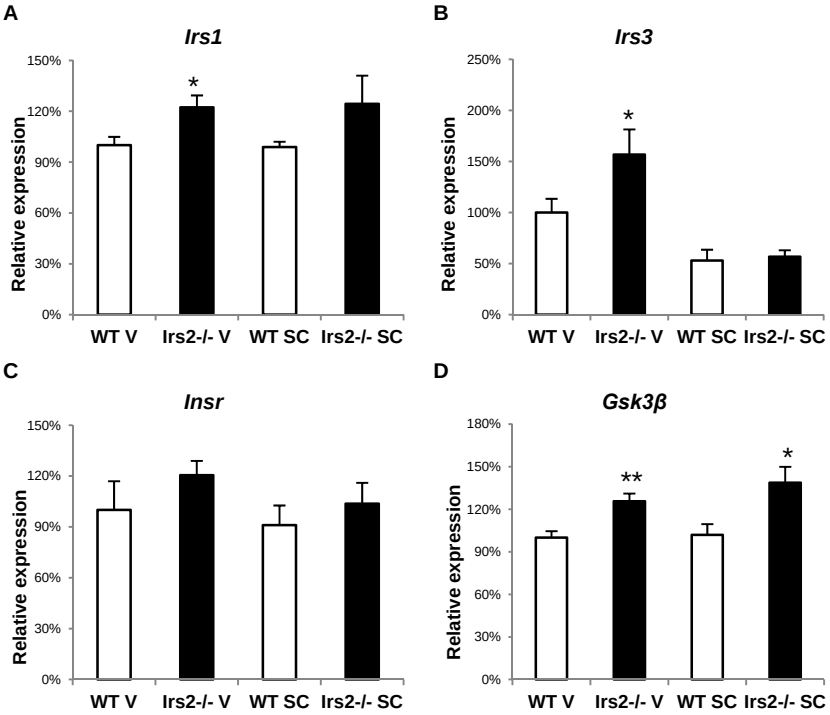

Figure 26: Gene expression analysis of insulin signalling components of WAT from WT and *Irs2*$^{-/-}$.
Total RNA was extracted from V and SC-WAT with Trizol®. RT-PCR was performed using TaqMan probes for the indicated genes. Each reaction was performed in duplicate and the value of the gene of interest was normalized to the expression of Ubiquitin C. Data was analyzed by the comparative Ct method ($2^{-\Delta\Delta Ct}$) (Livak and Schmittgen, 2001). Results are expressed as mean ± SEM. * $p<0.05$, ** $p<0.01$ and *** $p<0.001$. For data presentation, V-WAT of WT mice was considered as 100%. N= 5 mice of each genotype. Insulin receptor substrate 1 (**A**), Insulin receptor substrate 3 (**B**), Insulin receptor (**C**) and glycogen synthase kinase 3 (**D**).

4.5. Adipogenesis-related genes are altered in WAT from *Irs2*-deficient mice

Nuclear receptors are key regulators of adipogenesis as they form platforms for co-activator proteins and regulate the assembly of these cofactors into protein complexes on specific DNA sequences (Glass et al., 1997, Spiegelman, 1998, Moras and Gronemeyer, 1998, Wu et al.,

1999, Glass and Rosenfeld, 2000). Peroxisome proliferator activated receptor-γ (*Pparg*) is a nuclear hormone receptor that promotes the conversion of preadipocytes into fully differentiated adipocytes, including cell growth arrest, triglyceride accumulation, and improved insulin sensitivity (Walkey and Spiegelman, 2008). *Pparγ* expression was increased in both V-WAT and SC-WAT of *Irs2*-deficient mice as compared with control mice (Figure 27). Some co-activators have histone acetyltransferase activity that functions to 'open' the configuration of chromatin, allowing more efficient transcription (Puigserver and Spiegelman, 2003). Several co-activators, such as PPARγ co-activator‑1α (PGC-1α, gen *Ppargc1a*) enhance the activity of PPARγ. Consistent with attenuated expression of *Pparg,* the gene for PGC-1α was also down-regulated in WAT of *Irs2*$^{-/-}$ (Figure 27). PGC1α is crucial for liver gluconeogenesis and the altered expression of this co-activator has been implicated in hepatic insulin resistance of *Irs2*-deficient mice (Dong et al., 2006, Dong et al., 2008, Guo et al., 2009). Sterol Regulatory Element Binding Protein (SREBP) 1c (*Srebf1*) has emerged as a major protein involved not only in the regulation of genes related with carbohydrate and lipid metabolism in the liver, but also in adipose tissue, muscle and pancreatic beta cells (Tontonoz et al., 1993, Brown and Goldstein, 1997). *Srebf1* mediates the effects of insulin on gene expression and thus, favours glucose utilization and glycogen synthesis, as well as lipid synthesis from glucose and triglyceride storage into adipocytes (Kim et al., 1998, Fajas et al., 1999). This expression of this gene was increased significantly in V-WAT of *Irs2*$^{-/-}$ (Figure 27). Up-regulation of *Srebf1* may reflect an effort to increase lipid storage or alternatively, may represent the effects of chronic hyperinsulinemia in *Irs2*-deficient mice.

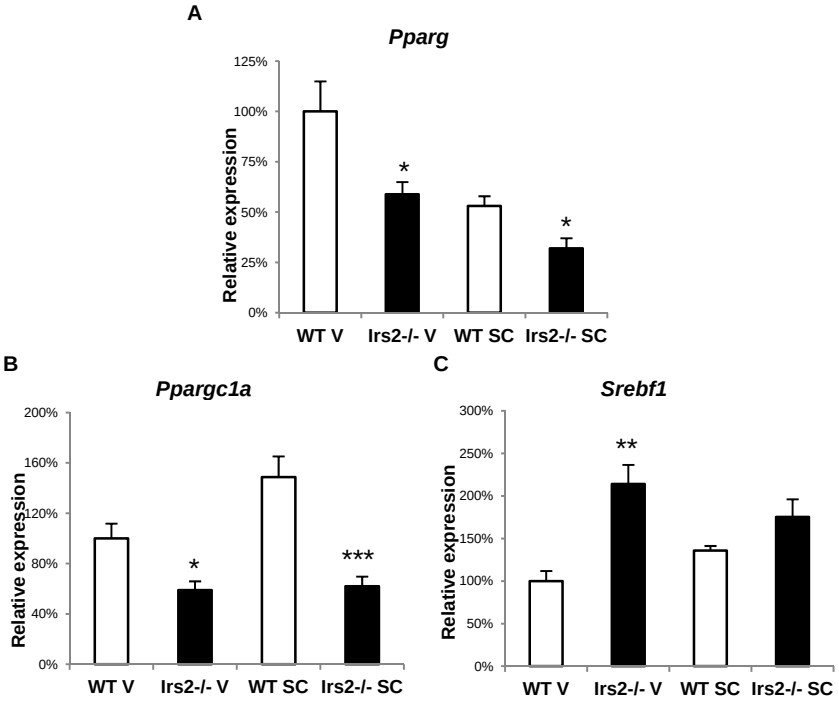

Figure 27: Gene expression of adipogenesis markers in WT and *Irs2*$^{-/-}$ WAT.
Total RNA was extracted from V and SC-WAT with Trizol®. RT-PCR was performed using TaqMan probes for the indicated genes. Each reaction was performed in duplicate and the value of the gene of interest was normalized to the expression of Ubiquitin C. Data was analyzed by the comparative Ct method ($2^{-\Delta\Delta Ct}$) (Livak and Schmittgen, 2001). Results are expressed as mean ± SEM. * $p<0.05$, ** $p<0.01$ and *** $p<0.001$. For data presentation, V-WAT of WT mice was considered as 100%. N= 5 mice of each genotype. Relative gene expression of Peroxisome proliferator activated receptor-γ (**A**), PPARγ co-activator‑1α (**B**) and Sterol Regulatory Element Binding Protein 1c (**C**) are presented in the graphs.

One of the targets of PPARγ, the *Fabp4* gene encoding fatty acid binding protein (FABP4 or aP2), was increased in the *Irs2*$^{-/-}$ model, perhaps reflecting some compensation mechanism. Adipsin (*Adn*) and Fatty Acid Synthase (*Fasn*) are acquired during differentiation to mature adipocytes (Choy et al., 1992, Spiegelman et al., 1993) and both were down-regulated in both types of WAT from *Irs2*-deficient mice (Figure 28). A decrease of *Adn* and *Fasn* has been described in

other obesity models (Lowell et al., 1990). GLUT4 (*Slc2a4*), the main glucose transporter present in WAT, was increased in V-WAT but not SC-WAT of *Irs2*$^{-/-}$ females.

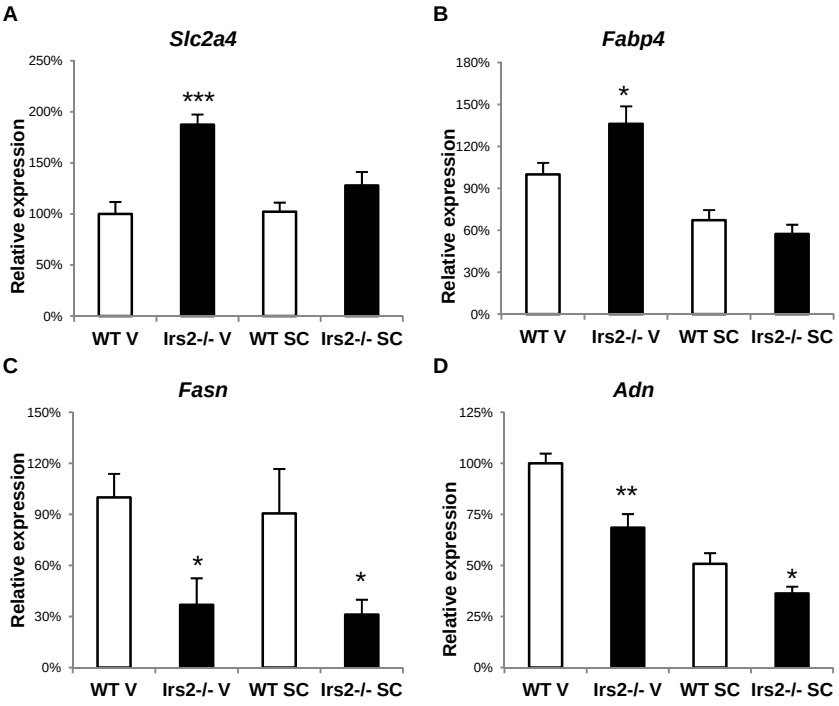

Figure 28: Gene expression of PPARγ targets in WT and *Irs2*$^{-/-}$ WAT.
Total RNA was extracted from V and SC-WAT with Trizol®. Real Time PCR was performed using TaqMan probes for the indicated genes. Each reaction was performed in duplicate and the value of the gene of interest was normalized to the expression of Ubiquitin C. Data was analyzed by the comparative Ct method ($2^{-\Delta\Delta Ct}$) (Livak and Schmittgen, 2001). Results are expressed as mean ± SEM. * $p<0.05$, ** $p<0.01$ and *** $p<0.001$. For data presentation, V-WAT of WT mice was considered as 100%. N= 5 mice of each genotype. Relative gene expression of Glucose transporter 4 (**A**), Fatty Acid Binding Protein 4 (**B**), Fatty acid synthase (**C**) and Adipsin (**D**) are shown in the graphs.

Synthesis of triacylglycerol (TG) involves acyl CoA diacylglycerol acyltransferase (*Dgat*) enzymes, which catalyze a reaction with diacylglycerol and fatty acid (FA) acyl CoA substrates (Bell and Coleman, 1980, Cases et al., 1998). Cellular TG storage is directly

correlated with levels of DGAT activity. Interestingly, DGAT1 expression in adipocytes and WAT is regulated by PPARγ activation (Sugii et al., 2009). However, although PPARγ expression is reduced in *Irs2*$^{-/-}$ mice, only *Dgat1* expression from SC-WAT was reduced in *Irs2*-deficient mice and it was equivalent between V-WAT samples of both genotypes (Figure 29). In sharp contrast, *Dgat2* was enhanced in both V and SC WAT of *Irs2*$^{-/-}$ females as compared to WT controls.

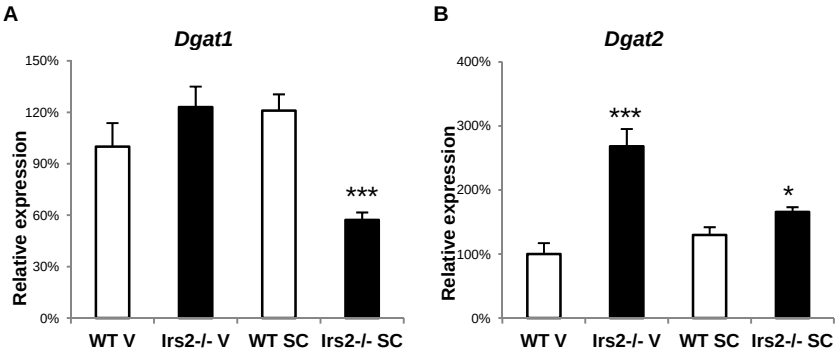

Figure 29: Gene expression of TG synthesis in WT and *Irs2*$^{-/-}$ WAT.
Total RNA was extracted from V and SC-WAT with Trizol®. Real Time PCR was performed using TaqMan probes for the indicated genes. Each reaction was performed in duplicate and the value of the gene of interest was normalized to the expression of Ubiquitin C. Data was analyzed by the comparative Ct method ($2^{-\Delta\Delta Ct}$) (Livak and Schmittgen, 2001). Results are expressed as mean ± SEM. * $p<0.05$, ** $p<0.01$ and *** $p<0.001$. For data presentation, V-WAT of WT mice was considered as 100%. N= 5 mice of each genotype. Relative gene expression of acyl CoA diacylglycerol acyltransferase 1 (**A**) and acyl CoA diacylglycerol acyltransferase 2 (**B**) are presented.

4.6. Adipocyte progenitor cells (APCs) are increased in V-WAT of *Irs2*$^{-/-}$ mice

The development of insulin resistance and its complications are related with abdominal adipose tissue accumulation and adipocyte enlargement rather than peripheral obesity, which is usually associated with a recruitment of new preadipocytes (hyperplasia) (Isakson et al., 2009). Since mature adipocytes are postmitotic

(Simon, 1965), adipocyte hyperplasia in adults requires that new adipocytes be produced from the differentiation of precursor cells. Previous reports have shown that cells derived from the stroma-vascular fraction (SVF) of WAT from mice and humans can differentiate into several lineages, including adipocytes (Zuk et al., 2002). Based on results presented above, the increased adiposity observed in *Irs2*$^{-/-}$ females is not due to cell hypertrophy since adipocyte size was similar to control mice. Alternatively, the moderate obesity of this model might be due to increased production of new adipocytes from APC.

4.6.1. Establishment of FACS method for isolation of APC

To assess the effects of *Irs2*-deficiency on APCs, a FACS-based strategy was developed to isolate this population of cells from SVF preparations of V-WAT and SC-WAT (Figure 30). WAT was digested enzymatically to obtain the SVF fraction which was then sorted based on lack of expression of CD45 (hematopoietic marker), CD31 (endothelial marker) and Ter119 (erythroid marker) to obtain a negative lineage (Lin$^-$). The Lin$^-$ subpopulation was further separated based on expression of stem cell antigen 1 (Sca1) and CD34 (preadipocyte/stroma marker), markers that are associated with the population of primary preadipocytes (Rodeheffer et al., 2008, Tang et al., 2008, Joe et al., 2009).

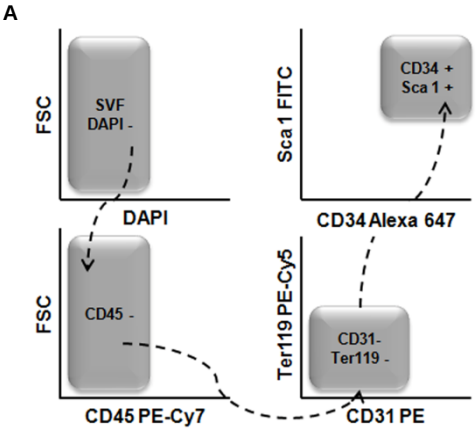

Figure 30: Strategy for APCs isolation by FACS.
After the selection of live cells (DAPI-), the sequential isolation of CD45-, CD31- and Ter119- cells guarantees that all the haematopoietic cells (CD45+), endothelial cells (CD31+) and erythroid cells (Ter119+) are discarded from the selected fraction. The population was then selected positively for CD34 and Sca1.

The population resulting from the FACS strategy displayed the following characteristics: CD45- CD31- Ter119- CD34+ Sca-1+. These cells were recovered from the Cell Sorting MoFlo and corrected to the weight of the starting material (grams of WAT). The APC population obtained from *Irs2*$^{-/-}$ V-WAT was 2.5-fold higher than WT but there were no significant differences between genotypes in the APC isolated from SC-WAT (Figure 31). After cell sorting the cells were plated and the primary culture was established as show the pictures

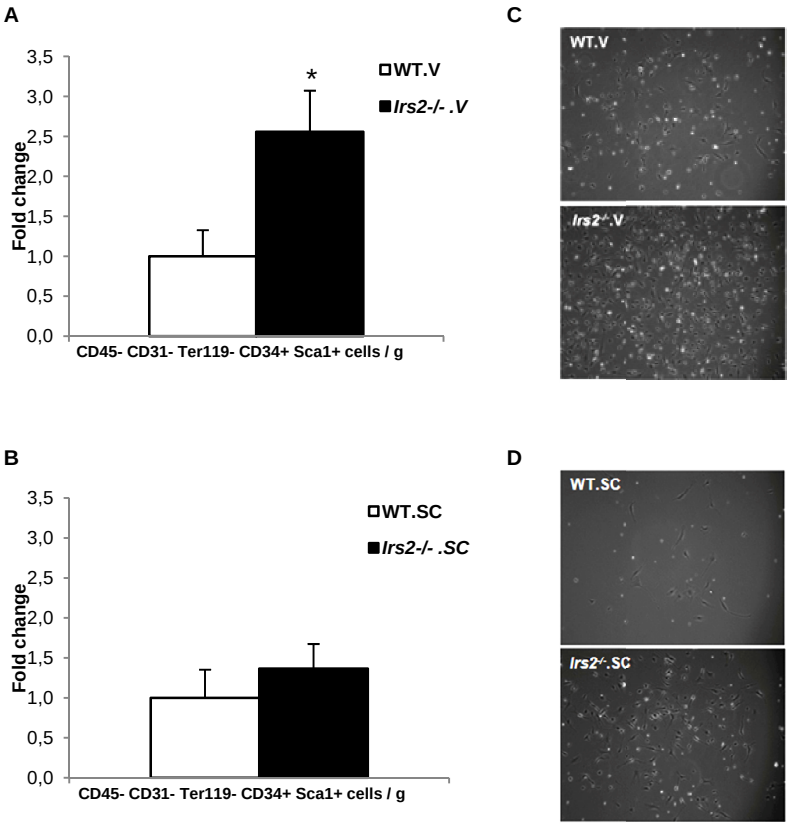

Figure 31: Quantification of APC from WT and *Irs2*$^{-/-}$ WAT.
Quantification of APC from V-WAT (**A**) and SC-WAT (**B**) obtained with FACS strategy. Results were corrected for weight of original WAT sample and then compared to WT V-WAT which was assigned the value of 1. Shown are representative phase contrast images of APC after FACS isolation from V-WAT (**C**) and SC-WAT (**D**). Results are expressed as mean ± SEM. * p<0.05, ** p<0.01 and *** p<0.001. N=3 mice of each genotype were used to generate the SVF and five independent isolation experiments were analyzed.

4.6.2. FACS reveals an increase of inflammatory cells in WAT of *Irs2*$^{-/-}$ mice

Based on the expression profile of inflammatory-related genes in WAT obtained from RT-PCR, the FACS data were used to estimate cell populations that might correlate with the observed gene changes. Thus, after selection for live cells (DAPI-), CD45+ (marker of

hematopoietic lineage) CD34- (stroma/preadipocyte cell marker) and Sca1- (stem cell marker) (Figure 32) were isolated from the SVF fractions of both V and SC WAT.

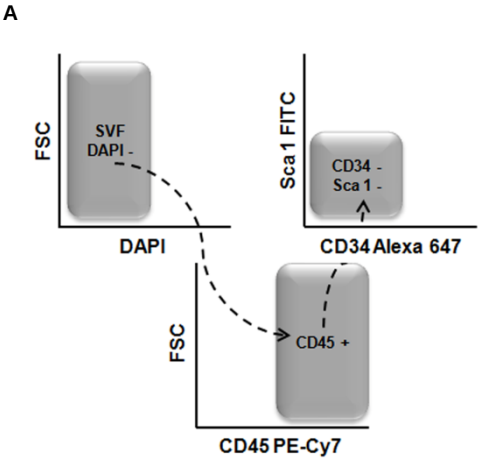

Figure 32: Scheme for FACS isolation of inflamation-related cells.
After the selection of the live cells (DAPI-), the isolation of CD45+ cells enriches for haematopoietic cells in the selected fraction. Negative selection for CD34 - and Sca1 - cells eliminates adult stem cells.

The population CD45+CD34-Sca1- was normalized to cells per gram of WAT and was 3-fold higher in V-WAT from *Irs2*$^{-/-}$, whereas this population isolated from SC-WAT was equivalent between genotypes (Figure 33).

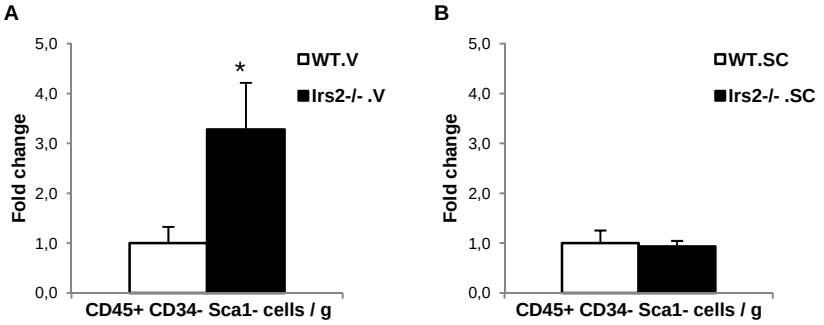

Figure 33: Quantification of inflammatory-related cells in WT and *Irs2*$^{-/-}$ WAT.
The CD45+ CD34- Sca1- population was isolated from the SVF fraction of V-WAT (**A**) and SC-WAT (**B**) as outlined in Figure 32. Results are expressed as mean ± SEM. * p<0.05, ** p<0.01 and *** p<0.001. N=3 mice of each genotype were used to generate the SVF and five independent isolation experiments were analyzed.

4.6.3. Validation of FACS strategy and long-term maintenance of APC phenotype

To confirm that the population obtained by the FACS strategy indeed represented APCs, Western blotting was performed to assess expression of an independent marker of adult adipose stem cells, the platelet-derived growth factor (PDGF) receptor. PDGFRβ is considered one of the main markers in adult stem cells from WAT since it is involved in the angiogenesis when new cells are differentiated from the precursors (Carmeliet, 2003, Armulik et al., 2005, Tang et al., 2008). After APC differentiate to a mature adipocyte, expression of PDGFRβ is drastically reduced. Consistent with this, PDGFRβ was expressed in only the APC population (CD45- CD31- Ter119- CD34+ Sca1+) isolated from both genotypes (Figure 34).

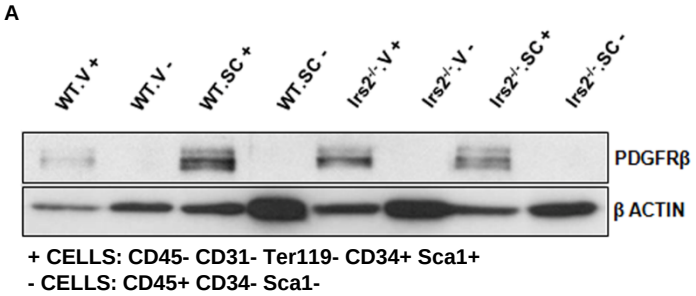

Figure 34 : Western blot analysis of APC obtained by FACS from WAT of WT and *Irs2*$^{-/-}$ mice.
Sorted cells were lysed and protein was extracted for Western blot analysis of APC marker PDGFRβ. βActin was used as a loading control. PDGFR: platelet-derived growth factor receptor.

To ensure that when cultured *in vitro* the APC population maintained a stem cell phenotype, FACS was repeated after culturing the SVF preparation for five days and compared to cells freshly isolated from SVF. The percentage of non-stem cell populations was higher in fresh preparations than when the SVF was cultured one week (DMEM + 10% FcBS + 10ng/mL βFGF). The CD45+ CD31+ Ter119+ cells basically disappeared when the cells were cultured (Figure 35B). Thus, the CD34+ Sca1+ population represented almost 90% of the cells in culture.

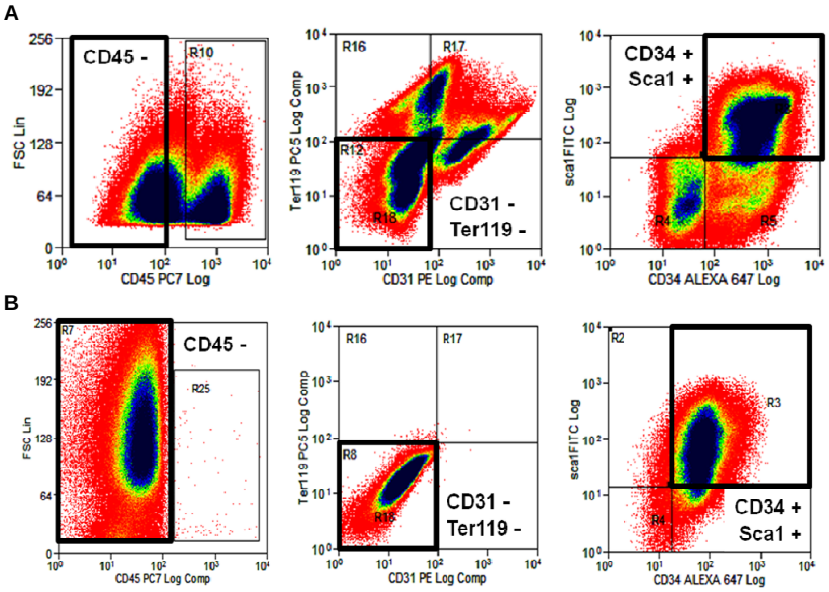

Figure 35: Comparison of FACS analysis from freshly isolated SVF or after 5 days in culture.
(**A**) FACS analysis of SVF directly isolated from the WAT. (**B**) FACS analysis of isolated APC after one week of culture. Enrichment of CD34+ Sca1+ population was approximately 90%.

4.7. Adipogenesis is impaired in *Irs2*-deficient APC

4.7.1. Characterization of WAT maturation in vivo

To validate the RT-PCR results of adipogenesis markers and to obtain biologically relevant profile of protein expression changes during the adipogenic program, WAT from 4-week old mice (recently weaned) was compared with WAT from 8-week old mice by Western blotting. This analysis revealed that the expression of IRS2 increased dramatically in V-WAT of WT mice but remained constant in SC-WAT during this time period (Figure 36). Interestingly, IRS2 was expressed equally in V and SC- WAT of WT animals. As expected, IRS2 was not detected in *Irs2*$^{-/-}$ samples. A slight increase of IRS1 expression was

detected from 4 to 8 weeks but expression of IRS3 as well as IRβ remained constant in both genotypes. Consistent with RT-PCR results, Glut4 was up-regulated V-WAT of *Irs2*-deficient mice (see Figure 28 and Figure 36). The expression of various proteins involved in the adipocyte metabolism was reduced in WAT from *Irs2*$^{-/-}$ mice including hormone sensitive lipase (HSL) and the leptin receptor (ObR). Concerning proteins with a clear role in the adipogenesis, PPARγ expression was increased in WAT of WT mice at 8-weeks of age compared to 4-week old mice. However, the expression of PPARγ was greatly reduced in *Irs2*-deficient WAT at both time points, consistent with qPCR data (see Figure 27 and Figure 36).

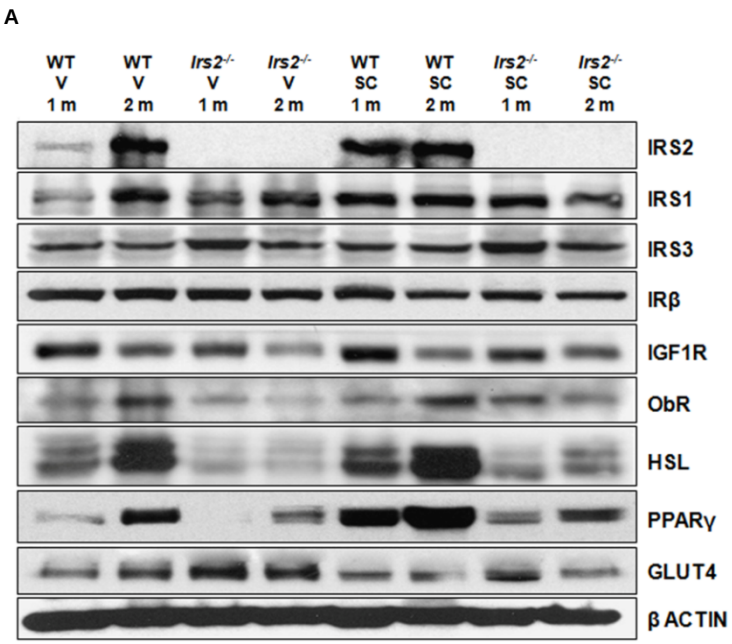

Figure 36: Western blot from WAT of 4 and 8 weeks old WT and *Irs2*$^{-/-}$ mice.
WAT from 4 and 8-week old mice was lysed and Western blot analysis was performed for IRS proteins and the main regulators markers of adipogenesis. β-actin was used as a loading control. IRS2, insulin receptor substrate 2; IRS1, Insulin receptor substrate 1; IRS3, insulin receptor substrate 3; IRβ, Insulin receptor; IGF1R, insulin growth factor receptor; ObR, leptin receptor, HSL, hormone sensitive lipase; PPARγ peroxisome proliferator-activated receptor gamma; GLUT4, glucose transporter 4.

4.7.2. Differentiation *in vitro* of *Irs2*$^{-/-}$ APC to adipocytes is impaired

Adipocytes are postulated to derive from multipotent mesenchymal stem cells (Pittenger et al., 1999). During the first phase of adipogenesis adult stem cells commit to the adipocyte lineage. In the second phase, which is known as terminal differentiation, the pre-adipocyte acquires the characteristics of mature adipocyte: transport and synthesis of lipids, insulin sensitivity and the secretion of adipocyte-specific proteins (Rosen and Spiegelman, 2000, Rosen and MacDougald, 2006). To examine the role of IRS2 in adipocyte differentiation, APC isolated from SVF were plated (day -3) and cultured until confluent (day 0). Adipocyte differentiation was induced by a standard protocol that employs a cocktail of insulin, glucocorticoids, and isobutylmethylxanthine (see Figure 15 page 93).

At the onset and conclusion of the 10-day differentiation protocol, images were captured to assess the morphology of APC cultures. As expected, all cultures were fully confluent on Day 0 of the protocol. Lipid droplets were observed in cultures of both V and SC APCs isolated from WAT of WT mice (Figure 37 B and F). However, few if any lipid droplets were noted in 10-day cultures of *Irs2*$^{-/-}$ APC, suggesting that adipogenesis might be impaired in WAT of this model (Figure 37 D and H). It is also noteworthy that under the experimental conditions used for this study, the adipogenic differentiation of APC from SC-WAT was higher than V-WAT in control samples.

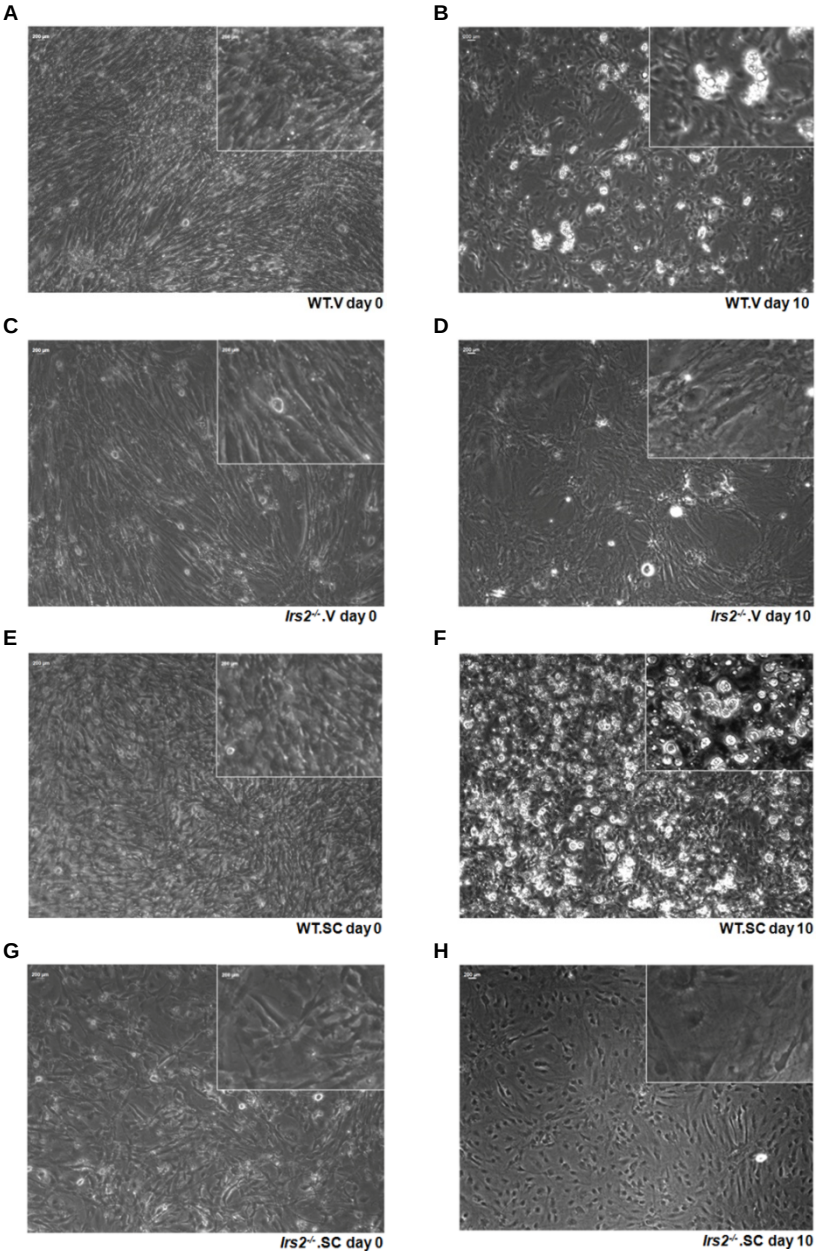

Figure 37: Phase contrast images of APC cultures from WT and *Irs2*$^{-/-}$ WAT subjected to adipocyte differentiation protocol.
Phase contrast images of APC at day 0 and day 10 of adipocyte differentiation. **A,B**) WT V-WAT; **C,D**) *Irs2* V-WAT; **E,F**) WT SC-WAT; **G,H**) *Irs2* SC-WAT. Images were captured with 20x objective and 40x objectives (right of the picture). Representative images from 3 different experiments are shown.

Mature adipocytes are highly specialized for the storage of excess lipid and contain triacylglycerol-rich lipid droplets (Björntorp, 1991a, Henry et al., 2006). Fluorescent lipophilic dyes, which partition into the nonpolar lipid droplet core, are useful lipid droplet markers. Thus, BODIPY 493/503 was used to more precisely quantify the differentiation of APC to adipocytes. Cells were fixed with 4% paraformaldehyde and incubated with BODIPY 493/503 to reveal lipid droplets. At day 0, all cultures were devoid of lipid droplets but after 4 days in adipogenic medium, WT APC display lipid droplets inside the cells as detected by BODIPY staining (Figure 38). Consistent with the results observed using light microscopy, cultures of *Irs2*$^{-/-}$ APC were negative for BODIPY staining, suggestive of impaired adipocyte differentiation. APC isolated from SC-WAT differentiated more efficiently than V-WAT in WT control cultures. It is interesting that the DAPI staining revealed differences in cell and nuclei size between WT and *Irs2*$^{-/-}$ APC.

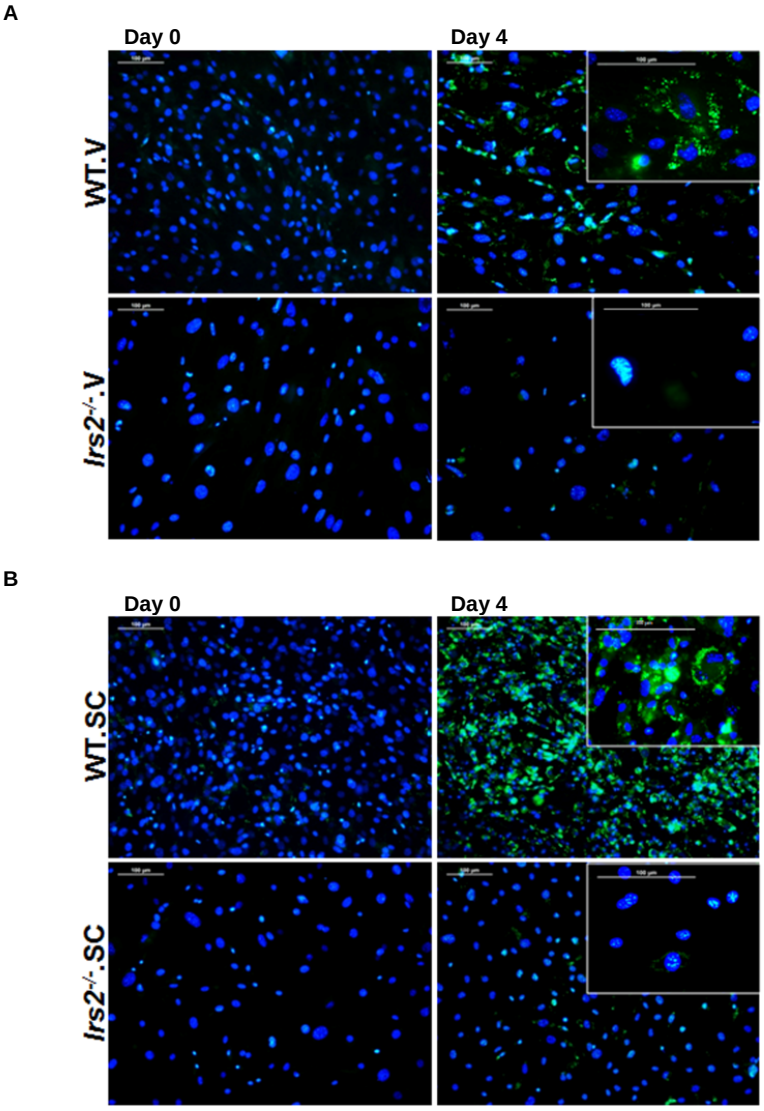

Figure 38: BODIPY staining at day 0 and day 4 of differentiation of APC to adipocytes.
The presence of lipids droplets was detected with BODIPY 493/503 (green). DAPI (blue) was used to reveal cell nuclei. **A**) APC from V-WAT; **B**) APC from SC-WAT. Scale bars represent 100µm.

Flow cytometry analysis was employed to quantify the differentiation of APC to adipocytes. Cells at different points of differentiation program (day 0, 4 and 10) were stained first with BODIPY to preserve lipid droplets. Subsequently, these cells were incubated with anti-Sca-1 antibody to assess loss of this stem cell marker during the differentiation to adipocyte. BODIPY staining was analyzed in linear amplification to estimate the time when the cells started to accumulate lipids. The fluorescence intensity of BODIPY detected in cultures of V-WAT APC from WT was higher at both day 4 and day 10 than *Irs2*$^{-/-}$ cultures (Figure 39). WT acquired lipids faster than *Irs2*$^{-/-}$ since by day 4 the curve is completely shifted to right.

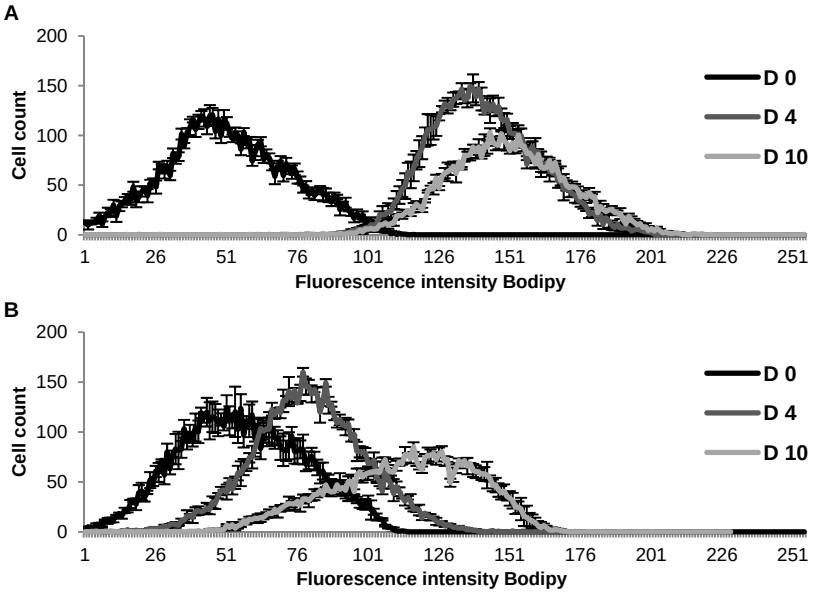

Figure 39: Quantification of BODIPY staining during the time-course of APC differentiation.
Lineal fluorescent intensity in X axis reflects BODIPY staining. (**A**) Differentiation of WT APC from V-WAT at days 0, 4 and 10. (**B**) Differentiation of *Irs2*$^{-/-}$ APC from V-WAT at days 0, 4 and 10. Results were expressed as mean ± SEM. N=3 different primary cell cultures were analyzed.

The profile BODIPY staining during the differentiation time-course was inversely related to Sca1 staining in WT cultures of APC: BODIPY increased steadily with adipocyte differentiation whereas the stem marker Sca1 decreased (Figure 40). However, in cultures of *Irs2*$^{-/-}$ V-APC Sca1 expression was not down-regulated along the course of differentiation and BODIPY staining was significantly lower as compared to V-APC (Figure 40).

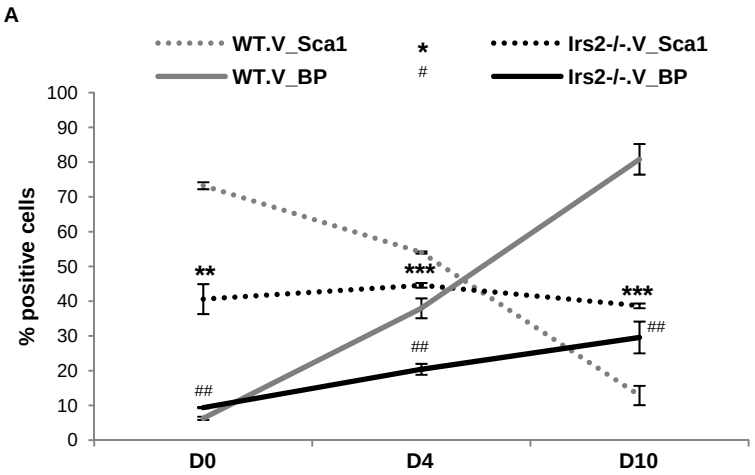

Figure 40: Comparison of BODIPY and Sca1 staining in ADP of APC from V-WAT. The % of total cells positive for BODIPY or Sca-1 was estimated by FACS. Results are expressed as mean ± $*^{/\#}$ p<0.05, $**^{/\#\#}$ p<0.01, and $***^{/\#\#\#}$ p<0.001. N=3 different primary cell cultures were analyzed.

Similar results were obtained with cultures of APC from SC-WAT, although the differences were more pronounced between WT and null samples since the differentiation to adipocytes was generally more efficient in these cultures. Between day 4 and 10, the majority of WT APC were positive for BODIPY, in contrast to *Irs2*$^{-/-}$ SC-WAT where only a limited number of cells contained lipid (Figure 41).

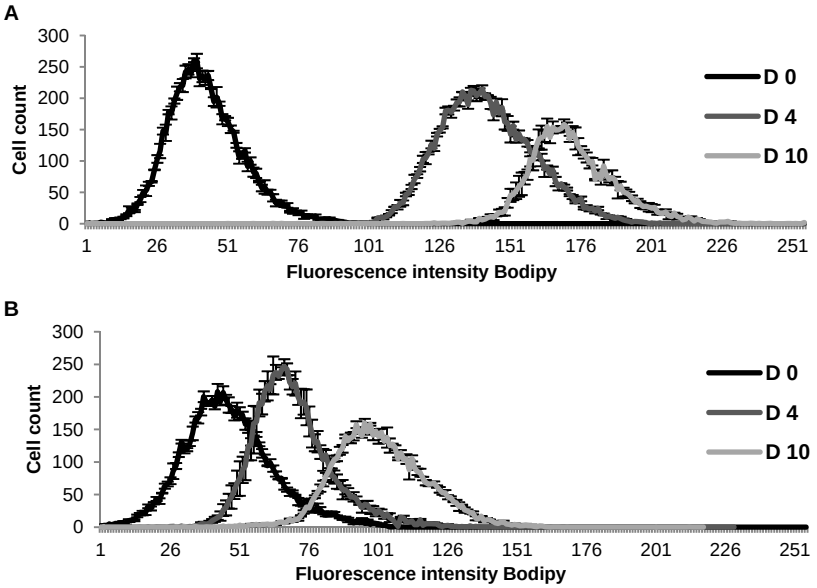

Figure 41: Quantification of BODIPY staining during the time-course of APC differentiation from SC-WAT.
Lineal fluorescent intensity in X axis reflects BODIPY staining. (**A**) Differentiation of WT APC from SC-WAT at days 0, 4 and 10. (**B**) Differentiation of *Irs2*$^{-/-}$ APC from SC-WAT at days 0, 4 and 10. Results were expressed as mean ± SEM. N=3 different primary cell cultures were analyzed.

Sca1 expression declined only slight from day 0 to day 10 in cultures of to *Irs2*$^{-/-}$ SC-WAT, whereas the adipogenic protocol caused a dramatic reduction of this stem marker in WT cultures (Figure 42).

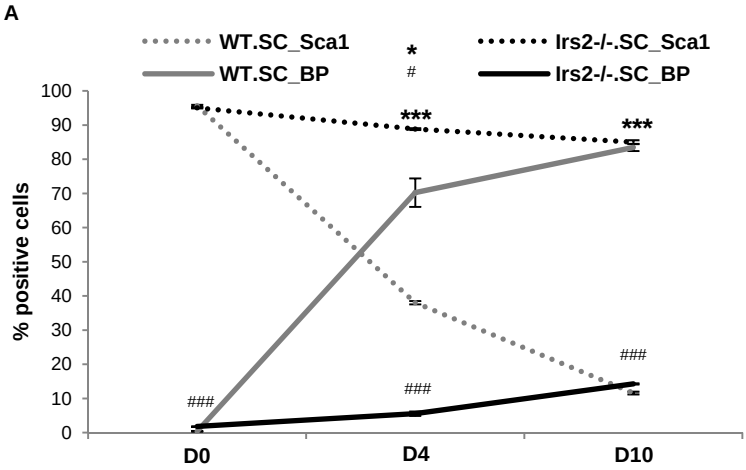

Figure 42: Comparison of BODIPY and Sca-1 staining in ADP of APC from SC-WAT.
The % of total cells positive for BODIPY or Sca-1 was estimated by FACS. Results are expressed as mean ± $*^{/\#}$ p<0.05, $**^{/\#\#}$ p<0.01, and $***^{/\#\#\#}$ p<0.001. N=3 different primary cell cultures were analyzed.

4.7.3. Western blot analysis of APC differentiation

To identify potential molecular mechanisms underlying the differential capacity of WT versus *Irs2*$^{-/-}$ APC to differentiate, Western blot analysis was performed at various time points during the adipogenic protocol. Interestingly, the expression of IRS2 increased significantly from day 0 to day 4 during the differentiation of both V and SC APC isolated from WT mice (Figure 43). Conversely, IRS1 levels decreased from day 0 to day 4, consistent with a role for IRS1 in regulating proliferation. PPARγ and C/EBPα were up-regulated as expected in cultures of WT APC. However, similar to RT-PCR results (see Figure 27), the basal expression of PPARγ was reduced in *Irs2*$^{-/-}$ APC and did not increase during with culture in adipogenic medium. These observations suggest that IRS2 may exert a specific role in promoting the adipogenic program and may explain, in part, the observed failure of *Irs2*$^{-/-}$ APC to differentiate to adipocytes.

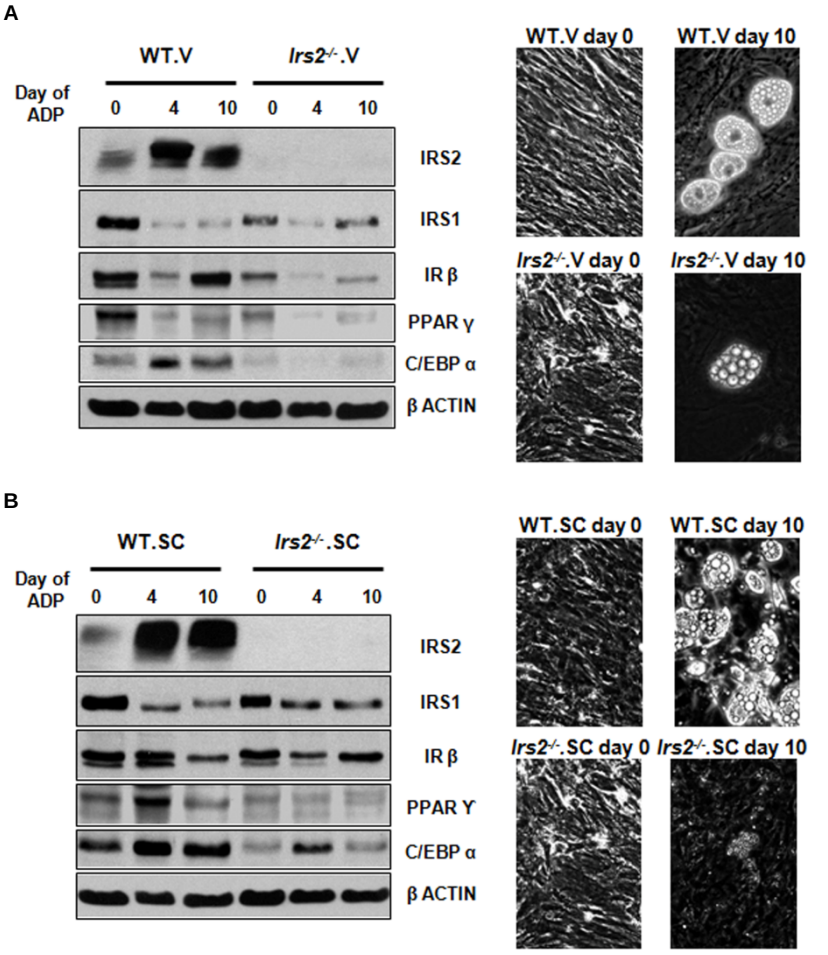

Figure 43: Western blot analysis of Adipocyte differentiation of APC.
APC cultures were harvested at the indicated days during adipocyte differentiation. (**A**) Western blot from differentiation of APC from V-WAT. (**B**) Western blot from differentiation of APC from SC-WAT. Shown is a representative image for 3 differentiation experiments. Anti-β Actin was used to assess protein loading.

4.8. *Irs2*-deficient APCs display altered proliferation in vitro

Proliferation of cells within adipose tissue is influenced both by circulating factors and neuronal inputs as well as by internal controls such as paracrine/autocrine factors secreted from the various cells

within adipose tissue (Hausman et al., 1993, Lau et al., 1996, Serrero and Lepak, 1996, Mohamed-Ali et al., 1998). Studies have shown that conditioned media from adipose tissue of obese subjects stimulates the proliferation of preadipocytes better than do those from lean individuals (Considine et al., 1996). Adipose tissue is a source of growth factors, such as IGF-I, IGF binding proteins, TNFα, angiotensin II, and Macrophage colony-stimulating factor (MCSF).

4.8.1. Characterization of cell growth and estimation of doubling time

Various wells of each culture were plated at the same density and proliferation was assessed by counting the cell number at 24-hour intervals during 5 days. After day 6, most of the cultures were confluent and contact inhibition occurred. Proliferation curves were generated by graphing the number of cells during consecutive days. In both genotypes, the proliferation rate was higher in SC-APC than V-APC (Figure 44). However, starting at day 3 of the analysis cell number was greater in *Irs2*$^{-/-}$ cultures as compared to WT controls. It should be noted that the curves in Figure 44 are not exponential growth curves since primary cultures and need to recover after the isolation procedure before their proliferation starts.

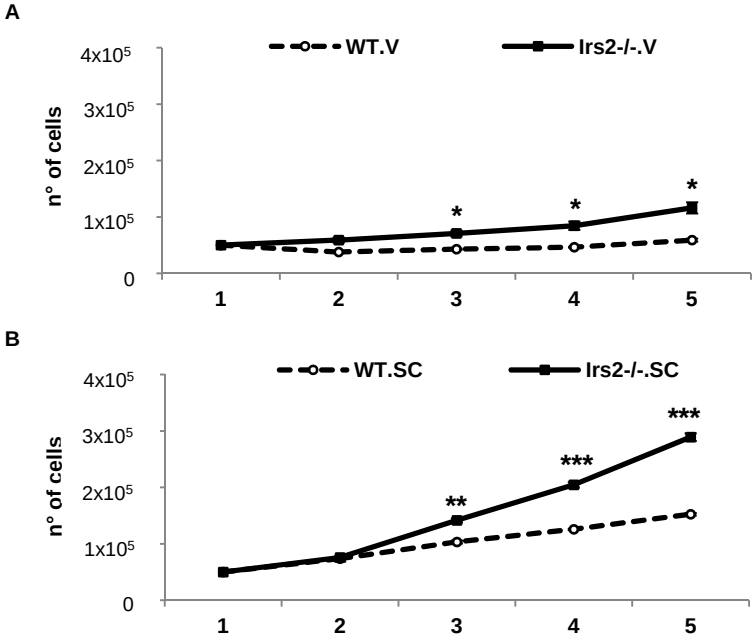

Figure 44: Growth curves estimated from cultures of APC.
APC cultures were harvested and counted on the indicated days from V (**A**) and SC (**B**) WAT. Results were expressed as mean *p<0.05, ** p<0.01 and *** p<0.001. N=3 different primary cell cultures were analyzed.

The doubling time of the various cultures was calculated using the daily cell counts and the online software (http://www.doubling-time.com/compute.php). *Irs2*$^{-/-}$ APC displayed a lower doubling time than WT APC, suggesting that they need less time to complete the cell-cycle (Figure 45).

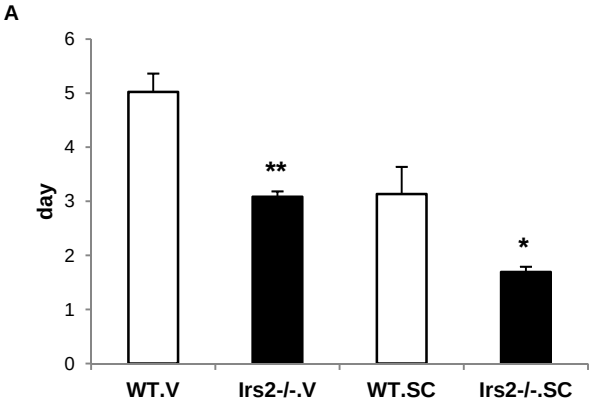

Figure 45: Estimated doubling time of APC cultures from WT and *Irs2*$^{-/-}$ mice. APC cultures were harvested and counted as indicated for Figure 45 and the doubling time was calculated by the online software (http://www.doubling-time.com/compute.php). Results are expressed as mean ± SEM.* p<0.05, ** p<0.01 and *** p<0.001. N=3 different primary cell cultures were analyzed.

4.8.2. Expression of proliferation markers Ki67 and phospho-Histone 3 are increased in *Irs2*$^{-/-}$ APC

The Ki67 protein (also known as MKI67) is a nuclear antigen specifically associated with cell proliferation (Gerdes et al., 1984). Expression of Ki67 occurs preferentially during late G1, S, G2 and M phases of the cell cycle but cannot be detected in G0 phase (Scholzen and Gerdes, 2000). Immunostaining for Ki67 was performed 24 hours after initial plating of APCs isolated from both genotypes. A greater proportion of *Irs2*$^{-/-}$ APC (both V and SC WAT) were positive for KI67 protein as compared to WT (Figure 46).

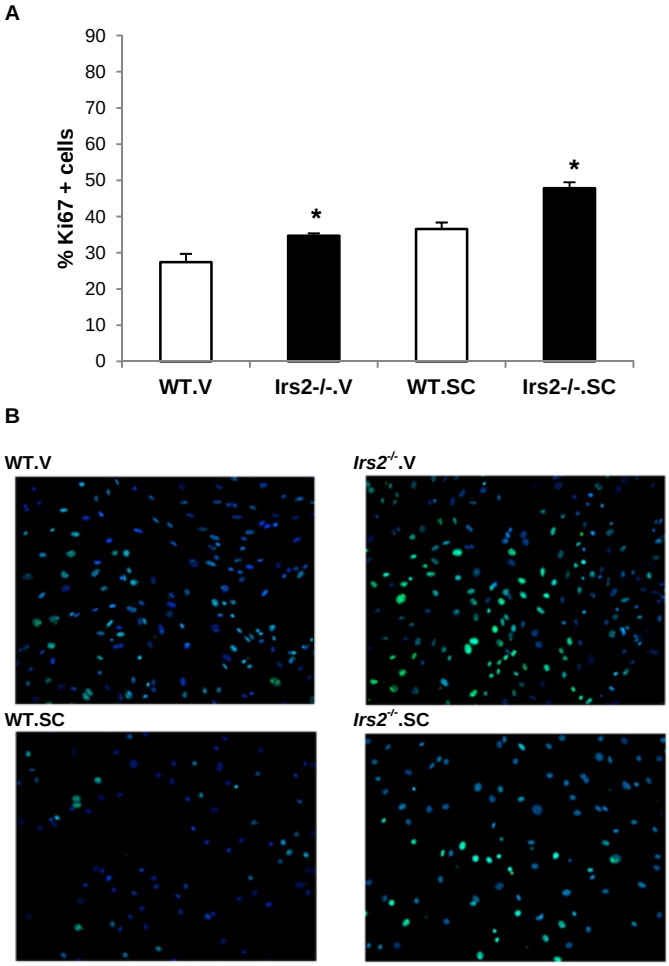

Figure 46: Quantification of Ki67 staining with In Cell® technology.
(**A)** InCell® quantification of Ki67 immunostaining. APCs were isolated from the indicated genotypes and plated. 24 hours later, cultures were fixed and stained for Ki67. (**B**) Representative images of APC stained with anti-Ki67 (green). DAPI was used to identify cell nuclei (blue). Results were expressed as mean ± SEM * p<0.05, ** p<0.01 and *** p<0.001. N=3 different primary cell cultures.

Another marker widely used to measure cell proliferation is the. phosphorylation of Histone 3 at Ser10, Ser28, and Thr11 which is tightly correlated with chromosome condensation during both mitosis and meiosis Thus, the nuclei of proliferating cells was stained using

Anti-pH3 Alexa 647 conjugated (red) and positive cells were quantified with In Cell® technology (see Figure 47). *Irs2*$^{-/-}$ APC from V-WAT showed an increase of pH3 staining whereas no differences were observed in APC from SC-WAT.

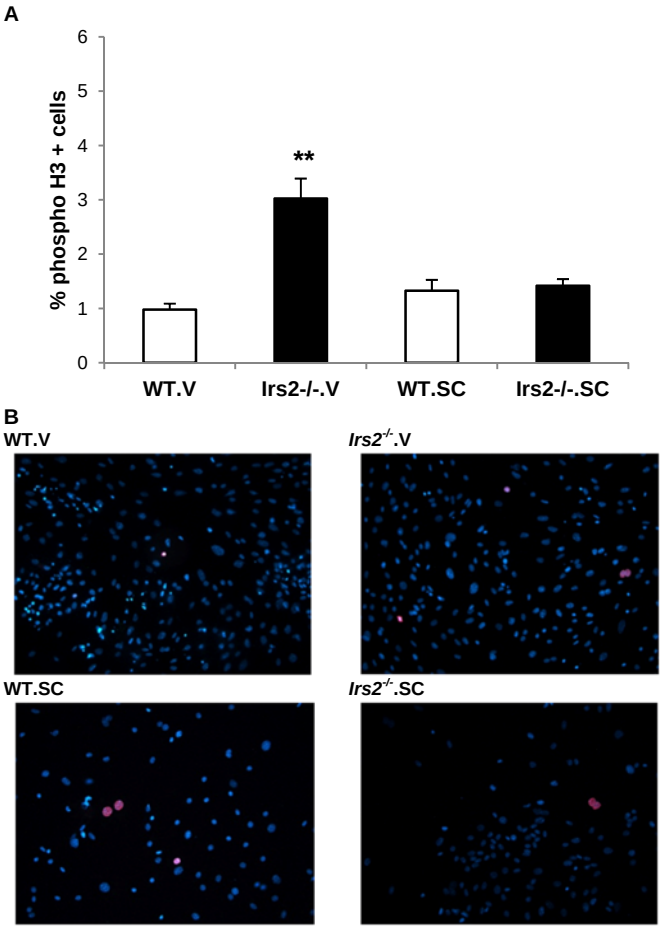

Figure 47: Quantification of anti-p-H3 in APC cultures.
(**A**) InCell® quantification of anti-phospho-Histone 3 immunostaining. APCs were isolated from the indicated genotypes and plated. 24 hours later, cultures were fixed and stained for p-H3. (**B**) InCell® quantification of p-H3 immunostaining (red). DAPI (blue) was used to reveal cell nuclei. Results are expressed as mean ± SEM. * $p<0.05$, ** $p<0.01$ and *** $p<0.001$. Three different primary cell cultures were analyzed.

4.8.3. Cell cycle analysis by Flow Cytometry reveals abnormalities in APC from *Irs2*-deficient mice

To gain further insight into the enhanced proliferation observed in *Irs2*$^{-/-}$ APC cultures, the cell-cycle was assessed with propidium iodide (PI). PI is a DNA fluorochrome used for cell-cycle analysis of single-cell suspensions. Flow cytometry analysis revealed enrichment of cells with double-quantity of DNA (4n) in *Irs2*$^{-/-}$APC, suggesting a population which is compounded by polyploidy cells as a result of DNA replication in the absence of mitosis. However, no differences in cells in S phase were observed. These results might suggest a increase in cells undergoing mitosis and/or a failure in cell-cycle control in *Irs2*$^{-/-}$ APC (Figure 48).

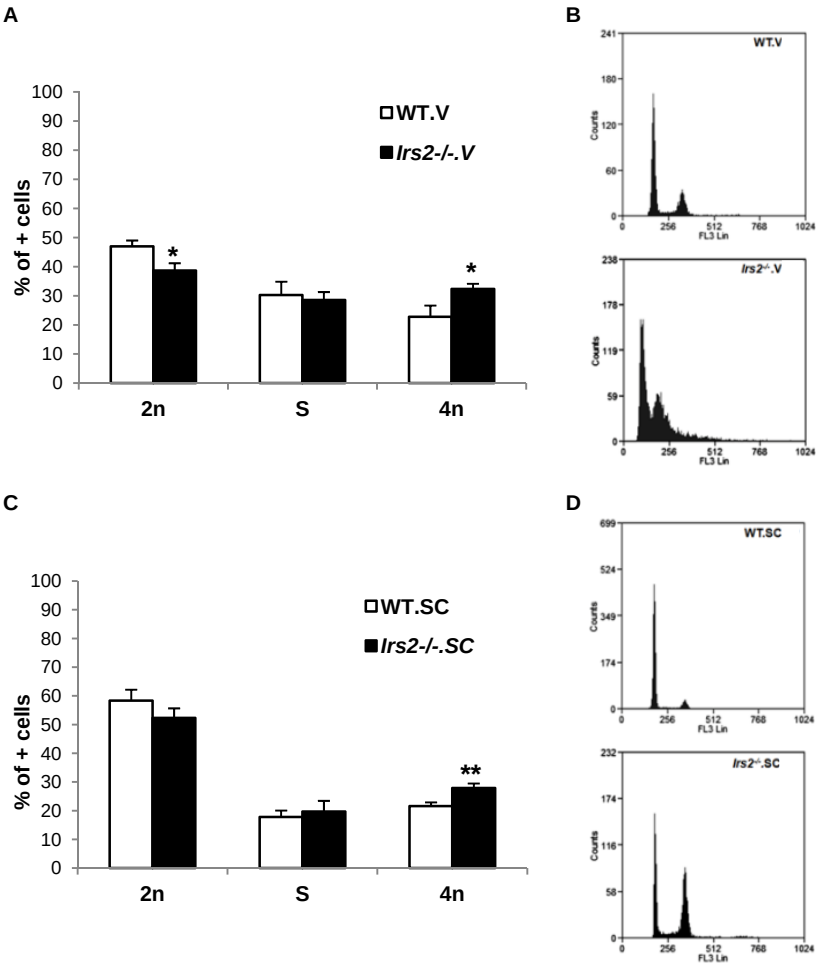

Figure 48: Analysis of DNA content by PI staining of APC from WT and *Irs2*$^{-/-}$ mice.
Cells adhering to the dish and detached cells (mitotic) were collected and subjected to PI nuclei staining and flow cytometry analysis. **A** and **C,** % of cells with different DNA content: 2n (normal cells G_0-G_1), S (synthesis phases of diploidy cells) and 4n (diploidy cells in mitosis and G_0-G_1 tetraploidy cells). **B** and **D**, DNA content on a logarithmic scale, determined by PI staining. Cells with 2n and 4n DNA are detected at 150 and 300, respectively, whereas cells between these two populations are cell in S phase. Results were expressed as mean ± SEM. * $p<0.05$, ** $p<0.01$ and *** $p<0.001$. N=5 primary cell cultures.

4.8.4. Apoptosis is not increased in APC cultures of *Irs2*-deficient mice

To determine whether *Irs2* deficiency might also alter apoptosis in APC, flow cytometry analysis was performed with Annexin V conjugated to FITC. Apoptotic cells were identified as cells positive for both Annexin V and PI. For this study, cells were maintained in normal growth medium (DMEM + 10% Serum), apoptotic conditions (DMEM without serum) or with supplemented βFGF (DMEM + 10ng/mL βFGF) during 24h. All samples were assayed in duplicate. Basal rates of apoptosis in APC cultures were similar between *Irs2*$^{-/-}$ APC and WT cultures. Serum withdrawal induced apoptosis in cultures of both V and SC APC and no differences were observed between genotypes (Figure 49). SC-APCs were more sensitive to serum withdrawal than V-APC, since the % of cell death was higher in these cultures. βFGF alone in the medium prevented apoptosis in response to serum withdrawal.

A

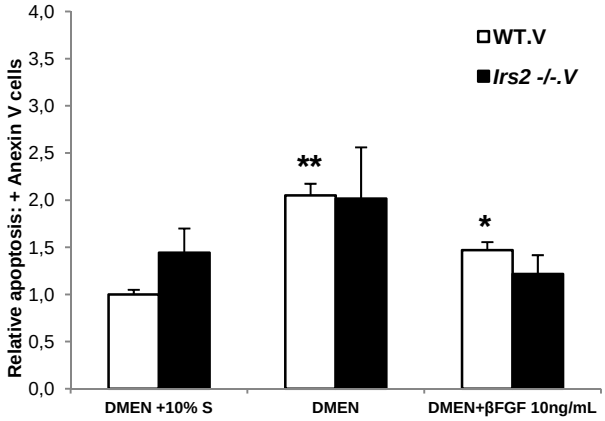

B

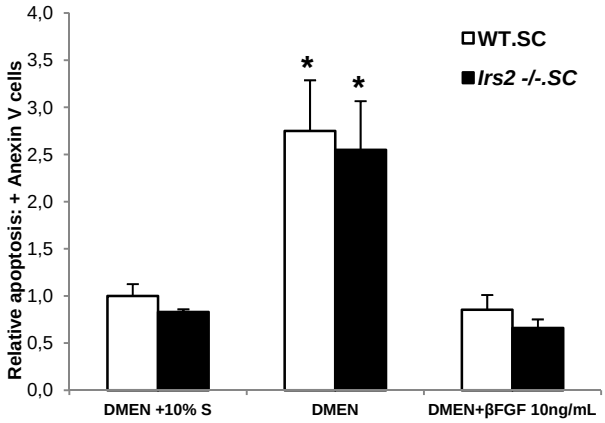

Figure 49: Detection of apoptosis by flow cytometry analysis of Annexin V. Apoptotic cells of APC from V-WAT (**A**) or SC-WAT (**B**). Results are expressed as mean ± SEM.* p<0.05, ** p<0.01 and *** p<0.001. N=3 different primary cell cultures were analyzed.

4.9. Osteopontin deficiency (*Spp1*$^{-/-}$) reduces inflammatory markers in WAT

Chronic inflammation appears to underlie obesity-induced metabolic deterioration including insulin resistance and DT2 (Dandona et al., 2004, Dandona et al., 2005, Hotamisligil, 2006). Osteopontin (OPN) is up-regulated in adipose tissue of obese humans and murine models of obesity. OPN acts as a chemokine and an inflammatory cytokine that is expressed in many cell types including adipose tissue macrophages (M Zeyda, 2007, Kiefer et al., 2010, Zeyda et al., 2011). Moreover, OPN added to the medium of primary adipocyte impairs differentiation as determined by PPAR γ and adiponectin gene expression (Zeyda et al., 2011). Given the impaired differentiation of *Irs2*-deficient APC, the relationship between insulin and OPN signalling in WAT was investigated. The results of this section were obtained in the laboratory of Dr. Thomas Stulnig of the University of Vienna.

4.9.1. Characterization of metabolic parameters in *Spp1*-deficient females

To assess the role of *Spp1* in adipose tissue inflammation and insulin resistance, female *Spp1*$^{-/-}$ and WT mice were maintained on a normal diet. Most of the previous studies with these mice were performed using high-fat diet but components of high-fat chow can themselves induce inflammation. Body weight was similar between WT and *Spp1* as were levels of fasting glucose (Figure 50). Adiposity was expressed as the quantity of WAT (g) divided by total body weight (g). Although there was a tendency for the WAT depots of *Spp1*$^{-/-}$ mice to weigh

less than WT, these differences were not statistically significant (Figure 50).

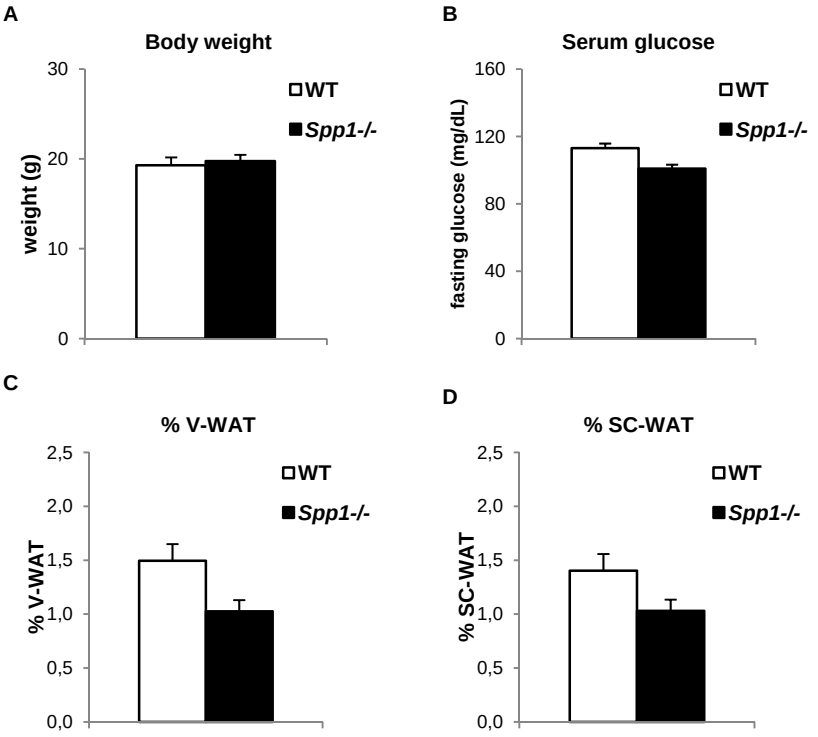

Figure 50: Metabolic parameters of WT and *Spp1*$^{-/-}$.
WT and *Spp1*$^{-/-}$ mice were fed a normal diet for 12 weeks. Mice were weighed (**A**) fasted overnight and blood glucose was measured using a glucometer (**B**). V and SC-WAT were excised and weighed (**C,D**). Results are expressed as mean ± SEM. N=10 mice of each genotype. Results are expressed as mean ± SEM. * $p<0.05$, ** $p<0.01$ and *** $p<0.001$.

4.9.2. *Spp1*-deficiency in mice alters the expression of adipokines and inflammatory markers

Based on the results presented in Figure 18 and Figure 21, *Irs2* knockout mice display increased circulating levels of insulin, leptin, TNFα and inflammation markers, suggestive of a state of obesity-induced inflammation and pre-diabetes. To assess the role of OPN in WAT and adipose tissue inflammation, gene expression studies were performed with V and SC-WAT of *Spp1*$^{-/-}$ and WT mice. All results were compared to expression in V-WAT that was considered as 100%. Similar to *Irs2*-deficient animals, adiponectin and *Rbp4* were up-regulated in both types of WAT from *Spp1* knockout mice (Figure 51). Resistin and IL6 were reduced in *Spp1*$^{-/-}$ mice as compared to control samples, which is the opposite of what was observed in *Irs2*$^{-/-}$ females. Other markers related with inflammation were measured in WAT. The genes for IL6, TNFα and MCP1 were all down-regulated in V and SC-WAT of *Spp1*$^{-/-}$ mice (Figure 51), suggesting that loss of *Spp1* reduces inflammatory cytokines in WAT.

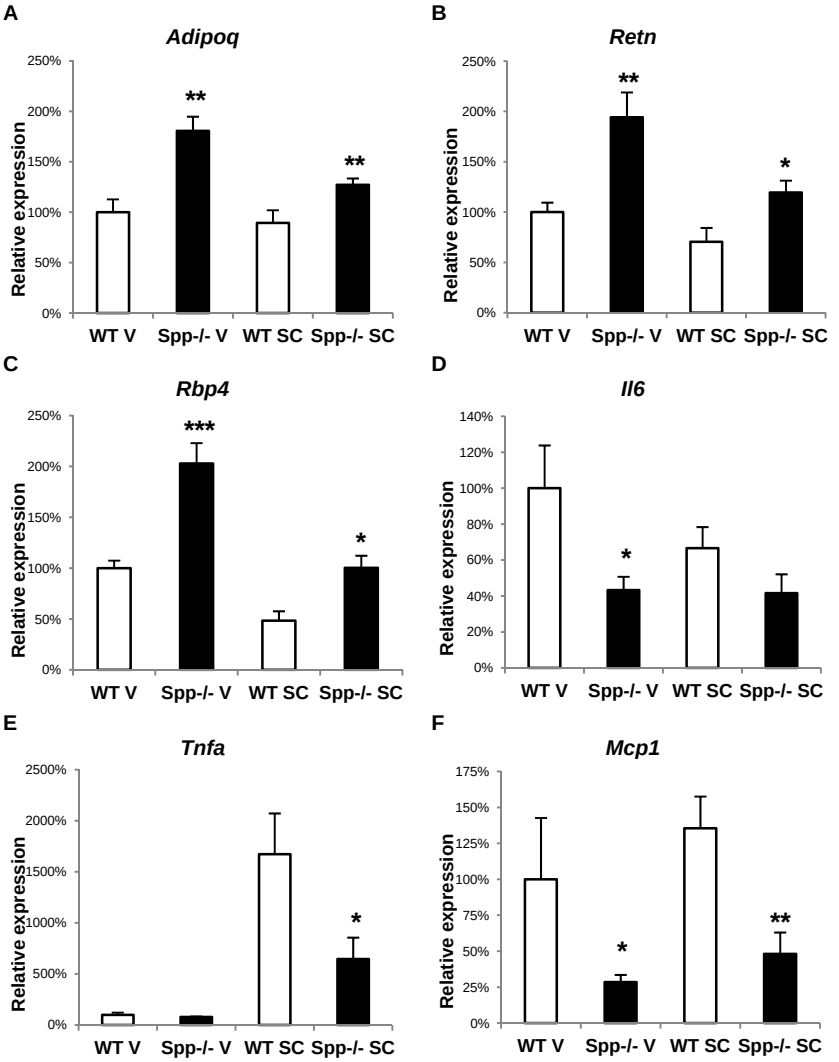

Figure 51: Gene expression of adipokines in WAT from WT and *Spp1*$^{-/-}$.
Total RNA was extracted from V and SC-WAT with Trizol®. RT-PCR was performed using TaqMan probes for the indicated genes. Each reaction was performed in duplicate and the value of the gene of interest was normalized to the expression of Ubiquitin C. Data was analyzed by the comparative Ct method ($2^{-\Delta\Delta Ct}$) (Livak and Schmittgen, 2001). Results are expressed as mean ± SEM. * $p<0.05$, ** $p<0.01$ and *** $p<0.001$. For data presentation, V-WAT of WT mice was considered as 100%. N= 5 mice of each genotype. Relative gene expression of Adiponectin (**A**), Resistin (**B**), Retinol Binding Protein 4 (**C**), Interluekine 6 (**D**), Tumor necrosis factor α (**E**) and Monocyte Chemotactic Protein 1 (**F**) are shown in the graphs.

Markers of inflammatory cells were studied next. To determine whether macrophage infiltration was altered in WAT of *Spp1*-deficienct mice, F4/80 (*Emr1*) was analyzed by RT-PCR and the expression of this marker was diminished in both WAT sources (Figure 51), indicative of a reduced macrophage infiltration. Expression of the mRNA for Leukocyte marker CD45 was also lower in *Spp1*$^{-/-}$ mice as compared with WT WAT. Taken together with the reduction of the T-cell infiltration markers CD3 (*Cd3e*) and CD8 (*Cd8a*), these results indicate reduced inflammation in WAT of *Spp1*$^{-/-}$.

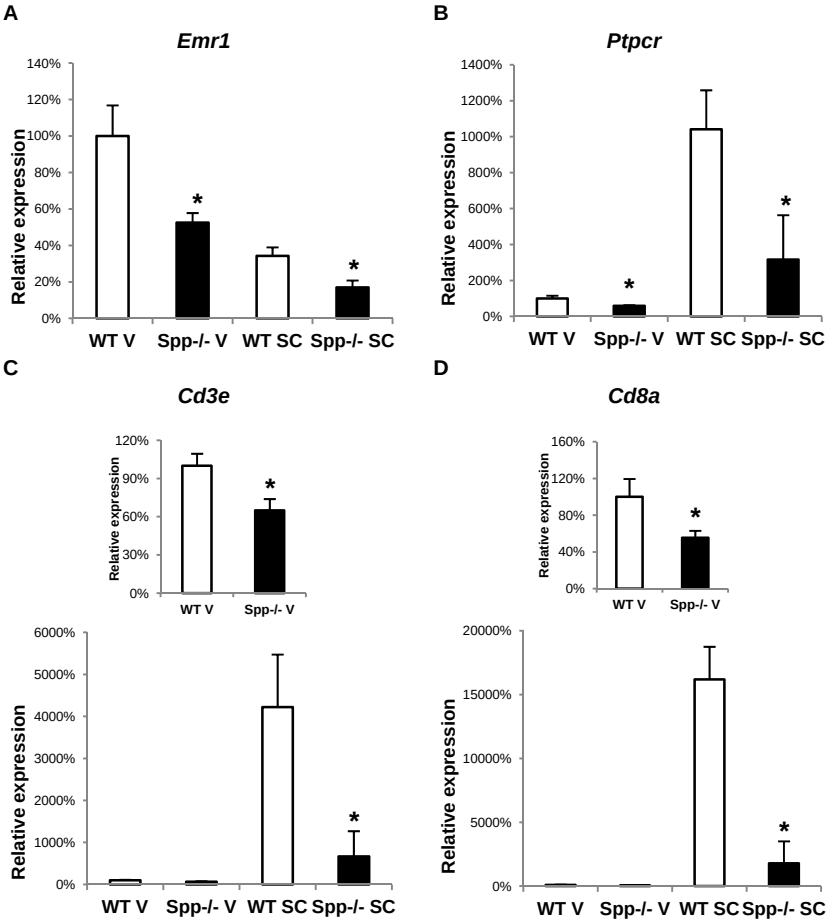

Figure 52: Gene expression of inflammatory-related markers in WAT from WT and *Spp1*$^{-/-}$.

Total RNA was extracted from V and SC-WAT with Trizol®. RT-PCR was performed using TaqMan probes for the indicated genes. Each reaction was performed in duplicate and the value of the gene of interest was normalized to the expression of Ubiquitin C. Data was analyzed by the comparative Ct method ($2^{-\Delta\Delta Ct}$) (Livak and Schmittgen, 2001). Results are expressed as mean ± SEM. * $p<0.05$, ** $p<0.01$ and *** $p<0.001$. For data presentation, V-WAT of WT mice was considered as 100%. N= 5 mice of each genotype. Relative gene expression of macrophage infiltration marker F4/80 (**A**), leukocyte marker CD45 (**B**) and T lymphocyte marker CD3 (**C**) and CD8 (**D**) are showed in the graphs.

4.10. Hypoxia markers are down-regulated in *Spp1*$^{-/-}$ WAT

In the *Irs2*-deficient model, enhanced expression of inflammatory-related markers was also associated with up-regulation of the principal markers of hypoxia, HIFα and VEGF (see Figure 25), suggesting low oxygen availability in WAT. HIFα was down-regulated in both types of WAT in *Spp1*$^{-/-}$ as compared to WT controls (Figure 53). However no differences were founded in VEGF.

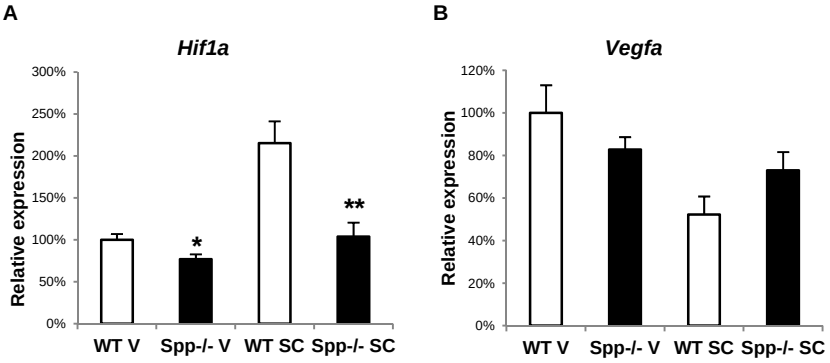

Figure 53: Gene expression studies of hypoxia markers in WAT from WT and *Spp1*$^{-/-}$.
Total RNA was extracted from V and SC-WAT with Trizol®. RT-PCR was performed using TaqMan probes for the indicated genes. Each reaction was performed in duplicate and the value of the gene of interest was normalized to the expression of Ubiquitin C. Data was analyzed by the comparative Ct method ($2^{-\Delta\Delta Ct}$) (Livak and Schmittgen, 2001). Results are expressed as mean ± SEM. * $p<0.05$, ** $p<0.01$ and *** $p<0.001$. For data presentation, V-WAT of WT mice was considered as 100%. N= 5 mice of each genotype. Relative gene expression of Hypoxic inducible factor α (**A**) and Vascular endothelial growth factor A (**B**) are shown in the graphs.

4.11. Expression of *Irs2* mRNA is increased in WAT of *Spp1*$^{-/-}$

To explore the relation between the reduced inflammation mediated by *Spp1*-deficiency and insulin action in WAT, various genes of the insulin signaling were studied by RT-PCR. Interestingly, *Irs2* mRNA was up-regulated in both depots of *Spp1*$^{-/-}$ WAT (Figure 54), suggesting that a general reduction of the inflammatory milieu might positively regulate IRS2 expression and thereby increase insulin sensitivity. The expression of *Irs1* and *Irs3* were decreased in *Spp1*$^{-/-}$ WAT whereas they were up-regulated in WAT of *Irs2*-deficient mice (Figure 54). The *Insr* was also reduced in V-WAT or SC-WAT from *Spp1*$^{-/-}$ mice. The expression of GLUT4 (*Slc2a4*) was increased in V-WAT of Spp1-deficient mice suggesting an increased glucose uptake but there were no differences in the expression of Gs*k3β* between genotypes.

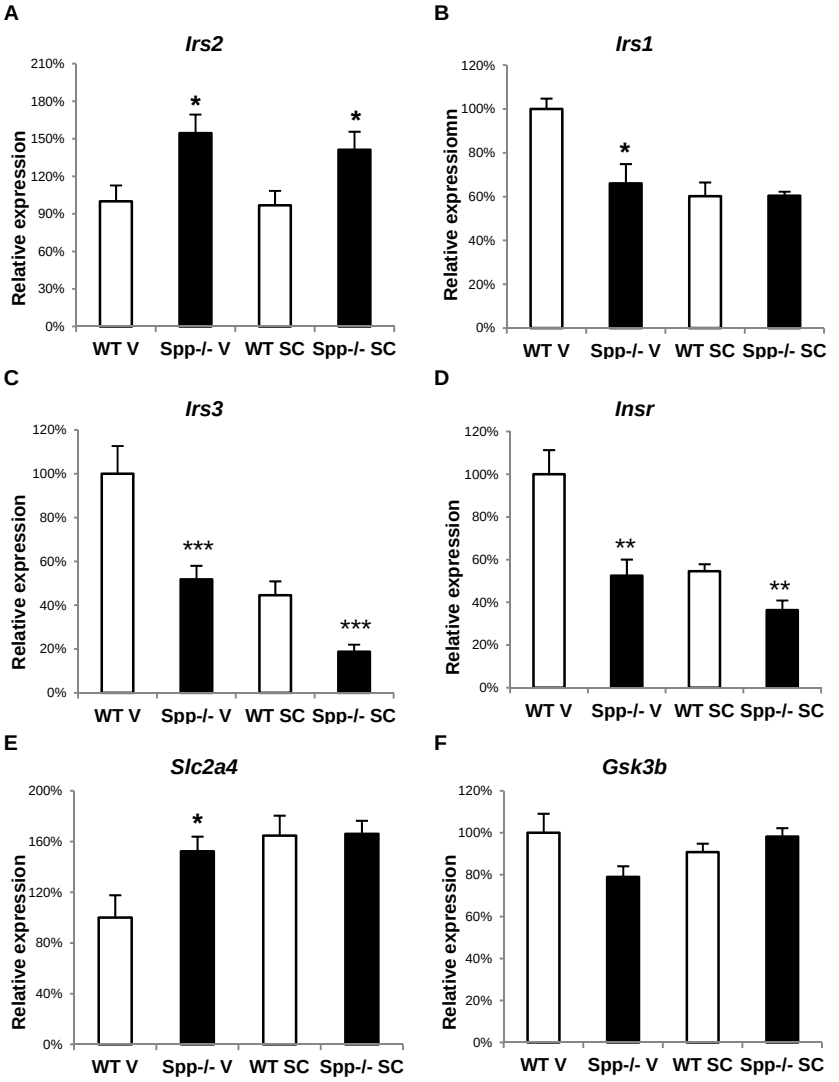

Figure 54: Analysis of genes of the insulin signalling pathway in WAT from WT and *Spp1*$^{-/-}$.
Total RNA was extracted from V and SC-WAT with Trizol®. RT-PCR was performed using TaqMan probes for the indicated genes. Each reaction was performed in duplicate and the value of the gene of interest was normalized to the expression of Ubiquitin C. Data was analyzed by the comparative Ct method ($2^{-\Delta\Delta Ct}$) (Livak and Schmittgen, 2001). Results are expressed as mean ± SEM. * $p<0.05$, ** $p<0.01$ and *** $p<0.001$. For data presentation, V-WAT of WT mice was considered as 100%. N= 5 mice of each genotype. Relative gene expression of Insulin receptor substrate 2 (**A**), Insulin receptor substrate 2 (**B**), Insulin receptor substrate 3 (**C**), Insulin receptor (**D**), Glucose transporter 4 (**E**) and glycogen synthase kinase 3 (**F**) are presented in the graphs.

4.12. The major genes associated with adipogenesis are up-regulated in WAT from *Spp1*$^{-/-}$ mice

To further assess potential differences in *Spp1* versus *Irs2* deficiency for WAT physiology, adipogenic-related genes were measured by RT-PCR. *Pparγ* was increased in V-WAT in *Spp1*$^{-/-}$ mice (Figure 55), contrasting the decrease observed in *Irs2*-deficient females (see Figure 27). *Fabp4*, *Fasn*, and *Adn* were also increased in WAT from OPN deficient mice (Figure 55).

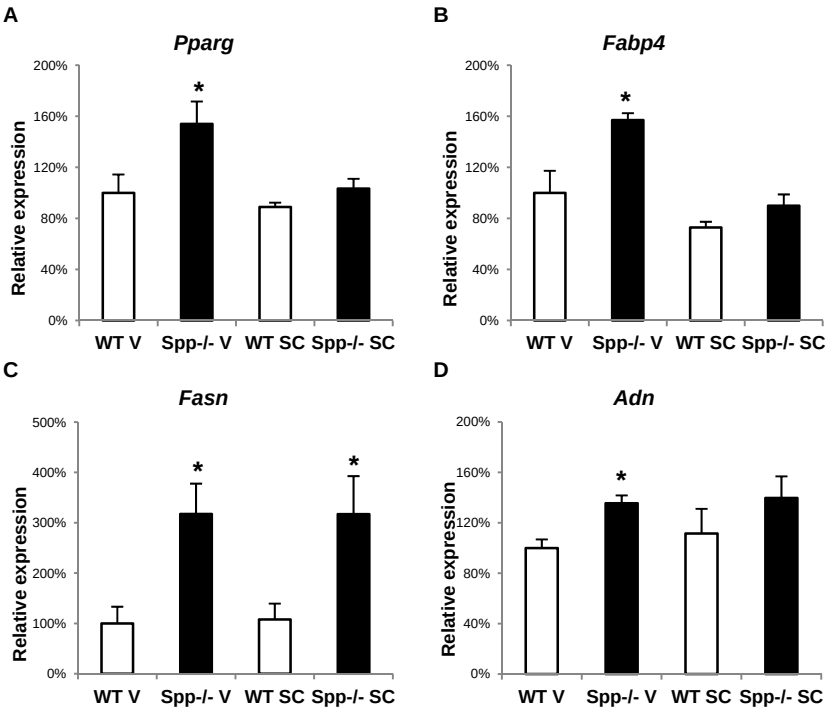

Figure 55: Gene expression of adipogenesis markers in WAT from WT and *Spp1*$^{-/-}$. RT-PCR was performed using TaqMan probes for the indicated genes. Data was analyzed by the comparative Ct method ($2^{-\Delta\Delta Ct}$) (Livak and Schmittgen, 2001). Results are expressed as mean ± SEM. * $p<0.05$, ** $p<0.01$ and *** $p<0.001$. For data presentation, V-WAT of WT mice was considered as 100%. N= 5 mice of each genotype. Relative gene expression of Peroxisome proliferator activated receptor-γ (**A**), Fatty acid binding protein 4 (**B**), Fatty acid synthase (**C**) and Adipsin (**D**) are shown in the graphs.

The expression of adipogenesis co-regulators *Pgc1α* and *Srebf1* was similar between WT and *Spp1*$^{-/-}$ except that *Srebf1* was reduced in SC-WAT from *Spp1*$^{-/-}$ mice (Figure 56). Expression of the two enzymes implicated in the synthesis of triacylglycerol, *Dgat1* and *Dgat2,* were enhanced in WAT from *Spp1*$^{-/-}$ mice, suggesting that adipocytes lacking OPN may display an increased energy storage capacity. Consistent with these results, addition of OPN to culture medium has been shown to inhibit the differentiation of progenitors to adipocytes (Zeyda et al., 2011).

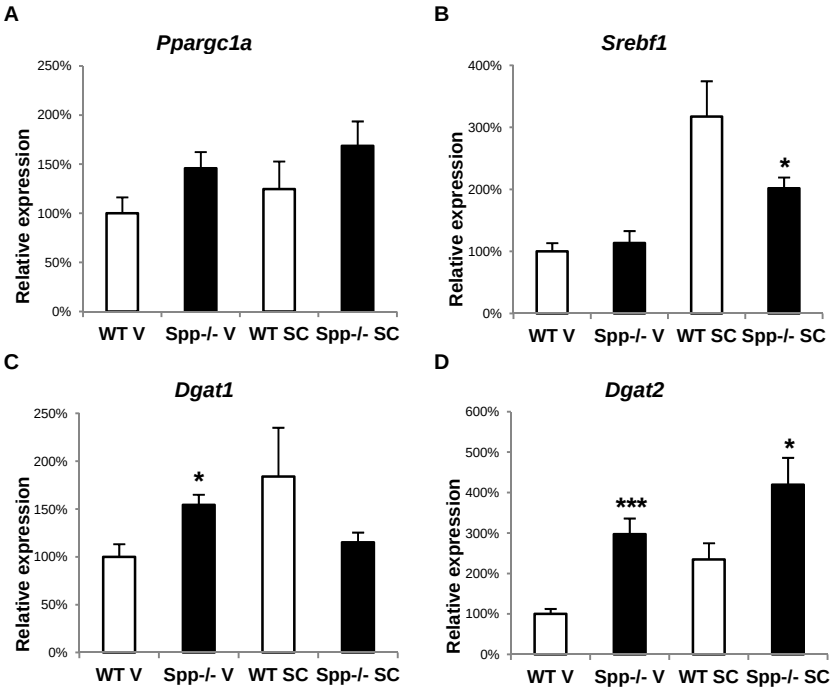

Figure 56: Gene expression of adipogenic coactivators in WAT from WT and Spp1$^{-/-}$.
RT-PCR was performed using TaqMan probes for the indicated genes. Each reaction was performed in duplicate and the value of the gene of interest was normalized to the expression of Ubiquitin C. Data was analyzed by the comparative Ct method ($2^{-\Delta\Delta Ct}$) (Livak and Schmittgen, 2001). Results are expressed as mean ± SEM. * $p<0.05$, ** $p<0.01$ and *** $p<0.001$. For data presentation, V-WAT of WT mice was considered as 100%. N= 5 mice of each genotype. Relative gene expression of PPARγ co-activator‑1α (**A**), Sterol Regulatory Element Binding Protein 1c (**B**), Acyl CoA diacylglyceron acyltransferase 1 (**C**) and Acyl CoA diacylglyceron acyltransferase 2 (**D**) are shown in the graphs.

4.13. Flow cytometry analysis reveals a decrease of APC isolated from SC-WAT from *Spp1*$^{-/-}$ mice

Mice lacking the osteopontin gene are resistant to diet-induced obesity (Kiefer et al., 2011), perhaps owing to reduced inflammation. Adipose mass is determined by many factors which ultimately regulate adipocyte cell size and/or adipocyte cell number. To gain further insight into the role of OPN in WAT regulation, APC were isolated from the SVF *Spp1*$^{-/-}$ WAT, as described previously for *Irs2*-deficient mice. The cells were analyzed by Flow cytometry to identify the APC population of CD45- CD31- Ter119- CD34+ Sca1+ cells. The % of APC obtained from V-WAT was similar between *Spp1*$^{-/-}$.and WT controls (Figure 57). Surprisingly, the population of APC from SC-WAT of *Spp1*$^{-/-}$ mice was reduced, suggesting that an anti-inflammatory niche may reduce adult stems cells in WAT.

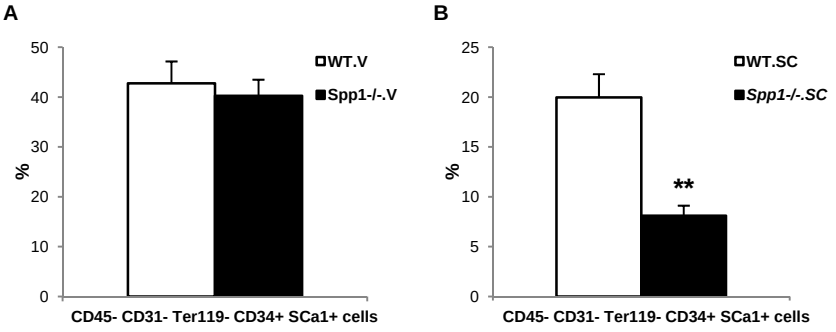

Figure 57: Analysis of APC population in WAT from WT and *Spp1*$^{-/-}$.
Flow cytometry analysis was used to quantify the APC population (CD45-CD31-Ter119-CD34+Sca1+ cells) in V-WAT (**A**) and SC-WAT (**B**). Results are expressed as mean ± SEM. * p<0.05, ** p<0.01 and *** p<0.001. The SVF was isolated from 3 mice of each genotype in 3 independent experiments for a total n of 9 mice of each genotype.

4.14. *Spp1*$^{-/-}$ APCs differentiate more efficiently to adipocytes *in vitro*

Previous studies have demonstrated that addition of OPN to cultures of human preadipocytes did not grossly alter adipogenesis as assessed by lipid droplet formation but analysis of gene expression revealed a concentration-dependent inhibition of PPARγ and adiponectin expression (Zeyda et al., 2011). *Spp1* gene expression is up-regulated in obese humans (Gómez-Ambrosi et al., 2007, Nomiyama et al., 2007, Bertola et al., 2009). A recent publication suggests that OPN deficiency improves diet-induced insulin resistance (Kiefer et al., 2011). Therefore, the capacity of *Spp1*$^{-/-}$.APC to differentiate to adipocytes was tested *in vitro.* APC were isolated from SVF with MACS® technology (see Figure 14 page 91) to obtain cells of the following immunophenotype: CD45- CD31- Ter119- CD34+ and Sca1+. The differentiation method was the same as used for APC from the *Irs2*-deficient model. APC were grown to confluence (day 0) and then exposed to the differentiation medium. After 10 days, the presence of lipid accumulation was assessed by phase contrast microscopy. The differentiation of SC-APC was more robust than V-APC in both genotypes. However, *Spp1*$^{-/-}$.APC differentiated more efficiently to adipocytes than WT controls based on the enhanced accumulation of lipid droplets in these cultures (Figure 58). These results contrast those obtained with *Irs2*$^{-/-}$APC where differentiation was impaired compared to control cultures (see Figure 37).

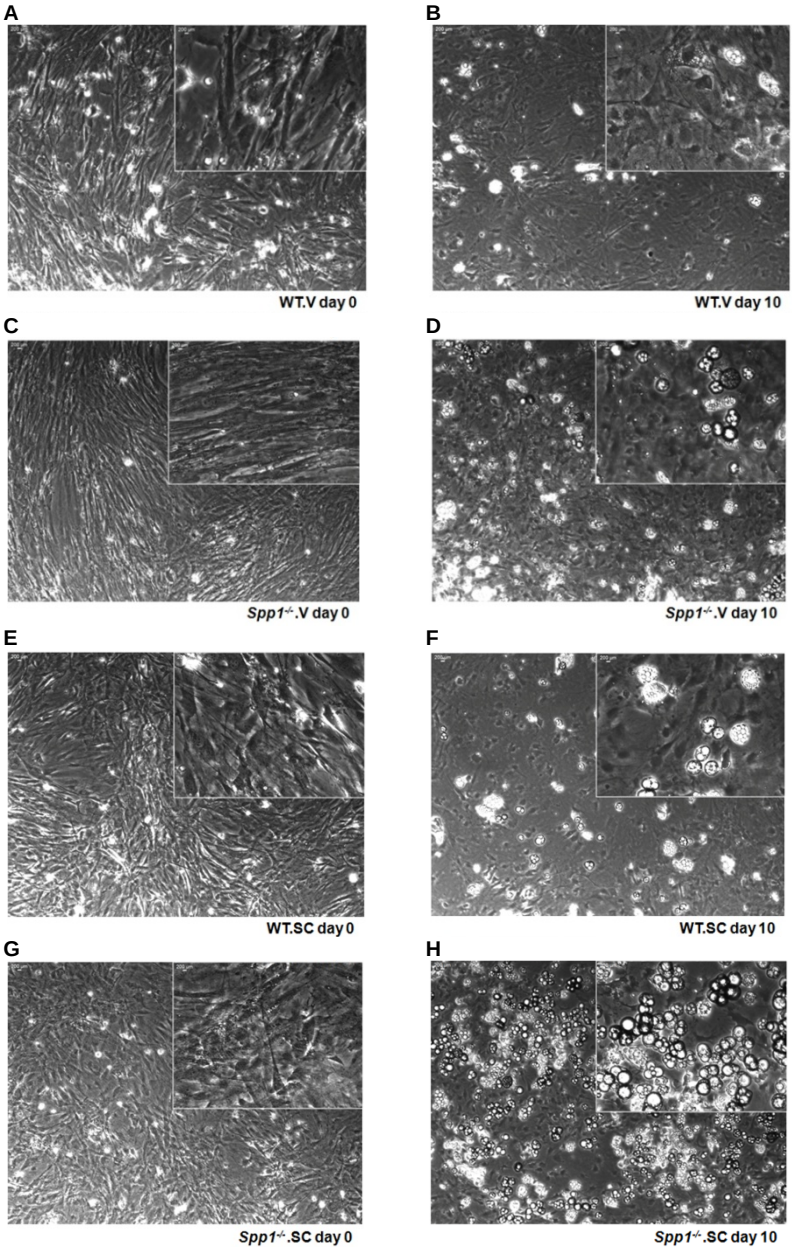

Figure 58: Phase contrast images of APC cultures from WT and *Spp1*$^{-/-}$ WAT subjected to adipocyte differentiation protocol.

Phase contrast images of APC at day 0 and day 10 of adipocyte differentiation. **A,B**) WT V-WAT; **C,D**) *Spp1*$^{-/-}$ V-WAT; **E,F**) WT SC-WAT; **G,H**) *Spp1*$^{-/-}$ SC-WAT. Images were captured with 20x objective and 40x objectives (right of the picture). Representative images from 2 different experiments are shown.

To characterize the molecular changes during the differentiation of *Spp1*$^{-/-}$ APC into adipocytes, RT-PCR analysis was performed at various time points (day -3, 0, 3, 7 and 10) during the adipogenic program. In both V-APC and SC-APC, *Irs2* expression increased at day 3 but then was down-regulated between day 7 and 10, depending on WAT source (Figure 59). Consistent with RT-PCR analysis observations in WAT (see Figure 54), *Irs2* expression was greater in *Spp1*$^{-/-}$ cultures of V-APC at day 10 and SC-APC at day -3. The expression profile of IRβ (*Insr*) was also distinct different between WT and *Spp1*$^{-/-}$ cultures (Figure 59); in V-APC the expression peaked at day 3 whereas in SC-APC, this peak occurred at the end of differentiation at day 10. GLUT4 *(Slc2a4)* expression was significantly higher in *Spp1*$^{-/-}$ SC-APC at day 10.

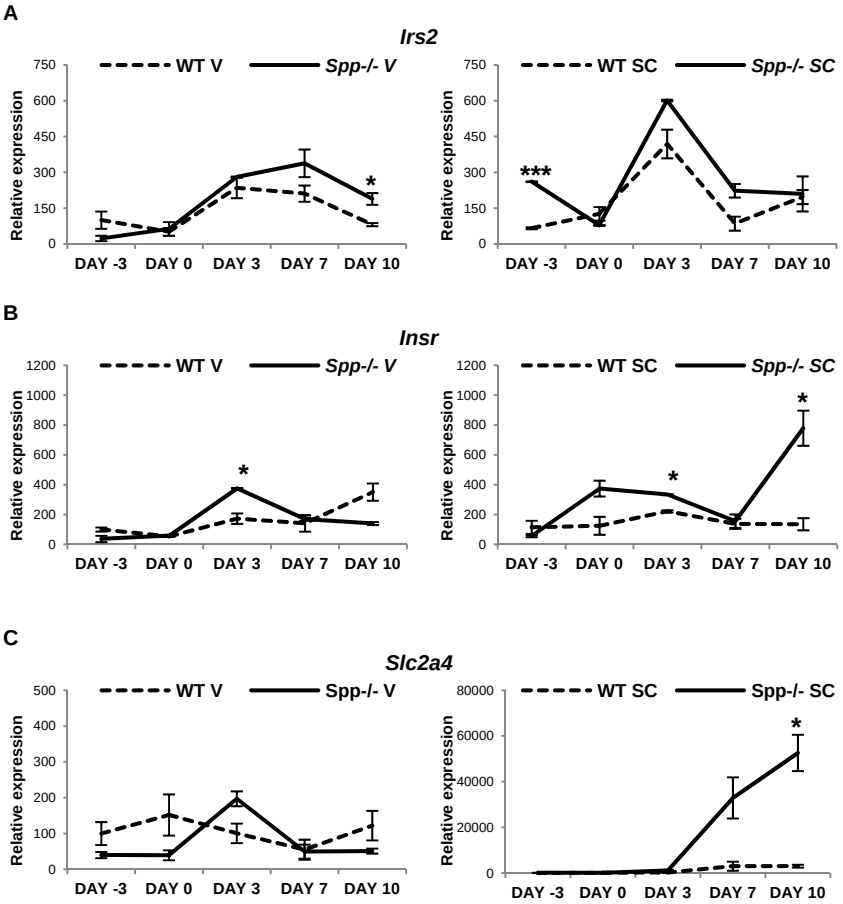

Figure 59: Gene expression analysis of insulin signaling related genes in APC from WT and *Spp1*$^{-/-}$ during differentiation of APC to adipocytes *in vitro*.
APC cultures were collected at the indicated days and used to prepare total RNA with Trizol®. RT-PCR was performed using TaqMan probes for the indicated genes. Each reaction was performed in duplicate and the value of the gene of interest was normalized to the expression of Ubiquitin C. Data was analyzed by the comparative Ct method ($2^{-\Delta\Delta Ct}$) (Livak and Schmittgen, 2001). Results are expressed as mean ± SEM. * p<0.05 , ** p<0.01 and *** p<0.001. For data presentation, APC from V-WAT of WT mice collected at day -3 was considered as 100%. N= 2 independent experiments. Insulin receptor substrate 2 (**A**), Insulin receptor β (**B**) and Glucose transporter 4 (**C**) are shown in the graphs.

Pparγ, the master regulator of adipogenesis, remained constant in WT V-APC cultures from day 0 to 10 but peaked sharply at day 3 in SC-APC. Additionally, the relative expression of *Pparγ* was higher in SC than V APC. The expression of *Pparγ* in *Spp1*$^{-/-}$ APC was higher at

day 7 in both V and SC cultures as compared to WT controls. *Fsn* expression was similar between WT and *Spp1*$^{-/-}$ with respect to V-WAT but in APC from SC-WAT, *Spp1*$^{-/-}$ APC had higher levels than WT APC. The peaks of *Adn* expression were significantly higher in *Spp1*$^{-/-}$ APC (see Figure 60).

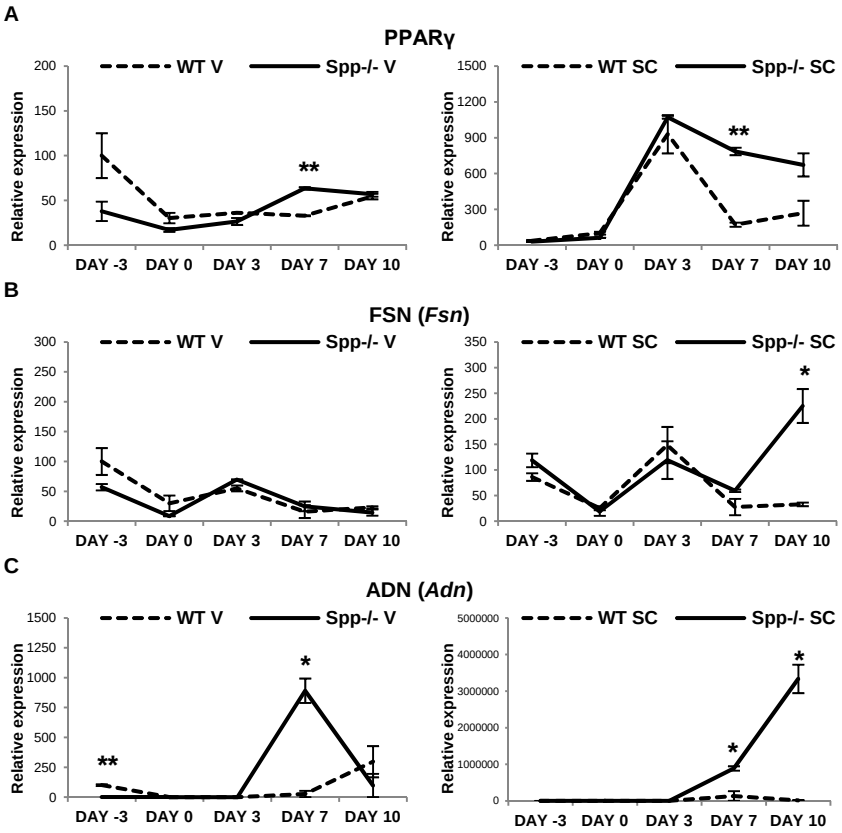

Figure 60: Gene expression analysis of adipogenesis related genes in APC from WT and *Spp1*$^{-/-}$ during differentiation of APC to adipocytes *in vitro*.
APCs were collected at the indicated days and used to prepare total RNA with Trizol®. RT-PCR was performed using TaqMan probes for the indicated genes. Each reaction was performed in duplicate and the value of the gene of interest was normalized to the expression of Ubiquitin C. Data was analyzed by the comparative Ct method ($2^{-\Delta\Delta Ct}$) (Livak and Schmittgen, 2001). Results are expressed as mean ± SEM. * $p<0.05$, ** $p<0.01$ and *** $p<0.001$. For data presentation, APC from WT V-WAT collected by day -3 was considered as 100%. N= 2 independent experiments. Peroxisome-proliferating receptor γ (**A**), Fatty acid synthase (**B**) and Adipsin (**C**).

CHAPTER 5

DISCUSSION

5. DISCUSSION

Lipids stored in adipose tissue represent the largest reserve of energy in the human body. In normal-weight adult humans, white adipose tissue represents 10 to 29% of body weight but this mass increases in obesity (Wang et al., 2008). Western dietary habits and a sedentary lifestyle have produced a worldwide epidemic of obesity. Indeed, at least one in 13 annual deaths in the European Union are likely to be related to excess weight (Banegas et al., 2003). Obesity predisposes patients to the development of cardiovascular disease and T2D, most likely due to the state of low-grade chronic inflammation which characterizes increased adipose mass. In recent years, various lines of evidence have demonstrated that activation of pro-inflammatory pathways can modulate insulin action via a number of mechanisms including down-regulation of insulin signalling pathway proteins (Starr et al., 1997, Hotamisligil, 2003). IRS proteins are the principal targets of the insulin receptor tyrosine kinase. Tissues from insulin-resistant and diabetic humans exhibit defects in IRS-dependent signalling (Copps et al., 2010, Copps and White, 2012), implicating their dysregulation in the initiation and progression of metabolic disease. Loss of *Irs2* expression is associated with beta cell insufficiency in both mice and humans with T2D (Withers et al., 1998, Gunton et al., 2005). The I*rs2*-deficient mouse model has demonstrated a crucial role for this signalling molecule in hepatic insulin sensitivity, brain and photoreceptor development, and hypothalamic regulation of appetite (Withers et al., 1998, Kubota et al., 2000, Burks et al., 2000, Withers, 2001, Burks and White, 2001, Schubert et al., 2003, Valverde et al., 2004, Choudhury et al., 2005, Taguchi et al., 2007). However, the role of IRS2 in adipose tissue has not been characterized. The results of the present project reveal that deletion of *Irs2* causes an increase in

stores of both V and SC WAT which is accompanied by a pro-inflammatory profile of cytokines and immune markers.

The role of IRS2 in WAT was examined initially by comparing V and SC fat between *Irs2*$^{-/-}$ and control mice. The increased body weight of female *Irs2*-deficient mice was associated with larger stores of both V and SC WAT. The % of total body weight reflected by V and SC-WAT was almost doubled in *Irs2*$^{-/-}$ females as compared with control mice. It is important to note that only female mice were used in the study since male *Irs2*$^{-/-}$ develop severe diabetes and die by 16 weeks of age (Garcia-Barrado et al., 2011). Thus, the study of female mice permitted the analysis of *Irs2* deficiency without the complications of hyperglycemia. Circulating levels of leptin were increased in *Irs2*$^{-/-}$ females but adiponectin was also increased which is surprising since adiponectin levels are reduced in obese subjects (Hu et al., 1996). However, this may be explained by recent studies which suggest that adiponectin levels reflect adipose tissue triglyceride storage capacity (Vega and Grundy, 2013). RT-PCR analysis of WAT depots revealed that expression of the genes for TNFα, IL6, and MCP1 are also increased in *Irs2*-deficient females. This is consistent with the observation that adipose tissue of obese humans contains increased numbers of macrophages, and once activated, these macrophages are responsible for the expression of various cytokines including TNFα, IL6, and MCP1 (Weisberg et al., 2003). TNFα is an important mediator of insulin resistance in obesity and diabetes through its ability to decrease the tyrosine kinase activity of the insulin receptor and inactivate IRS proteins. The present results suggest that reduced IRS2 signaling could contribute to obesity in at least two ways, first through the simple impairment of insulin signaling pathways and second, by increasing the expression of cytokines such as TNFα in

WAT which would compound insulin resistance by inhibiting the activity of the insulin receptor.

Increased WAT mass can arise through an increase in cell size, cell number, or both. Adipose cells are quite variable in size which depends principally on the amount of stored triglycerides. Mild obesity mainly reflects an increased adipose cell size (hypertrophic obesity) while more severe obesity or obesity arising in childhood derives from an increased fat cell number (hyperplastic obesity) (Spiegelman and Flier, 1996). Recent studies indicate that the adipocyte population is more dynamic than previously believed. In humans, adipocyte number increases dramatically throughout the first two decades of life and continues to turn over at the rate of about 10% per year throughout adulthood (Spalding et al., 2008, Jo et al., 2009). Individuals with early-onset obesity develop increased numbers of adipocytes, suggesting the concept of a "fixed body weight" since even after significant weight loss the number of adipocytes remains constant in these individuals. In the *Irs2*-deficient model, the increase in adipose mass was not due to an increase in cell size as a consequence of hypertrophy, suggesting that enhanced WAT mass might be attributable to increased adipocyte number. This notion was corroborated by the upregulation of the main markers of hypoxia HIFα and VEGFa in WAT of *Irs2*$^{-/-}$ females. Several laboratories have proposed that hypoxia in WAT occurs as a result of adipocyte hyperplasia which reduces the O_2 supply from the vasculature (Kabon et al., 2004, Pasarica et al., 2009).

Although how pre-adipocytes differentiate into adipocytes has been defined through extensive study of *in vitro* models such as 3T3-L1, very little is known about the development and regulation of preadipocytes *in vivo*. As key parts of a homeostatic system that

modulates energy balance, the identification of the signaling mechanisms that regulate preadipocyte cell growth and differentiation are of extreme interest since they represent potential targets for controlling obesity. Embryonic mesoderm is thought to give rise to mesenchymal stem cells, which in turn give rise to common early precursors or adipoblasts (Gesta et al., 2007). Under appropriate conditions, adipoblasts develop into committed white and brown preadipocytes and, ultimately mature adipocytes. Due to absence of specific markers, the specific steps in lineage commitment and differentiation, and the factors controlling these pathways have not been defined. During the last several years, various laboratories have identified APC in the SVF using lineage tracing studies in mouse models (Tang et al., 2008). These specialized cells express PPARγ, Sca1, and CD34. Although advances have been made towards the identification of the APC *in vivo*, no studies have yet addressed the role of insulin signaling in regulating this population in WAT. Based on the results of the present study, insulin sensitivity may play a key role in establishing the number of APC *in vivo*. The number of APCs isolated from V-WAT of *Irs2*$^{-/-}$ females was increased more than 2-fold. However, it remains to be determined whether the increase of V-WAT progenitors observed in this model is due directly to the loss of *Irs2* expression or whether it more accurately reflects systemic inflammation resulting from *Irs2*-deficiency.

WAT depots in different parts of the body have different developmental timing and different physiological effects. Although an increase of both V and SC fat was observed in *Irs2*$^{-/-}$ females, the population of APC was increased in V but not SC-WAT when compared to control mice. This observation is consistent with the fact that visceral adiposity, but not subcutaneous adiposity, is associated with diabetes and other metabolic diseases (Gesta et al., 2007).

Increasing evidence suggest that subcutaneous fat is not related to many of the classic obesity-induced pathologies but rather might play a protective role. The typically female, pear-shape of body fat distribution is subcutaneous fat, and appears to pose less of a health risk compared to visceral fat (Kissebah and Krakower, 1994).

Under the experimental conditions employed, the differentiation of SC-APC to adipocytes was more robust than V-APC in both genotypes. An interesting observation from this study is the fact that IRS2 expression increased greatly during the early phases of the differentiation of WT APC in vitro. In contrast, IRS1 and IRS3 were slightly down-regulated, suggesting that IRS2 signals may be important for initiating the transcriptional program that directs adipogenesis. Consistent with this hypothesis, cultures of *Irs2*$^{-/-}$ APC from both V and SC-WAT differentiated poorly to adipocytes in vitro as determined by the accumulation of lipid by BODIPY. The impaired differentiation of *Irs2*$^{-/-}$ APC correlated with decreased expression of the principal adipogenic transcription factors PPARγ and C-EBPα and markers of adipocyte function. Moreover, cultures of both V and SC *Irs2*$^{-/-}$ APC proliferated more rapidly than control cells, suggesting that enhanced doubling time might explain, in part, the failure of *Irs2*-deficient precursors to differentiate (Figure 61). The mitotic index of mature adipocytes is quite low since these cells exit the cell cycle in order to differentiate and mature functionally. The increased proliferation might be explained by the observation that IRS1 signaling, unopposed by IRS2, is mitogenic as evidenced by the hyperplasia of beta cells in *Irs1*-deficient mice (Withers et al., 1998).

How is possible that *Irs2*$^{-/-}$ APC display impaired differentiation to adipocytes *in vitro* yet *Irs2*-deficiency causes moderate obesity *in vivo*? Interestingly, it has been recently reported that the differentiation

potential of human preadipocytes is inversely correlated with obesity, whereas the pool of precursors cells was positively correlated to BMI, suggesting that the obese microenvironment is capable of inducing proliferation of human preadipocytes while inhibiting their differentiation (Permana et al., 2004, Isakson et al., 2009). Medium conditioned by macrophages stimulates proliferation of human preadipocytes in vitro (Lacasa et al., 2007, Keophiphath et al., 2009). The expression of MCP1 was increased in V-WAT but not SC-WAT of *Irs2*$^{-/-}$ females, providing yet an additional explanation for the enhanced proliferation and impaired proliferation of the APC population. Therefore, it seems quite likely that pro-inflammatory signals or cells that accumulate within adipose tissue with obesity might contribute to fat mass enlargement through paracrine effects on progenitor cells. In addition to increased expression of cytokines and adipokines, the population of immune cells was increased in V-WAT. Moreover, the expression of enzymes involved in synthesis and storage of lipids was altered in WAT of *Irs2*-deficienct mice, suggesting the possibility that although there are more adipocytes present in the WAT of these animals, these cells are not fully mature at a functional level. Indeed, WAT of *Irs2*$^{-/-}$ females regulation of lipolyis is resistant to catecholamines due to increased expression of HSL (Garcia-Barrado et al., 2011).

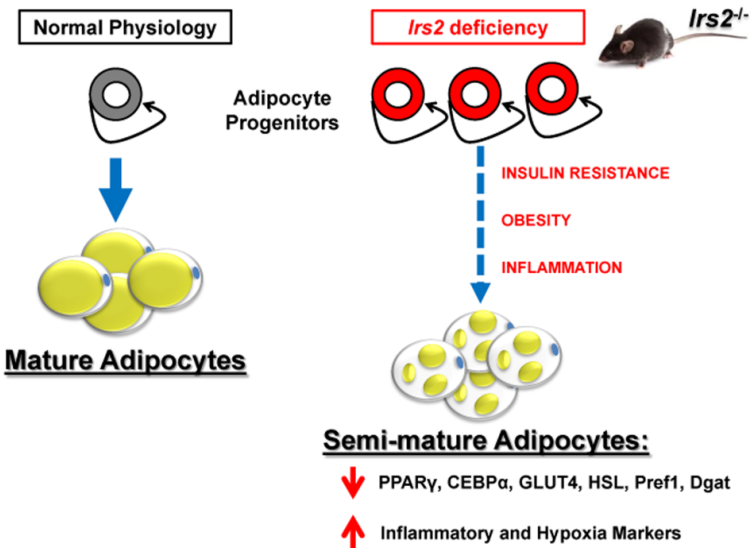

Figure 61: Propose model of the role of IRS2 in regulation of WAT.

OPN is up-regulated in adipose tissue of obese humans and murine models of obesity. OPN acts as a chemokine and an inflammatory cytokine that is expressed in many cell types including adipose tissue macrophages (M Zeyda, 2007, Kiefer et al., 2010, Zeyda et al., 2011). Loss of osteopontin *(Spp1$^{-/-}$)* prevents high-fat diet-induced obesity, and markedly improves insulin signalling and insulin sensitivity in the liver by reducing the presence of infiltrating macrophages. However, the relationship between OPN and insulin signalling has not been clearly defined. Thus, mice deficient for OPN (*Spp1*$^{-/-}$) were used to investigate the potential interaction between cytokine action and IRS2 signals. Additionally, the *Spp1*-deficient model was used to contrast the cytokine/adipokine profiles between an insulin resistant and an insulin sensitive model. *Spp1*$^{-/-}$ females maintained on a normal diet displayed a normal body weight. In contrast to the proinflammatory profile observed in *Irs2*$^{-/-}$ females, the expression of cytokines such as

IL6 and MCP1 were greatly reduced in WAT of *Spp1*$^{-/-}$ mice as were makers of hypoxia such as HIF1α and VEGFa. Interestingly, the expression of *Irs2* was up-regulated in WAT of *Spp1*$^{-/-}$ mice, whereas the expression of *Irs1* and *Irs3* were moderately down-regulated, an opposite pattern to that observed in *Irs2*$^{-/-}$ WAT. Additionally, the expression of the insulin receptor gene was also decreased in WAT of these mice, perhaps reflecting the presence of general insulin sensitivity. These observations suggest a relationship between inflammation, *Irs2* expression, and insulin sensitivity whereby *Irs2* is increased in an anti-inflammatory setting and diminished in a pro-inflammatory environment.

OPN inhibits expression of PPARγ and adiponectin in cultures of human preadipocytes (Zeyda et al., 2011) However, the precise role of OPN in regulating APC development and differentiation has not been characterized. The results of the present study reveal that the expression of genes required for efficient adipogenesis such as PPARγ are increased in WAT of *Spp1*$^{-/-}$ mice. Quantification of APC progenitors revealed a decrease in this population isolated from SC-WAT, whereas the population from V-SC was similar to WT controls. However, these *Spp1*$^{-/-}$ APC from SC-WAT differentiated more efficiently to adipocytes than WT controls based on the enhanced accumulation of lipid droplets in these cultures (Figure 62). These results contrast those obtained with *Irs2*$^{-/-}$APC where differentiation was impaired. The genetic approach used for this study suggest that that adipogenesis and adipocyte physiology are improved in *Opn*-deficiency but impaired in the absence of IRS2 signals. The key to these observations may be the presence of a pro-inflammatory environment in WAT of *Irs2*$^{-/-}$ females in contrast to the anti-inflammatory detected in *Spp1*$^{-/-}$ mice.

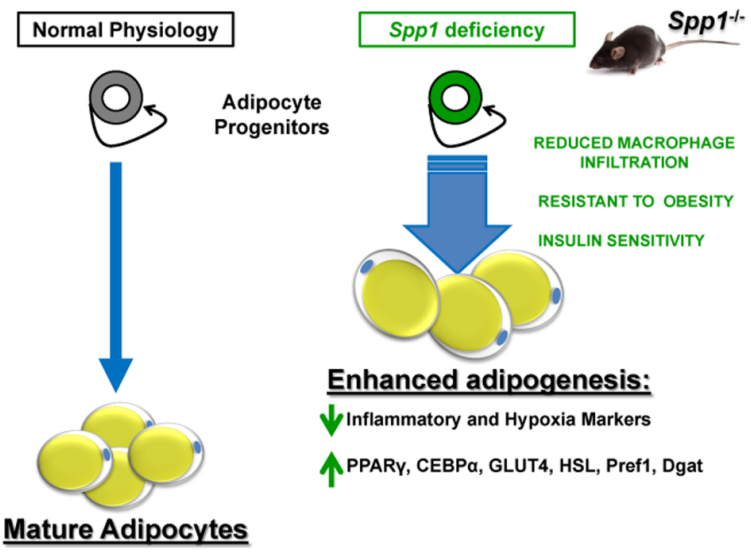

Figure 62: Propose model of the role of OPN in regulation of WAT.

Reversing or controlling the worldwide epidemic of obesity requires a more precise knowledge of adipogenesis and WAT function. Collectively, the observations of this study suggest that inflammation and loss of insulin sensitivity negatively modulate the population of adipocyte precursors which reside in WAT in vivo. Reduced IRS2 function causes insulin resistance and is associated with inflammation and impaired differentiation of APC to adipocytes. In contrast, loss of the cytokine OPN increase insulin sensitivity, reduces inflammation, and enhances adipogenesis. These findings reveal a potential therapeutic strategy of targeting obesity-associated inflammatory mediators including lifestyle changes and/or drugs that promote IRS2 expression.

CHAPTER 6

CONCLUSIONS

6. CONCLUSIONS

I. Deletion of *Irs2* causes increased accumulation of both visceral and subcutaneous adipose tissue in female mice. This adiposity may reflect a specific role for IRS2 signaling in the regulation of energy stores and/or the effects produced directly by *Irs2*-deficiency in pancreatic beta cells and liver.

II. The expression of cytokines and adipokines are dysregulated in *Irs2*-deficient female mice, reflecting a profile consistent with obesity-induced inflammation. The results of this study suggest that *Irs2* null mice represent a physiologically relevant model for studying the role of inflammation in the progression from pre-diabetes to diabetes.

III. The population of adipocyte progenitor cells located within the stroma-vascular fraction was increased in visceral WAT of I*rs2*-deficienct mice. *Irs2*-deficient progenitor cells from both visceral and subcutaneous WAT failed to differentiate to adipocytes *in vitro*. Impaired differentiation was associated with reduced expression of key adipogenic transcription factors such as PPARγ and C/EBPα *in vitro* and *in vivo*. Additionally *Irs2*-deficient APCs proliferated more rapidly in culture. Collectively, these results implicate a role for IRS2 signals in regulating the development and differentiation of adipocyte progenitors. IRS2 signaling may mediate the insulin-dependent transcriptional program of adipogenesis as well as in the regulation of proliferation. Maturation to

functional adipocytes may be particularly sensitive to loss of IRS2.

IV. In contrast to the *Irs2* model, the expression of cytokines and markers of inflammation are reduced in WAT of mice deficient for osteopontin (*Spp1*). *Irs2* expression was enhanced in *Spp1*$^{-/-}$ WAT. These observations suggest that reduced *Irs2* expression is associated with obesity and inflammation whereas anti-inflammatory settings such as *Spp1*-deficiency are associated with enhanced *Irs2* expression.

V. Adipocyte progenitors isolated *Spp1*$^{-/-}$ mice differentiate more efficiently to adipocytes *in vitro* than WT control progenitors. The enhanced differentiation was associated with increased expression of PPARγ. These findings suggest that cytokines such as osteopontin may negatively regulate adipocyte differentiation.

7. RESUMEN

INTRODUCCIÓN

Insulina y acciones fisiológicas

La insulina es la hormona anabolizante más importante, es secretada por las células β pancreáticas de los islotes de Langerhans y es responsable del control de los niveles de glucosa circulantes. Además posee importantes acciones a nivel de desarrollo, diferenciación y crecimiento. A nivel de metabolismo, los órganos diana de la insulina son el hígado, el músculo y el tejido adiposo. Sus funciones incluyen la regulación de la incorporación de glucosa en el músculo y en el tejido adiposo, la gluconeogénesis y lipogénesis en el hígado así como la lipogénesis y la adipogénesis en el tejido adiposo. También tiene la capacidad de influir en el apetito al actuar sobre el hipotálamo junto con la acción de la leptina. Además, la insulina, a través de su ruta se señalización puede participar en la expresión de genes, en la síntesis de proteínas y en proliferación y supervivencia celular.

La insulina ejerce su función a través de su interacción con el receptor de insulina (IR) que transmite la señal a través de la fosforilación, gracias a su actividad quinasa, a las proteínas IRS (del inglés Insulin Receptor Substrate). A partir de aquí se activan una serie de rutas en las que están involucradas otras proteínas tales como AKT y MAP quinasas entre otras, cuya consecuencia final es la activación de proteínas y factores de transcripción que regulan la expresión génica con consecuencias en el metabolismo, crecimiento, diferenciación y supervivencia celular.

Modelo deficiente en IRS2: ratón *Irs2*$^{-/-}$.

Los ratones deficientes en la proteína IRS2 son un 10% más pequeños que los silvestres, muestran un descenso en la masa de células β que junto con la resistencia a insulina que también acompaña a este modelo, desencadenan la aparición de diabetes tipo 2. Además, las hembras deficientes en IRS2 desarrollan obesidad por un incremento del tejido adiposo y una desregulación del sistema hipotalámico que a través de la leptina regula el apetito, provocando una mayor ingesta de alimento en ratones deficientes para IRS2. Añadir además la relación entre el sistema reproductivo y la función de IRS2, siendo las hembras *Irs2*$^{-/-}$ infértiles.

Diabetes Mellitus tipo 2

La diabetes Mellitus (DM) es una enfermedad metabólica caracterizada por niveles altos de glucosa en sangre. Principalmente existen dos tipos de DM. La DM tipo 1 es una enfermedad autoinmune en la que se desarrollan anticuerpos que atacan a las células beta del páncreas, encargadas de la síntesis de insulina, resultando en una falta total de ésta, y por lo tanto, una necesidad absoluta de aporte exógeno. El otro tipo es la DM tipo 2, mucho más frecuente que la anterior, que se desarrolla por una resistencia a la acción de la insulina sobre los tejidos periféricos (hígado, musculo y tejido adiposo principalmente) que acaba por un fallo en la secreción de ésta, apareciendo una hiperinsulinemia inicial que trata de compensar la falta de acción, seguida de un fallo en la síntesis debida a la desaparición progresiva de las células β pancreáticas, que por tanto desencadena la aparición de DM. La estrategia terapéutica seguida en la DM tipo 1 es el aporte exógeno de insulina, mientras

que en la DM tipo 2, acciones en la dieta y ejercicio pueden regular inicialmente la glucemia de los pacientes, aunque a medida que aparecen las complicaciones de la resistencia a insulina, fármacos hipoglucemiantes e incluso en último caso, insulina exógena, acaban siendo necesarias para el control de la glucemia.

El estudio “Di@betes” es el estudio epidemiológico más importante hecho hasta ahora en territorio español, tasa en un 13,8% la prevalencia de DM en población mayor de 18 años. Mientras que a nivel mundial los estudios estiman que en 2025 habrá 300 millones de personas con DM, suponiendo esto un 5,4% de la población mundial, siendo el aumento más pronunciado en países en desarrollo.

La DM forma parte del conjunto de enfermedades presentes en el Síndrome Metabólico (SM) y, junto con la obesidad, es considerada por la Organización Mundial de la Salud (WHO, por sus siglas en inglés) como el mayor riesgo para padecer muerte cardiovascular.

Además de las consecuencias de la glucotoxicidad y la resistencia a insulina presente en la DM, ésta a su vez se acompaña de un estado inflamatorio reactivo que causa una retroalimentación a la DM empeorando la deficiente señalización por insulina en los tejidos periféricos e impidiendo en normal funcionamiento de la célula β pancreática. Citoquinas como Factor de Necrosis Tumoral α (TNF-α por sus siglas en inglés) o las interleuquinas 1 y 6 (IL-1, IL-6) son ya reconocidos como agentes que entorpecen la acción de la insulina inhibiendo/promoviendo fosforilaciones que dificultan la transmisión de la señal, por ejemplo, inactivando a las proteínas IRS mediante fosforilación en residuos de serina/treonina.

Obesidad y tejido adiposo

La obesidad ha sido descrita por la WHO como la pandemia del siglo XXI afectando a más de 1 billón de personas en todo el mundo. Se define como un exceso de masa corporal como consecuencia de un desequilibrio entre un mayor aporte de energía a la que es capaz de consumir el organismo, agravada a su vez por factores ambientales, genéticos y psicosociales. El índice de masa corporal (BMI por sus siglas en inglés) es la herramienta que ha sido utilizada para diagnosticar los distintos grados de obesidad, aunque hoy en día se encuentre en entredicho por la importancia que está adquiriendo la distribución de la grasa en el cuerpo. El BMI es un parámetro obtenido al dividir el peso en kilogramos entre el cuadrado de la altura en metros (BMI=kg/m^2), considerando individuos con sobrepeso a aquellos con un BMI≥ 25 y obesidad cuando BMI ≥ 30.

En la obesidad se produce un aumento del tejido adiposo, fenómeno que ha sido explicado por dos teorías, la hiperplasia y la hipertrofia de los adipocitos, aunque actualmente se postula que lo que ocurre es una combinación de ambas. La hiperplasia es un aumento del tejido adiposo por un aumento en el número de adipocitos tras la diferenciación de células progenitoras presentes en el nicho del tejido adiposo, sin embargo, la hipertrofia es un aumento del tamaño de los adipocitos ya presentes, aumentando así su capacidad para almacenar triglicéridos.

El tejido adiposo es el órgano encargado de almacenar el exceso de energía en forma de lípidos y es uno de los tejidos más importantes metabólicamente hablando, tanto como almacén de lípidos como por ser el encargado de su movilización ante necesidades. Además de este papel pasivo de depósito energético, hoy en día se considera al tejido adiposo cómo un órgano metabólicamente activo con funciones

endocrinas, paracrinas y autocrinas que influyen de una forma importante en la homeostasis general del organismo, influyendo en el metabolismo lípidos y glucosa, inflamación y regulación del apetito entre otros.

El origen embrionario del tejido adiposo es el mesodermo, junto con músculo y huesos. Las células mesenquimales (MSC por sus siglas en inglés) provenientes de esta capa embrionaria son capaces de diferenciarse a adipocitos, osteoblastos, condrocitos y mioblastos, aunque el número exacto de pasos hasta que las MSC se convierten en adipocitos maduros no está bien establecido.

Existen dos tipos de tejido adiposo: blanco y marrón, con un mismo origen embrionario pero con funciones metabólicas muy distintas. El tejido adiposo blanco (WAT, por sus siglas en inglés) está encargado principalmente para la reserva energética y el tejido adiposo marrón (BAT, por sus siglas en inglés), por el contrario, está encargado de disipar la energía que sobra en forma de calor por un proceso denominado termogénesis. Ambos tipos de tejido adiposo se distribuyen por el cuerpo de forma distinta, mientras que los mayores depósitos de WAT se localizan principalmente en la zona intra-abdominal (tejido visceral) y de una forma subcutánea en nalgas, muslos y abdomen. Por el contrario, depósitos de BAT son más abundantes en la etapa postnatal reduciéndose en el etapa adulta a pequeños depósitos en la zona cervical, supraclavicular y paravertebral. Ambos no presentan diferencias única y exclusivamente en cuanto a coloración, sino también en cuanto a su morfología, distribución, expresión genes y función. También hay diferencias en cuanto a vascularización, tamaño celular, expresión de receptores de esteroides y factores de crecimiento y expresión de proteínas. Además, tanto WAT como BAT están enervados por

distintos sistemas, mientras que el sistema adrenérgico está encargado del control del WAT, el noradrenérgico se encarga del BAT. El tejido adiposo marrón posee adipocitos multiloculares con abundantes mitocondrias que expresan altas cantidades de proteína desacoplante 1 (UCP-1), la cual es responsable de la actividad termogénica de este tejido. Por el contrario, el tejido adiposo blanco está formado por adipocitos uniloculares, que al contrario que los adipocitos del BAT, producen por ejemplo, leptina, una hormona que informa al cerebro del estado nutricional para regular la ingesta y el gasto energético. Además de las diferencias existentes entre el WAT y el BAT, dentro del WAT, en función de su localización, también existen diferencias entre el tejido adiposo blanco visceral (V) o subcutáneo (SC). Adipocitos de depósitos V son menos sensibles a la insulina que los que se localizan en el tejido SC, y por tanto, a los efectos lipogénicos de ésta. La capacidad reguladora del metabolismo de los lípidos la ejercen los adipocitos gracias a un conjunto de proteínas reguladoras, entre otras cabe destacar: lipoproteína Lipasa (LPL), transportadores de ácidos grasos, proteínas de unión a ácidos grasos (FABP, por sus siglas en inglés), fosfoenolpiruvato carboxilasa (PEPCK, por sus siglas en inglés), perilipina, hormona sensible a la lipasa (HSL, por sus siglas en inglés) y por último, los transportadores de glucosa (GLUT), en concreto GLUT4.

Cómo se ha comentado antes, la función principal del WAT es almacenar triglicéridos (TG) en los momentos de exceso energético o liberar ácidos grasos (AG) cuando las necesidades energéticas así lo requieran, pero además en el WAT se produce la síntesis de adipoquinas, hormonas y citoquinas tanto por lo adipocitos como por otras células presentes en el tejido adiposo, como macrófagos y linfocitos T, de ahí el importante papel del WAT a nivel endocrino,

autocrino y paracrino. Entre las adipoquinas y citoquinas que se sintetizan desde el WAT cabe destacar: la LEPTINA (gen *ob*), la ADIPONECTINA (gen *adipoq*); la RESISTINA (gen *retn*); la Proteína de unión al retinol 4 (RBP4, por sus siglas en inglés, gen *rbp4*); TNFα, (gen *tnfa*); IL6 (gen *il6*); Proteína quimioatrayente de monocitos 1 (MCP1, por sus siglas en inglés, gen *Ccl2*). Estas moleculas son el nexo de unión entre la obesidad, la diabetes y la inflamación que construyen una compleja red de retroalimentación en la que también se implican otros sistemas del organismo.

Células progenitoras de adipocitos (APC)

Son las células madre adultas presentes en el tejido adiposo procedentes de células mesenquimales. Aunque las células progenitoras son más abundantes en las etapas tempranas de la vida, también están presentes en la etapa adulta del organismo. Se pueden localizar en la fracción estroma-vascular del tejido adiposo (SVF, por sus siglas en inglés) tras una digestión enzimática del WAT y un posterior aislamiento mediante marcajes específicos con anticuerpos, entre ellos Sca1+ (antígeno específico de células madre de ratón), CD45- (antígeno común de leucocitos), CD34+ (proteína presente en células del estroma) y Ter119– (molécula de superficie de plaquetas) entre otros. Hay que destacar las diferencias existentes en cuanto a proliferación, capacidad de diferenciación y expresión de genes de APC aisladas de distintas fuentes de tejido adiposo, por lo que acaban siendo funcionalmente diferentes. El proceso por el cual los progenitores acaban siendo adipocitos maduros y funcionales se denomina adipogénesis y aparece tanto en etapas jóvenes como adultas ante la necesidad de renovación celular cómo la de nuevas células para aumentar la masa de tejido adiposo en obesidad. La adipogénesis conlleva 4 estadios: interrupción de proliferación,

expansión clonal, diferenciación temprana y diferenciación tardía. Esta última etapa ha sido ampliamente estudiada en líneas celulares de preadipocitos murinos como los 3T3L1 y en ella intervienen numerosos factores, entre los que cabe destacar:

- PPARγ: receptor nuclear clave en la adipogénesis cuya expresión es obligatoria para la diferenciación completa hacia adipocitos maduros.
- Familia C/EBPs: formadas por las proteínas C/EBP α, β, δ, ε, ξ. Las isoformas α, β y δ son las implicadas en la adipogénesis.
- ADD1/ SREBP1: proteína que se expresa de forma tardía en la diferenciación. Interactúa directamente con PPARγ y con ello regula la actividad de genes relacionados con el metabolismo de ácigos grasos y TGC.

Osteopontina

La osteopontina es una molécula expresada por macrófagos activos, linfocitos T, osteoclastos, hepatocitos y células endoteliales, epiteliales y de la musculatura lisa de la vasculatura. Tiene un papel esencial en la respuesta inmunitaria y en los procesos de inflamación a nivel sistémico además de estar involucrada en la patología de la esteatosis hepática no alcohólica asociada a la obesidad (NAFDL, por sus siglas en inglés). Además la OPN favorece la infiltración de macrófagos en obesidad que ayuda al desarrollo de resistencia a insulina en el tejido adiposo, con consecuencias ya mencionadas previamente.

Durante la estancia en el laboratorio del Dr. Thomas Stulnig en Viena se utilizaron ratones deficientes en Osteopontina (OPN, gen *Spp1*). Se ha descrito que el modelo deficiente en osteopontina *Spp1*$^{-/-}$ es

resistente a las complicaciones metabólicas e inflamatorias que se desarrollan en la obesidad inducida por una dieta rica en grasa, tanto a nivel hepático, evitando la esteatosis, como a nivel del tejido adiposo, mejorando la sensibilidad a la insulina y disminuyendo la infiltración de macrófagos responsables del aumento de marcadores de inflamación. Por ello, este modelo es una importante herramienta para estudiar la importancia de la inflamación, o mejor dicho, la ausencia de ésta en el proceso de diferenciación hacia adipocitos de las células progenitoras residentes en el tejido adiposo.

HIPÓTESIS Y OBJETIVOS

Defectos en la señalización por insulina están implicados en la aparición de DM tipo 2 y obesidad. La deficiencia en *Irs2* produce resistencia a insulina y defectos en las células beta pancreática en ratones. Además las hembras deficientes en *Irs2* desarrollan obesidad y resistencia a leptina y catecolaminas. Sin embargo, la función exacta que desempeña IRS2 en el tejido adiposo está aún por esclarecer. Además, teniendo en cuenta el papel de la osteopontina en la inflamación del tejido adiposo, postulamos que puede existir una relación entre la función de la osteopontina en el WAT y la señalización por IRS2. Para definir el papel de IRS2 en adipogénesis y obesidad se proponen los siguientes objetivos:

1. Caracterización del tejido adiposo blanco de hembras deficientes en *Irs2* estudiando marcadores funcionales de adipocitos, de inflamación así como de la señalización de insulina.

2. Aislamiento y caracterización de APC de grasa y determinación del papel de IRS2 en la diferenciación y proliferación de estas células.
3. Evaluar la posible relación fisiológica entre la señalización por IRS2 y la citoquina OPN mediante el estudio de tejido adiposo procedente de ratones hembras *Irs2*$^{-/-}$ y *Spp1*$^{-/-}$.

MATERIAL Y MÉTODOS

Animales de estudio

Hembras silvestres y deficientes en IRS2 (*Irs2*$^{-/-}$) de la cepa C57BL/6J de 12-16 semanas de edad. Los procedimientos empleados están aprobados por el Comité de Ética y Bienestar Animal (CEBA) del CIPF. Animales silvestres y deficientes en osteopontina (*Spp1*$^{-/-}$) de la cepa C57BL/6J de 12-14 semanas de edad del laboratorio del Dr. Stulnig en Viena utilizados durante la colaboración científica.

Análisis de glucosa y hormonas en sangre

Extracción de suero de la sangre de los ratones en ayunas y posterior determinación de glucosa (tiras reactivas), insulina (ELISA) y adipoquinas y otras citoquinas por Luminex®.

Análisis histológico del tejido adiposo

Cortes histológicos en parafina y análisis morfológico de los adipocitos mediante tinción de Hematoxilina/Eosina.

Análisis de la grasa V y SC del modelo deficiente para *Irs2* y para Osteopontina (*Spp1*$^{-/-}$).

Extracción de mRNA mediante Trizol® y posterior estudio por PCR cuantitativa de los genes involucrados en la señalización de insulina, la adipogénesis e inflamación en el tejido adiposo V y SC así como estudio mediante western blot de las proteínas más importantes de los procesos señalados anteriormente.

Aislamiento e identificación de APC

Para el aislamiento enzimático se siguió un protocolo modificado del publicado por Smith-Hall J et al. y posteriormente se identificaron utilizando los marcadores: Sca1, CD34, CD45, CD31 y Ter119, junto con DAPI para el marcaje de viabilidad.

- Aislamiento de APC mediante MACS®: utilizando anticuerpos conjugados a microbolas magnéticas. Las poblaciones celulares se aíslan haciendo usos de imanes y las distintas combinaciones de los anticuerpos.
- Aislamiento de APC mediante FACS: utilizando anticuerpos conjugados con fluorocromos. Las poblaciones celulares se aíslan utilizando un clitómetro High Speed Cell Sorter MoFlo equipado con 3 láseres con los que excitar los distintos fluorocromos y poder así aislar las poblaciones de interés.

Cultivo de las APC

Para el cultivo rutinario, tras su aislamiento por FACS o MACS se cultivaron en medio DMEM, 10% Suero Bovino Fetal de un clon específico (FcBS) y 10ng/mL de FGFβ. Se realizaron ensayos celulares de proliferación y apoptosis.

Para la diferenciación hacia adipocitos maduros, las APC se dejaron crecer hasta 100% de confluencia con el medio de cultivo descrito anteriormente y luego se cultivaron en un medio formado por DMEM avanzado (aDMEM/F12) y suero bovino fetal (FBS, por sus siglas en inglés) con diferentes factores (insulina (INS), dexametasona (DXM) e isobutilmetilxantina (IBMX)) para la diferenciación hacia adipocitos maduros como se indica en la tabla:

día -3 a 0	**día 0 a 4**	**día 4 a 7**	**día 7 a 12**
DMEM	aDMEM/F12	aDMEM/F12	aDMEM/F12
10% FcBS	5% FBS	5% FBS	5% FBS
10ng/mL βFGF	INS 20µg/mL	INS 20µg/mL	
	DXM 10µM		
	IBMX 0.5mM		

Se tomaron muestras a días 0, 4 y 10 para su posterior estudio molecular con técnicas de inmunotinción, citometría de flujo, western blot y PCR cuantitativa para evaluar la diferenciación mediante la expresión de marcadores clave en la adipogénesis tales como las proteínas relacionadas con la señalización de insulina así como aquellas que directamente intervienen en la adipogenesis como PPARγ.

Análisis estadístico

Para evaluar si las diferencias obtenidas en los resultados eran estadísticamente significativas, se utilizaron los programas GraphPad Prism 5 y Microsoft Excel con la función del test *t* de Student.

CONCLUSIONES

I. La ausencia en ratones hembras de *Irs2* en provoca un aumento del tejido adiposo tanto visceral como subcutáneo. Este aumento puede relacionar la señalización por IRS2 con la regulación de las reservas energéticas.

II. Los niveles de expresión de citoquinas y adipoquinas en el tejido adiposo están alterados en hembras deficientes para *Irs2*, algo relacionado con la inflamación presente en la obesidad. Por ello el modelo deficiente en *Irs2* podría ser relevante para estudiar que papel juega la inflamación en la progresión desde un estado prediabético a la aparición de diabetes.

III. Hay un aumento de células progenitoras de adipocitos en el tejido adiposo visceral de ratones deficientes para *Irs2* pero estas células tienen alterado el mecanismo molecular de la adipogenesis *in vitro.* Además los progenitores aislados del tejido adiposo de ratones deficientes para *Irs2* proliferan más rápido que los controles. Todo ello indica que IRS2 está involucrada en la diferenciación dependiente de insulina de los adipocitos así como en la regulación de la proliferación.

IV. La deficiencia de osteopontina causa una reducción en todos los marcadores de inflamación en el tejido adiposo. Adamas la expresión de *Irs2* está aumentada en grasa.

V. Celulas progenitoras de adipocitos aisladas del tejido adiposo de ratones deficientes para osteopontina diferencian mejor que los progenitores aislados de ratones controles. Por ellos citoquinas como la osteopontina entorpecen la diferenciación completa hacia adipocitos.

REFERENCES

ADILSON GUILHERME, J. V. V., VISHWAJEET PURI & MICHAEL P. CZECH 2008. Adipocyte dysfunctions linking obesity to insulin resistance and type 2 diabetes. *Nature Reviews Molecular Cell Biology,* 9**,** 367-377.

ALARCON, B., BERKHOUT, B., BREITMEYER, J. & TERHORST, C. 1988. Assembly of the human T cell receptor-CD3 complex takes place in the endoplasmic reticulum and involves intermediary complexes between the CD3-gamma. delta. epsilon core and single T cell receptor alpha or beta chains. *Journal of Biological Chemistry,* 263**,** 2953-2961.

AMOS, A. F., MCCARTY, D. J. & ZIMMET, P. 1997. The rising global burden of diabetes and its complications: estimates and projections to the year 2010. *Diabetic medicine,* 14**,** S7-S85.

ANTUNA-PUENTE, B., FEVE, B., FELLAHI, S. & BASTARD, J. P. 2008. Adipokines: The missing link between insulin resistance and obesity. *Diabetes & Metabolism,* 34**,** 2-11.

ARMULIK, A., ABRAMSSON, A. & BETSHOLTZ, C. 2005. Endothelial/pericyte interactions. *Circulation research,* 97**,** 512-523.

ASHKAR, S., WEBER, G. F., PANOUTSAKOPOULOU, V., SANCHIRICO, M. E., JANSSON, M., ZAWAIDEH, S., RITTLING, S. R., DENHARDT, D. T., GLIMCHER, M. J. & CANTOR, H. 2000. Eta-1 (Osteopontin): An Early Component of Type-1 (Cell-Mediated) Immunity. *Science,* 287**,** 860-864.

BANEGAS, J., LOPEZ-GARCIA, E., GUTIERREZ-FISAC, J., GUALLAR-CASTILLON, P. & RODRIGUEZ-ARTALEJO, F. 2003. A simple estimate of mortality attributable to excess weight in the European Union. *European Journal of Clinical Nutrition,* 57**,** 201-208.

BARBOSA-DA-SILVA, S., FRAULOB-AQUINO, J. C., LOPES, J. R., MANDARIM-DE-LACERDA, C. A. & AGUILA, M. B. 2012. Weight Cycling Enhances Adipose Tissue Inflammatory Responses in Male Mice. *PLoS ONE,* 7**,** e39837.

BASKIN, D. G., FIGLEWICZ LATTEMANN, D., SEELEY, R. J., WOODS, S. C., PORTE JR, D. & SCHWARTZ, M. W. 1999. Insulin and leptin: dual adiposity signals to the brain for the regulation of food intake and body weight. *Brain research,* 848**,** 114-123.

BASTARD, J.-P., JARDEL, C., BRUCKERT, E., BLONDY, P., CAPEAU, J., LAVILLE, M., VIDAL, H. & HAINQUE, B. 2000. Elevated levels of interleukin 6 are reduced in serum and subcutaneous adipose tissue of obese women after weight

loss. *Journal of Clinical Endocrinology & Metabolism,* 85**,** 3338-3342.
BASTARD, J.-P., MAACHI, M., VAN NHIEU, J. T., JARDEL, C., BRUCKERT, E., GRIMALDI, A., ROBERT, J.-J., CAPEAU, J. & HAINQUE, B. 2002. Adipose tissue IL-6 content correlates with resistance to insulin activation of glucose uptake both in vivo and in vitro. *Journal of Clinical Endocrinology & Metabolism,* 87**,** 2084-2089.
BEALE, E. G., FOREST, C. & HAMMER, R. E. 2003. Regulation of cytosolic phosphoenolpyruvate carboxykinase gene expression in adipocytes. *Biochimie,* 85**,** 1207-1211.
BELKINA, A. C. & DENIS, G. V. 2010. Obesity genes and insulin resistance. *Current Opinion in Endocrinology, Diabetes and Obesity,* 17**,** 472-477 10.1097/MED.0b013e32833c5c48.
BELL, G. I., PICTET, R. L., RUTTER, W. J., CORDELL, B., TISCHER, E. & GOODMAN, H. M. 1980. Sequence of the human insulin gene. *Nature,* 284**,** 26-32.
BELL, R. M. & COLEMAN, R. A. 1980. Enzymes of glycerolipid synthesis in eukaryotes. *Annual review of biochemistry,* 49**,** 459-487.
BERTOLA, A., DEVEAUX, V., BONNAFOUS, S., ROUSSEAU, D., ANTY, R., WAKKACH, A., DAHMAN, M., TORDJMAN, J., CLÉMENT, K. & MCQUAID, S. E. 2009. Elevated expression of osteopontin may be related to adipose tissue macrophage accumulation and liver steatosis in morbid obesity. *Diabetes,* 58**,** 125-133.
BIDDINGER, S. B. & KAHN, C. R. 2006. From mice to men: insights into the insulin resistance syndromes. *Annu Rev Physiol,* 68**,** 123-58.
BJÖRNHOLM, M., HE, A., ATTERSAND, A., LAKE, S., LIU, S., LIENHARD, G., TAYLOR, S., ARNER, P. & ZIERATH, J. 2002. Absence of functional insulin receptor substrate-3 (IRS-3) gene in humans. *Diabetologia,* 45**,** 1697-1702.
BJÖRNTORP, P. 1974. Size, number and function of adipose tissue cells in human obesity. *Hormone and metabolic research= Hormon-und Stoffwechselforschung= Hormones et métabolisme***,** 77.
BJÖRNTORP, P. 1990. "Portal" adipose tissue as a generator of risk factors for cardiovascular disease and diabetes. *Arteriosclerosis, Thrombosis, and Vascular Biology,* 10**,** 493-6.
BJÖRNTORP, P. 1991a. Adipose tissue distribution and function. *International Journal of Obesity,* 15 Suppl 2**,** 67-81.
BJÖRNTORP, P. 1991b. Metabolic implications of body fat distribution. *Diabetes Care,* 14**,** 1132-1143.

BJÖRNTORP, P., KARLSSON, M. & PETTERSSON, P. 1982. Expansion of adipose tissue storage capacity at different ages in rats. *Metabolism,* 31**,** 366-373.

BLÜHER, M., MICHAEL, M. D., PERONI, O. D., UEKI, K., CARTER, N., KAHN, B. B. & KAHN, C. R. 2002. Adipose tissue selective insulin receptor knockout protects against obesity and obesity-related glucose intolerance. *Developmental cell,* 3**,** 25-38.

BLUMBERG, R. S., LEY, S., SANCHO, J., LONBERG, N., LACY, E., MCDERMOTT, F., SCHAD, V., GREENSTEIN, J. L. & TERHORST, C. 1990. Structure of the T-cell antigen receptor: evidence for two CD3 epsilon subunits in the T-cell receptor-CD3 complex. *Proceedings of the National Academy of Sciences,* 87**,** 7220-7224.

BOARD, M., BOLLEN, M., STALMANS, W., KIM, Y., FLEET, G. & JOHNSON, L. 1995. Effects of C-1-substituted glucose analogue on the activation states of glycogen synthase and glycogen phosphorylase in rat hepatocytes. *Biochemical Journal,* 311**,** 845.

BÖHNI, R., RIESGO-ESCOVAR, J., OLDHAM, S., BROGIOLO, W., STOCKER, H., ANDRUSS, B. F., BECKINGHAM, K. & HAFEN, E. 1999. Autonomous Control of Cell and Organ Size by CHICO, a< i> Drosophila</i> Homolog of Vertebrate IRS1–4. *Cell,* 97**,** 865-875.

BOUCHARD, C. 1997. Genetic determinants of regional fat distribution. *Human reproduction,* 12**,** 1-5.

BOUCHARD, C., DESPRES, J.-P. & MAURIEGE, P. 1993. Genetic and nongenetic determinants of regional fat distribution. *Endocrine reviews,* 14**,** 72-93.

BOUCHARD, C. & PERUSSE, L. 1993. Genetics of Obesity. *Annual Review of Nutrition,* 13**,** 337-354.

BOURA-HALFON, S. & ZICK, Y. 2009. Phosphorylation of IRS proteins, insulin action, and insulin resistance. *American Journal of Physiology-Endocrinology And Metabolism,* 296**,** E581-E591.

BRADY, M. J. 2004. IRS2 takes center stage in the development of type 2 diabetes. *The Journal of Clinical Investigation,* 114**,** 886-888.

BROWN, M. S. & GOLDSTEIN, J. L. 1997. The SREBP Pathway: Regulation review of cholesterol metabolism by proteolysis of a membrane-bound transcription factor. *Cell,* 89**,** 331-340.

BRUNING, J. C., GAUTAM, D., BURKS, D. J., GILLETTE, J., SCHUBERT, M., ORBAN, P. C., KLEIN, R., KRONE, W., MULLER-WIELAND, D. & KAHN, C. R. 2000. Role of Brain Insulin Receptor in Control of Body Weight and Reproduction. *Science,* 289**,** 2122-2125.

BURKS, D. J., DE MORA, J. F., SCHUBERT, M., WITHERS, D. J., MYERS, M. G., TOWERY, H. H., ALTAMURO, S. L., FLINT, C. L. & WHITE, M. F. 2000. IRS-2 pathways integrate female reproduction and energy homeostasis. *Nature,* 407**,** 377-382.

BURKS, D. J., PONS, S., TOWERY, H., SMITH-HALL, J., MYERS JR, M. G., YENUSH, L. & WHITE, M. F. 1997. Heterologous pleckstrin homology domains do not couple IRS-1 to the insulin receptor. *Journal of Biological Chemistry,* 272**,** 27716-27721.

BURKS, D. J., WANG, J., TOWERY, H., ISHIBASHI, O., LOWE, D., RIEDEL, H. & WHITE, M. F. 1998. IRS pleckstrin homology domains bind to acidic motifs in proteins. *Journal of Biological Chemistry,* 273**,** 31061-31067.

BURKS, D. J. & WHITE, M. F. 2001. IRS proteins and beta-cell function. *Diabetes,* 50 Suppl 1**,** S140-5.

CAI, D., DHE-PAGANON, S., MELENDEZ, P. A., LEE, J. & SHOELSON, S. E. 2003. Two new substrates in insulin signaling, IRS5/DOK4 and IRS6/DOK5. *Journal of Biological Chemistry,* 278**,** 25323-25330.

CALABRO, P., SAMUDIO, I., WILLERSON, J. T. & YEH, E. T. H. 2004. Resistin Promotes Smooth Muscle Cell Proliferation Through Activation of Extracellular Signal–Regulated Kinase 1/2 and Phosphatidylinositol 3-Kinase Pathways. *Circulation,* 110**,** 3335-3340.

CALLE, M. C. & FERNANDEZ, M. L. 2012. Inflammation and type 2 diabetes. *Diabetes & Metabolism,* 38**,** 183-191.

CAMPBELL, I. W. 2000. Antidiabetic Drugs Present and Future. *Drugs,* 60**,** 1017-1028.

CANCELLO, R., HENEGAR, C., VIGUERIE, N., TALEB, S., POITOU, C., ROUAULT, C., COUPAYE, M., PELLOUX, V., HUGOL, D., BOUILLOT, J.-L., BOULOUMIÉ, A., BARBATELLI, G., CINTI, S., SVENSSON, P.-A., BARSH, G. S., ZUCKER, J.-D., BASDEVANT, A., LANGIN, D. & CLÉMENT, K. 2005. Reduction of Macrophage Infiltration and Chemoattractant Gene Expression Changes in White Adipose Tissue of Morbidly Obese Subjects After Surgery-Induced Weight Loss. *Diabetes,* 54**,** 2277-2286.

CANNON, B., HEDIN, A. & NEDERGAARD, J. 1982. Exclusive occurrence of thermogenin antigen in brown adipose tissue. *FEBS letters,* 150**,** 129-132.

CANNON, B. & NEDERGAARD, J. 2004. Brown adipose tissue: function and physiological significance. *Physiological reviews,* 84**,** 277-359.

CAO, Z., UMEK, R. M. & MCKNIGHT, S. L. 1991. Regulated expression of three C/EBP isoforms during adipose

conversion of 3T3-L1 cells. *Genes & development,* 5**,** 1538-1552.

CARMELIET, P. 2003. Angiogenesis in health and disease. *Nature medicine,* 9**,** 653-660.

CASES, S., SMITH, S. J., ZHENG, Y.-W., MYERS, H. M., LEAR, S. R., SANDE, E., NOVAK, S., COLLINS, C., WELCH, C. B. & LUSIS, A. J. 1998. Identification of a gene encoding an acyl CoA: diacylglycerol acyltransferase, a key enzyme in triacylglycerol synthesis. *Proceedings of the National Academy of Sciences,* 95**,** 13018-13023.

CINTI, S. 2001a. The adipose organ: endocrine aspects and insights from transgenic models. *Eating and weight disorders: EWD,* 6**,** 4.

CINTI, S. 2001b. The adipose organ: morphological perspectives of adipose tissues. *Proceedings of the Nutrition Society,* 60**,** 319-328.

CINTI, S. 2005. The adipose organ. *Prostaglandins, Leukotrienes and Essential Fatty Acids,* 73**,** 9-15.

COFFER, P. J., JIN, J. & WOODGETT, J. R. 1998. Protein kinase B (c-Akt): a multifunctional mediator of phosphatidylinositol 3-kinase activation. *Biochemical Journal,* 335**,** 1.

CONSIDINE, R. V. & CARO, J. F. 1997. Leptin and the regulation of body weight. *The international journal of biochemistry & cell biology,* 29**,** 1255-1272.

CONSIDINE, R. V., NYCE, M. R., MORALES, L., MAGOSIN, S. A., SINHA, M. K., BAUER, T. L., ROSATO, E. L., COLBERG, J. & CARO, J. 1996. Paracrine stimulation of preadipocyte-enriched cell cultures by mature adipocytes. *American Journal of Physiology-Endocrinology And Metabolism,* 270**,** E895-E899.

COPPS, K. & WHITE, M. 2012. Regulation of insulin sensitivity by serine/threonine phosphorylation of insulin receptor substrate proteins IRS1 and IRS2. *Diabetologia,* 55**,** 2565-2582.

COPPS, K. D., HANCER, N. J., OPARE-ADO, L., QIU, W., WALSH, C. & WHITE, M. F. 2010. Irs1 serine 307 promotes insulin sensitivity in mice. *Cell Metab,* 11**,** 84-92.

CRAIG, A. M. & DENHARDT, D. T. 1991. The murine gene encoding secreted phosphoprotein 1 (osteopontin): promoter structure, activity, and induction in vivo by estrogen and progesterone. *Gene,* 100**,** 163-171.

CROSS, D. A., ALESSI, D. R., COHEN, P., ANDJELKOVICH, M. & HEMMINGS, B. A. 1995. Inhibition of glycogen synthase kinase-3 by insulin mediated by protein kinase B. *Nature,* 378**,** 785-789.

CHANG, L., CHIANG, S.-H. & SALTIEL, A. R. 2004. Insulin signaling and the regulation of glucose transport. *Molecular medicine,* 10**,** 65.

CHOUDHURY, A. I., HEFFRON, H., SMITH, M. A., AL-QASSAB, H., XU, A. W., SELMAN, C., SIMMGEN, M., CLEMENTS, M., CLARET, M., MACCOLL, G., BEDFORD, D. C., HISADOME, K., DIAKONOV, I., MOOSAJEE, V., BELL, J. D., SPEAKMAN, J. R., BATTERHAM, R. L., BARSH, G. S., ASHFORD, M. L. J. & WITHERS, D. J. 2005. The role of insulin receptor substrate 2 in hypothalamic and beta cell function. *The Journal of Clinical Investigation,* 115**,** 940-950.

CHOY, L. N., ROSEN, B. & SPIEGELMAN, B. M. 1992. Adipsin and an endogenous pathway of complement from adipose cells. *Journal of Biological Chemistry,* 267**,** 12736-12741.

DANDONA, P., ALJADA, A. & BANDYOPADHYAY, A. 2004. Inflammation: the link between insulin resistance, obesity and diabetes. *Trends in immunology,* 25**,** 4-7.

DANDONA, P., ALJADA, A., CHAUDHURI, A., MOHANTY, P. & GARG, R. 2005. Metabolic Syndrome A Comprehensive Perspective Based on Interactions Between Obesity, Diabetes, and Inflammation. *Circulation,* 111**,** 1448-1454.

DANI, C. & BILLON, N. 2012. Adipocyte Precursors: Developmental Origins, Self-Renewal, and Plasticity

Adipose Tissue Biology. *In:* SYMONDS, M. E. E. (ed.). Springer New York.

DARZYNKIEWICZ, Z., HALICKA, H. D. & ZHAO, H. 2010. Analysis of Cellular DNA Content by Flow and Laser Scanning Cytometry

Polyploidization and Cancer. *In:* POON, R. Y. C. (ed.). Springer New York.

DEREK LEROITH MD, P., JERROLD M OLEFSKY MD , SIMEON I TAYLOR MD, PHD 2003. *Diabetes Mellitus A Fundamental and Clinical Text*.

DI GREGORIO, G. B., YAO-BORENGASSER, A., RASOULI, N., VARMA, V., LU, T., MILES, L. M., RANGANATHAN, G., PETERSON, C. A., MCGEHEE, R. E. & KERN, P. A. 2005. Expression of CD68 and macrophage chemoattractant protein-1 genes in human adipose and muscle tissues association with cytokine expression, insulin resistance, and reduction by pioglitazone. *Diabetes,* 54**,** 2305-2313.

DONG, X., PARK, S., LIN, X., COPPS, K., YI, X. & WHITE, M. F. 2006. Irs1 and Irs2 signaling is essential for hepatic glucose homeostasis and systemic growth. *Journal of Clinical Investigation,* 116**,** 101-114.

DONG, X. C., COPPS, K. D., GUO, S., LI, Y., KOLLIPARA, R., DEPINHO, R. A. & WHITE, M. F. 2008. Inactivation of hepatic

Foxo1 by insulin signaling is required for adaptive nutrient homeostasis and endocrine growth regulation. *Cell metabolism,* 8**,** 65-76.

DORHEIM, M. A., SULLIVAN, M., DANDAPANI, V., WU, X., HUDSON, J., SEGARINI, P. R., ROSEN, D. M., AULTHOUSE, A. L. & GIMBLE, J. M. 1993. Osteoblastic gene expression during adipogenesis in hematopoietic supporting murine bone marrow stromal cells. *Journal of cellular physiology,* 154**,** 317-328.

DUCKWORTH, W. C. 1988. Insulin degradation: mechanisms, products, and significance. *Endocrine reviews,* 9**,** 319-345.

DULL, T. J., GRAY, A., HAYFLICK, J. S. & ULLRICH, A. 1984. Insulin-like growth factor II precursor gene organization in relation to insulin gene family.

ENGELMAN, J. A., LUO, J. & CANTLEY, L. C. 2006. The evolution of phosphatidylinositol 3-kinases as regulators of growth and metabolism. *Nature Reviews Genetics,* 7**,** 606-619.

ENGFELDT, P., HELLMÉR, J., WAHRENBERG, H. & ARNER, P. 1988. Effects of insulin on adrenoceptor binding and the rate of catecholamine-induced lipolysis in isolated human fat cells. *Journal of Biological Chemistry,* 263**,** 15553-15560.

EPSTEIN, F. H., MOLLER, D. E. & FLIER, J. S. 1991. Insulin resistance—mechanisms, syndromes, and implications. *New England Journal of Medicine,* 325**,** 938-948.

EXCELLENCE, N. I. F. H. A. C. 2006. *Obesity: The Prevention, Identification, Assessment and Management of Overweight and Obesity in Adults and Children* London.

FAIN, J. N., MADAN, A. K., HILER, M. L., CHEEMA, P. & BAHOUTH, S. W. 2004. Comparison of the release of adipokines by adipose tissue, adipose tissue matrix, and adipocytes from visceral and subcutaneous abdominal adipose tissues of obese humans. *Endocrinology,* 145**,** 2273-2282.

FAJAS, L., AUBOEUF, D., RASPÉ, E., SCHOONJANS, K., LEFEBVRE, A.-M., SALADIN, R., NAJIB, J., LAVILLE, M., FRUCHART, J.-C. & DEEB, S. 1997. The organization, promoter analysis, and expression of the human PPARγ gene. *Journal of Biological Chemistry,* 272**,** 18779-18789.

FAJAS, L., SCHOONJANS, K., GELMAN, L., KIM, J. B., NAJIB, J., MARTIN, G., FRUCHART, J.-C., BRIGGS, M., SPIEGELMAN, B. M. & AUWERX, J. 1999. Regulation of peroxisome proliferator-activated receptor γ expression by adipocyte differentiation and determination factor 1/sterol regulatory element binding protein 1: implications for adipocyte differentiation and metabolism. *Molecular and cellular biology,* 19**,** 5495-5503.

FALCÃO-PIRES, I., CASTRO-CHAVES, P., MIRANDA-SILVA, D., LOURENÇO, A. P. & LEITE-MOREIRA, A. F. 2012. Physiological, pathological and potential therapeutic roles of adipokines. *Drug Discovery Today,* 17**,** 880-889.

FANTIN, V. R., LAVAN, B. E., WANG, Q., JENKINS, N. A., GILBERT, D. J., COPELAND, N. G., KELLER, S. R. & LIENHARD, G. E. 1999. Cloning, tissue expression, and chromosomal location of the mouse insulin receptor substrate 4 gene. *Endocrinology,* 140**,** 1329-1337.

FASSHAUER, M., KLEIN, J., UEKI, K., KRIAUCIUNAS, K. M., BENITO, M., WHITE, M. F. & KAHN, C. R. 2000. Essential role of insulin receptor substrate-2 in insulin stimulation of Glut4 translocation and glucose uptake in brown adipocytes. *Journal of Biological Chemistry,* 275**,** 25494-25501.

FAVELYUKIS, S., TILL, J. H., HUBBARD, S. R. & MILLER, W. T. 2001. Structure and autoregulation of the insulin-like growth factor 1 receptor kinase. *Nature Structural & Molecular Biology,* 8**,** 1058-1063.

FAVRE, C., GERARD, A., CLAUZIER, E., PONTAROTTI, P., OLIVE, D. & NUNES, J. 2003. DOK4 and DOK5: new Dok-related genes expressed in human T cells. *Genes and immunity,* 4**,** 40-45.

FINUCANE, O. M., REYNOLDS, C. M., MCGILLICUDDY, F. C. & ROCHE, H. M. 2012. Insights into the role of macrophage migration inhibitory factor in obesity and insulin resistance. *Proceedings of the Nutrition Society,* FirstView**,** 11.

FISHER, L., TORCHIA, D., FOHR, B., YOUNG, M. & FEDARKO, N. 2001. Flexible structures of SIBLING proteins, bone sialoprotein, and osteopontin. *Biochemical and Biophysical Research Communications,* 280**,** 460-465.

FRIED, S. K., BUNKIN, D. A. & GREENBERG, A. S. 1998. Omental and subcutaneous adipose tissues of obese subjects release interleukin-6: depot difference and regulation by glucocorticoid. *Journal of Clinical Endocrinology & Metabolism,* 83**,** 847-850.

FRIED, S. K., RUSSELL, C. D., GRAUSO, N. L. & BROLIN, R. E. 1993. Lipoprotein lipase regulation by insulin and glucocorticoid in subcutaneous and omental adipose tissues of obese women and men. *Journal of Clinical Investigation,* 92**,** 2191.

FRIEDMAN, J. E., ISHIZUKA, T., LIU, S., FARRELL, C. J., BEDOL, D., KOLETSKY, R. J., KAUNG, H. L. & ERNSBERGER, P. 1997. Reduced insulin receptor signaling in the obese spontaneously hypertensive Koletsky rat. *Am J Physiol,* 273**,** E1014-23.

FRIEDMAN, J. M. & HALAAS, J. L. 1998. Leptin and the regulation of body weight in mammals. *Nature,* 395**,** 763-770.

GAO, C., GUO, H., DOWNEY, L., MARROQUIN, C., WEI, J. & KUO, P. C. 2003. Osteopontin-dependent CD44v6 expression and cell adhesion in HepG2 cells. *Carcinogenesis,* 24**,** 1871-1878.

GAO, G. F. & JAKOBSEN, B. K. 2000. Molecular interactions of coreceptor CD8 and MHC class I: the molecular basis for functional coordination with the T-cell receptor. *Immunology today,* 21**,** 630-636.

GARCIA-BARRADO, M. J., IGLESIAS-OSMA, M. C., MORENO-VIEDMA, V., PASTOR MANSILLA, M. F., GONZALEZ, S. S., CARRETERO, J., MORATINOS, J. & BURKS, D. J. 2011. Differential sensitivity to adrenergic stimulation underlies the sexual dimorphism in the development of diabetes caused by Irs-2 deficiency. *Biochemical pharmacology,* 81**,** 279-288.

GAVIN, J. R., ROTH, J., NEVILLE, D. M., DE MEYTS, P. & BUELL, D. N. 1974. Insulin-dependent regulation of insulin receptor concentrations: a direct demonstration in cell culture. *Proceedings of the National Academy of Sciences,* 71**,** 84-88.

GERDES, J., LEMKE, H., BAISCH, H., WACKER, H.-H., SCHWAB, U. & STEIN, H. 1984. Cell cycle analysis of a cell proliferation-associated human nuclear antigen defined by the monoclonal antibody Ki-67. *The Journal of Immunology,* 133**,** 1710-1715.

GERIN, I., CHA, H. C. & MACDOUGALD, O. A. 2006. Chapter 8 Regulation of adipocyte differentiation and metabolism by Wnt signaling and C/EBP transcription factors. *In:* JACOB, E. F. (ed.) *Advances in Molecular and Cellular Endocrinology.* Elsevier.

GESTA, S., BLUHER, M., YAMAMOTO, Y., NORRIS, A. W., BERNDT, J., KRALISCH, S., BOUCHER, J., LEWIS, C. & KAHN, C. R. 2006. Evidence for a role of developmental genes in the origin of obesity and body fat distribution. *Proc Natl Acad Sci U S A,* 103**,** 6676-81.

GESTA, S., TSENG, Y. H. & KAHN, C. R. 2007. Developmental origin of fat: tracking obesity to its source. *Cell,* 131**,** 242-56.

GIACHELLI, C. M., LOMBARDI, D., JOHNSON, R. J., MURRY, C. E. & ALMEIDA, M. 1998. Evidence for a role of osteopontin in macrophage infiltration in response to pathological stimuli in vivo. *The American journal of pathology,* 152**,** 353.

GLASS, C. K., ROSE, D. W. & ROSENFELD, M. G. 1997. Nuclear receptor coactivators. *Current opinion in cell biology,* 9**,** 222-232.

GLASS, C. K. & ROSENFELD, M. G. 2000. The coregulator exchange in transcriptional functions of nuclear receptors. *Genes & development,* 14**,** 121-141.

GLATZ, J. F. & STORCH, J. 2001. Unravelling the significance of cellular fatty acid-binding proteins. *Current opinion in lipidology,* 12**,** 267-274.

GOCZE, P. M. & FREEMAN, D. A. 1994. Factors underlying the variability of lipid droplet fluorescence in MA-10 leydig tumor cells. *Cytometry,* 17**,** 151-158.

GÓMEZ-AMBROSI, J., CATALÁN, V., RAMÍREZ, B., RODRÍGUEZ, A., COLINA, I., SILVA, C., ROTELLAR, F., MUGUETA, C., GIL, M. J., CIENFUEGOS, J. A., SALVADOR, J. & FRÜHBECK, G. 2007. Plasma Osteopontin Levels and Expression in Adipose Tissue Are Increased in Obesity. *Journal of Clinical Endocrinology & Metabolism,* 92**,** 3719-3727.

GREENBERG, A. S., EGAN, J. J., WEK, S. A., MOOS JR, M. C., LONDOS, C. & KIMMEL, A. R. 1993. Isolation of cDNAs for perilipins A and B: sequence and expression of lipid droplet-associated proteins of adipocytes. *Proceedings of the National Academy of Sciences of the United States of America,* 90**,** 12035.

GREGOIRE, F. M., SMAS, C. M. & SUL, H. S. 1998. Understanding Adipocyte Differentiation. *Physiological Reviews,* 78**,** 783-809.

GRIGORIADIS, A. E., HEERSCHE, J. & AUBIN, J. E. 1988. Differentiation of muscle, fat, cartilage, and bone from progenitor cells present in a bone-derived clonal cell population: effect of dexamethasone. *The Journal of cell biology,* 106**,** 2139-2151.

GUNTON, J. E., KULKARNI, R. N., YIM, S., OKADA, T., HAWTHORNE, W. J., TSENG, Y.-H., ROBERSON, R. S., RICORDI, C., O'CONNELL, P. J. & GONZALEZ, F. J. 2005. Loss of ARNT/HIF1beta mediates altered gene expression and pancreatic-islet dysfunction in human type 2 diabetes. *Cell,* 122**,** 337-349.

GUO, S., COPPS, K. D., DONG, X., PARK, S., CHENG, Z., POCAI, A., ROSSETTI, L., SAJAN, M., FARESE, R. V. & WHITE, M. F. 2009. The Irs1 branch of the insulin signaling cascade plays a dominant role in hepatic nutrient homeostasis. *Molecular and cellular biology,* 29**,** 5070-5083.

HANKE, S. & MANN, M. 2009. The phosphotyrosine interactome of the insulin receptor family and its substrates IRS-1 and IRS-2. *Mol Cell Proteomics,* 8**,** 519-34.

HAUNER, H. & ENTENMANN, G. 1991. Regional variation of adipose differentiation in cultured stromal-vascular cells from the abdominal and femoral adipose tissue of obese women. *International journal of obesity,* 15**,** 121.

HAUNER, H., ENTENMANN, G., WABITSCH, M., GAILLARD, D., AILHAUD, G., NEGREL, R. & PFEIFFER, E. 1989. Promoting

effect of glucocorticoids on the differentiation of human adipocyte precursor cells cultured in a chemically defined medium. *Journal of Clinical Investigation,* 84**,** 1663.

HAUNERLAND, N. H. & SPENER, F. 2004. Fatty acid-binding proteins–insights from genetic manipulations. *Progress in lipid research,* 43**,** 328-349.

HAUSMAN, D. B., DIGIROLAMO, M., BARTNESS, T. J., HAUSMAN, G. J. & MARTIN, R. J. 2001. The biology of white adipocyte proliferation. *Obesity Reviews,* 2**,** 239-254.

HAUSMAN, G., WRIGHT, J., DEAN, R. & RICHARDSON, R. 1993. Cellular and molecular aspects of the regulation of adipogenesis. *Journal of Animal Science,* 71**,** 33-55.

HENRY, R. R., PHILLIPS, S. A., MUDALIAR, S. R. & CIARALDI, T. P. 2006. Chapter 6 The adipocyte and adipose tissue as endocrine organs: Impact on the insulin resistance phenotype. *In:* JACOB, E. F. (ed.) *Advances in Molecular and Cellular Endocrinology.* Elsevier.

HENRY, S. L., BENSLEY, J. G., WOOD-BRADLEY, R. J., CULLEN-MCEWEN, L. A., BERTRAM, J. F. & ARMITAGE, J. A. 2012. White adipocytes: More than just fat depots. *The International Journal of Biochemistry & Cell Biology,* 44**,** 435-440.

HIBUSE, T., MAEDA, N., NAGASAWA, A. & FUNAHASHI, T. 2006. Aquaporins and glycerol metabolism. *Biochimica et Biophysica Acta (BBA) - Biomembranes,* 1758**,** 1004-1011.

HIJIYA, N., SETOGUCHI, M., MATSUURA, K., HIGUCHI, Y., AKIZUKI, S. & YAMAMOTO, S. 1994. Cloning and characterization of the human osteopontin gene and its promoter. *Biochemical Journal,* 303**,** 255.

HILL, M. M., CLARK, S. F., TUCKER, D. F., BIRNBAUM, M. J., JAMES, D. E. & MACAULAY, S. L. 1999. A role for protein kinase Bβ/Akt2 in insulin-stimulated GLUT4 translocation in adipocytes. *Molecular and cellular biology,* 19**,** 7771-7781.

HIROSUMI, J., TUNCMAN, G., CHANG, L., GÖRGÜN, C. Z., UYSAL, K. T., MAEDA, K., KARIN, M. & HOTAMISLIGIL, G. S. 2002. A central role for JNK in obesity and insulin resistance. *Nature,* 420**,** 333-336.

HIRSCH, J. & BATCHELOR, B. 1976. Adipose tissue cellularity in human obesity. *Clinics in Endocrinology and Metabolism,* 5**,** 299-311.

HOFBAUER, K. G. 2002. Molecular pathways to obesity. *International Journal of Obesity,* International Journal of Obesity (2002) 26, Suppl 2, S18-S27. .

HOLM, C. 2003. Molecular mechanisms regulating hormone-sensitive lipase and lipolysis. *Biochemical Society Transactions,* 31**,** 1120-1124.

HORWITZ, D. L., STARR, J., MAKO, M., BLACKARD, W. & RUBENSTEIN, A. 1975. Proinsulin, insulin, and C-peptide concentrations in human portal and peripheral blood. *Journal of Clinical Investigation,* 55**,** 1278.

HOSOGAI, N., FUKUHARA, A., OSHIMA, K., MIYATA, Y., TANAKA, S., SEGAWA, K., FURUKAWA, S., TOCHINO, Y., KOMURO, R. & MATSUDA, M. 2007. Adipose tissue hypoxia in obesity and its impact on adipocytokine dysregulation. *Diabetes,* 56**,** 901-911.

HOTAMISLIGIL, G. 2003. Inflammatory pathways and insulin action. *International journal of obesity,* 27**,** S53-S55.

HOTAMISLIGIL, G. S. 2006. Inflammation and metabolic disorders. *Nature,* 444**,** 860-867.

HOTAMISLIGIL, G. S., PERALDI, P., BUDAVARI, A., ELLIS, R., WHITE, M. F. & SPIEGELMAN, B. 1996. IRS-1-Mediated Inhibition of Insulin Receptor Tyrosine Kinase Activity in TNF--and Obesity-Induced Insulin Resistance. *SCIENCE-NEW YORK THEN WASHINGTON-***,** 665-667.

HOTAMISLIGIL, G. S., SHARGILL, N. S. & SPIEGELMAN, B. M. 1993. Adipose expression of tumor necrosis factor-alpha: direct role in obesity-linked insulin resistance. *Science,* 259**,** 87-91.

HU, E., LIANG, P. & SPIEGELMAN, B. M. 1996. AdipoQ is a novel adipose-specific gene dysregulated in obesity. *Journal of Biological Chemistry,* 271**,** 10697-10703.

IKEDA, H., WEST, D., PUSTEK, J., FIGLEWICZ, D., GREENWOOD, M., PORTE JR, D. & WOODS, S. 1986. Intraventricular insulin reduces food intake and body weight of lean but not obese Zucker rats. *Appetite,* 7**,** 381-386.

ISAKSON, P., HAMMARSTEDT, A., GUSTAFSON, B. & SMITH, U. 2009. Impaired Preadipocyte Differentiation in Human Abdominal Obesity Role of Wnt, Tumor Necrosis Factor-α, and Inflammation. *Diabetes,* 58**,** 1550-1557.

JAMES, P. T., LEACH, R., KALAMARA, E. & SHAYEGHI, M. 2012. The worldwide obesity epidemic. *Obesity Research,* 9**,** 228S-233S.

JENSEN, M. D. 2008. Role of body fat distribution and the metabolic complications of obesity. *Journal of Clinical Endocrinology & Metabolism,* 93**,** s57-s63.

JO, J., GAVRILOVA, O., PACK, S., JOU, W., MULLEN, S., SUMNER, A. E., CUSHMAN, S. W. & PERIWAL, V. 2009. Hypertrophy and/or Hyperplasia: Dynamics of Adipose Tissue Growth. *PLoS Comput Biol,* 5**,** e1000324.

JOE, A. W. B., YI, L., EVEN, Y., VOGL, A. W. & ROSSI, F. M. V. 2009. Depot-Specific Differences in Adipogenic Progenitor

Abundance and Proliferative Response to High-Fat Diet. *STEM CELLS,* 27**,** 2563-2570.

JOHNSON, P., STERN, J., GREENWOOD, M. & HIRSCH, J. 1978. Adipose tissue hyperplasia and hyperinsulinemia in Zucker obese female rats: a developmental study. *Metabolism,* 27**,** 1941-1954.

JONO, S., PEINADO, C. & GIACHELLI, C. M. 2000. Phosphorylation of osteopontin is required for inhibition of vascular smooth muscle cell calcification. *Journal of Biological Chemistry,* 275**,** 20197-20203.

KABON, B., NAGELE, A., REDDY, D., EAGON, C., FLESHMAN, J. W., SESSLER, D. I. & KURZ, A. 2004. Obesity decreases perioperative tissue oxygenation. *Anesthesiology,* 100**,** 274.

KAHN, A. R. S. C. R. 2001. Insulin signalling and the regulation of glucose and lipid metabolism. *Nature* 414**,** 799-806.

KAHN, B. B. 1998. Type 2 Diabetes: When Insulin Secretion Fails to Compensate for Insulin Resistance. *Cell,* 92**,** 593-596.

KAHN, C., WHITE, M., SHOELSON, S., BACKER, J., ARAKI, E., CHEATHAM, B., CSERMELY, P., FOLLI, F., GOLDSTEIN, B. & HUERTAS, P. 1993. The insulin receptor and its substrate: molecular determinants of early events in insulin action. *Recent progress in hormone research,* 48**,** 291.

KANDA, H., TATEYA, S., TAMORI, Y., KOTANI, K., HIASA, K.-I., KITAZAWA, R., KITAZAWA, S., MIYACHI, H., MAEDA, S. & EGASHIRA, K. 2006. MCP-1 contributes to macrophage infiltration into adipose tissue, insulin resistance, and hepatic steatosis in obesity. *Journal of Clinical Investigation,* 116**,** 1494-1505.

KAZANECKI, C. C. 2007. *Osteopontin and cell adhesion: Role of post-translational modifications and the C-terminal region.* Doctor of Philosophy, ProQuest.

KAZANECKI, C. C., UZWIAK, D. J. & DENHARDT, D. T. 2007. Control of osteopontin signaling and function by post-translational phosphorylation and protein folding. *Journal of cellular biochemistry,* 102**,** 912-924.

KEOPHIPHATH, M., ACHARD, V., HENEGAR, C., ROUAULT, C., CLÉMENT, K. & LACASA, D. 2009. Macrophage-secreted factors promote a profibrotic phenotype in human preadipocytes. *Molecular Endocrinology,* 23**,** 11-24.

KERN, P. A., RANGANATHAN, S., LI, C., WOOD, L. & RANGANATHAN, G. 2001. Adipose tissue tumor necrosis factor and interleukin-6 expression in human obesity and insulin resistance. *American Journal of Physiology - Endocrinology And Metabolism,* 280**,** E745-E751.

KHAN, S. A., COOK, A. C., KAPPIL, M., GÜNTHERT, U., CHAMBERS, A. F., TUCK, A. B. & DENHARDT, D. T. 2005.

Enhanced cell surface CD44 variant (v6, v9) expression by osteopontin in breast cancer epithelial cells facilitates tumor cell migration: novel post-transcriptional, post-translational regulation. *Clinical and Experimental Metastasis,* 22**,** 663-673.

KIEFER, F. 2010. *Osteopontin in obesity-associated adipose tissue inflammation and insulin resistance and its interaction with monocyte chemoattractant protein-1.* Degree 'Doctor of Philosophy - PhD' Doctoral Thesis at the Medical University of Vienna for obtaining the Degree 'Doctor of Philosophy - PhD', Medical University of Vienna.

KIEFER, F., NESCHEN, S., PFAU, B., LEGERER, B., NEUHOFER, A., KAHLE, M., HRABÉ DE ANGELIS, M., SCHLEDERER, M., MAIR, M., KENNER, L., PLUTZKY, J., ZEYDA, M. & STULNIG, T. 2011. Osteopontin deficiency protects against obesity-induced hepatic steatosis and attenuates glucose production in mice. *Diabetologia,* 54**,** 2132-2142.

KIEFER, F. W., ZEYDA, M., GOLLINGER, K., PFAU, B., NEUHOFER, A., WEICHHART, T., SÄEMANN, M. D., GEYEREGGER, R., SCHLEDERER, M. & KENNER, L. 2010. Neutralization of osteopontin inhibits obesity-induced inflammation and insulin resistance. *Diabetes,* 59**,** 935-946.

KIEFER, F. W., ZEYDA, M., TODORIC, J., HUBER, J., GEYEREGGER, R., WEICHHART, T., ASZMANN, O., LUDVIK, B., SILBERHUMER, G. R. & PRAGER, G. 2008. Osteopontin expression in human and murine obesity: extensive local up-regulation in adipose tissue but minimal systemic alterations. *Endocrinology,* 149**,** 1350-1357.

KIGUCHI, N., MAEDA, T., KOBAYASHI, Y., FUKAZAWA, Y. & KISHIOKA, S. 2009. Leptin enhances CC-chemokine ligand expression in cultured murine macrophage. *Biochemical and biophysical research communications,* 384**,** 311-315.

KIM, J. B., SARRAF, P., WRIGHT, M., YAO, K. M., MUELLER, E., SOLANES, G., LOWELL, B. B. & SPIEGELMAN, B. M. 1998. Nutritional and insulin regulation of fatty acid synthetase and leptin gene expression through ADD1/SREBP1. *Journal of Clinical Investigation,* 101**,** 1.

KIM, J. B. & SPIEGELMAN, B. M. 1996. ADD1/SREBP1 promotes adipocyte differentiation and gene expression linked to fatty acid metabolism. *Genes & development,* 10**,** 1096-1107.

KIM, J. B., SPOTTS, G. D., HALVORSEN, Y.-D., SHIH, H.-M., ELLENBERGER, T., TOWLE, H. C. & SPIEGELMAN, B. M. 1995. Dual DNA binding specificity of ADD1/SREBP1 controlled by a single amino acid in the basic helix-loop-helix domain. *Molecular and cellular biology,* 15**,** 2582-2588.

KING, H., AUBERT, R. E. & HERMAN, W. H. 1998. Global Burden of Diabetes, 1995–2025: Prevalence, numerical estimates, and projections. *Diabetes Care,* 21**,** 1414-1431.

KISSEBAH, A. H. & KRAKOWER, G. R. 1994. Regional adiposity and morbidity. *Physiol Rev,* 74**,** 761-811.

KLAMMT, J., GARTEN, A., BARNIKOL-OETTLER, A., BECK-SICKINGER, A. G. & KIESS, W. 2005. Comparative analysis of the signaling capabilities of the insulin receptor-related receptor. *Biochem Biophys Res Commun,* 327**,** 557-64.

KLIP, A. & PÂQUET, M. R. 1990. Glucose transport and glucose transporters in muscle and their metabolic regulation. *Diabetes Care,* 13**,** 228-243.

KOOPMAN, G., REUTELINGSPERGER, C., KUIJTEN, G., KEEHNEN, R., PALS, S. & VAN OERS, M. 1994. Annexin V for flow cytometric detection of phosphatidylserine expression on B cells undergoing apoptosis. *Blood,* 84**,** 1415-1420.

KRISTIANSEN, O. P. & MANDRUP-POULSEN, T. 2005. Interleukin-6 and Diabetes. *Diabetes,* 54**,** S114-S124.

KUBOTA, N., TERAUCHI, Y., MIKI, H., TAMEMOTO, H., YAMAUCHI, T., KOMEDA, K., SATOH, S., NAKANO, R., ISHII, C., SUGIYAMA, T., ETO, K., TSUBAMOTO, Y., OKUNO, A., MURAKAMI, K., SEKIHARA, H., HASEGAWA, G., NAITO, M., TOYOSHIMA, Y., TANAKA, S., SHIOTA, K., KITAMURA, T., FUJITA, T., EZAKI, O., AIZAWA, S., NAGAI, R., TOBE, K., KIMURA, S. & KADOWAKI, T. 1999. PPARγ Mediates High-Fat Diet–Induced Adipocyte Hypertrophy and Insulin Resistance. *Molecular cell,* 4**,** 597-609.

KUBOTA, N., TERAUCHI, Y., TOBE, K., YANO, W., SUZUKI, R., UEKI, K., TAKAMOTO, I., SATOH, H., MAKI, T., KUBOTA, T., MOROI, M., OKADA-IWABU, M., EZAKI, O., NAGAI, R., UETA, Y., KADOWAKI, T. & NODA, T. 2004. Insulin receptor substrate 2 plays a crucial role in beta cells and the hypothalamus. *The Journal of Clinical Investigation,* 114**,** 917-927.

KUBOTA, N., TOBE, K., TERAUCHI, Y., ETO, K., YAMAUCHI, T., SUZUKI, R., TSUBAMOTO, Y., KOMEDA, K., NAKANO, R., MIKI, H., SATOH, S., SEKIHARA, H., SCIACCHITANO, S., LESNIAK, M., AIZAWA, S., NAGAI, R., KIMURA, S., AKANUMA, Y., TAYLOR, S. I. & KADOWAKI, T. 2000. Disruption of insulin receptor substrate 2 causes type 2 diabetes because of liver insulin resistance and lack of compensatory beta-cell hyperplasia. *Diabetes,* 49**,** 1880-1889.

LACASA, D., TALEB, S., KEOPHIPHATH, M., MIRANVILLE, A. & CLEMENT, K. 2007. Macrophage-secreted factors impair human adipogenesis: involvement of proinflammatory state in preadipocytes. *Endocrinology,* 148**,** 868-877.

LAFONTAN, M. & BERLAN, M. 2003. Do regional differences in adipocyte biology provide new pathophysiological insights? *Trends in pharmacological sciences,* 24**,** 276-283.

LANG, D., MATTHEWS, D., PETO, J. & TURNER, R. 1979. Cyclic oscillations of basal plasma glucose and insulin concentrations in human beings. *New England Journal of Medicine,* 301**,** 1023-1027.

LAU, D., SCHILLABEER, G., LI, Z., WONG, K., VARZANEH, F. & TOUGH, S. 1996. Paracrine interactions in adipose tissue development and growth. *International journal of obesity and related metabolic disorders: journal of the International Association for the Study of Obesity,* 20**,** S16.

LAUSTSEN, P. G., MICHAEL, M. D., CRUTE, B. E., COHEN, S. E., UEKI, K., KULKARNI, R. N., KELLER, S. R., LIENHARD, G. E. & KAHN, C. R. 2002. Lipoatrophic diabetes in Irs1−/−/Irs3−/− double knockout mice. *Genes & development,* 16**,** 3213-3222.

LAVAN, B. E., LANE, W. S. & LIENHARD, G. E. 1997. The 60-kDa phosphotyrosine protein in insulin-treated adipocytes is a new member of the insulin receptor substrate family. *Journal of Biological Chemistry,* 272**,** 11439-11443.

LEE, Y. H., GIRAUD, J., DAVIS, R. J. & WHITE, M. F. 2003. c-Jun N-terminal kinase (JNK) mediates feedback inhibition of the insulin signaling cascade. *Journal of Biological Chemistry,* 278**,** 2896-2902.

LIEBERMAN, L. S. 2003. DIETARY, EVOLUTIONARY, AND MODERNIZING INFLUENCES ON THE PREVALENCE OF TYPE 2 DIABETES. *Annual Review of Nutrition,* 23**,** 345-377.

LIN, X., TAGUCHI, A., PARK, S., KUSHNER, J. A., LI, F., LI, Y. & WHITE, M. F. 2004. Dysregulation of insulin receptor substrate 2 in beta cells and brain causes obesity and diabetes. *The Journal of Clinical Investigation,* 114**,** 908-916.

LISTENBERGER, L. L. & BROWN, D. A. 2007. Fluorescent detection of lipid droplets and associated proteins. *Current Protocols in Cell Biology***,** 24.2. 1-24.2. 11.

LITTHAUER, D. & SERRERO, G. 1992. The primary culture of mouse adipocyte precursor cells in defined medium. *Comparative Biochemistry and Physiology Part A: Physiology,* 101**,** 59-64.

LIVAK, K. J. & SCHMITTGEN, T. D. 2001. Analysis of Relative Gene Expression Data Using Real-Time Quantitative PCR and the 2−ΔΔCT Method. *Methods,* 25**,** 402-408.

LONDOS, C., BRASAEMLE, D. L., SCHULTZ, C. J., SEGREST, J. P. & KIMMEL, A. R. Year. Perilipins, ADRP, and other proteins that associate with intracellular neutral lipid droplets in animal cells. *In:* Seminars in cell & developmental biology, 1999. 51.

LOWELL, B. B., NAPOLITANO, A., USHER, P., DULLOO, A. G., ROSEN, B. S., SPIEGELMAN, B. M. & FLIER, J. S. 1990. Reduced Adipsin Expression in Murine Obesity: Effect of Age and Treatment with the Sympathomimetic-Thermogenic Drug Mixture Ephedrine and Caffeine. *Endocrinology,* 126**,** 1514-1520.

M ZEYDA, D. F., J TODORIC, O ASZMANN, M SPEISER, G GYÖRI, G J ZLABINGER AND T M STULNIG 2007. Human adipose tissue macrophages are of an anti-inflammatory phenotype but capable of excessive pro-inflammatory mediator production. *International Journal of Obesity,* 31**,** 1420–1428.

MARCUELLO, C., CALLE-PASCUAL, A. L., FUENTES, M., RUNKLE, I., SORIGUER, F., GODAY, A., BOSCH-COMAS, A., BORDI, #XFA, , E., CARMENA, R., CASAMITJANA, R., CASTA, #XF1, O, L., CASTELL, C., CATAL, #XE1, , M., DELGADO, E., FRANCH, J., GAZTAMBIDE, S., GIRB, #XE9, S, J., GOMIS, R., GUTI, RREZ, G., #XF3, PEZ-ALBA, A., MART, #XED, NEZ-LARRAD, M. T., MEN, NDEZ, E., MORA-PECES, I., ORTEGA, E., PASCUAL-MANICH, G., ROJO-MART, NEZ, G., SERRANO-RIOS, M., VALD, S, S., ZQUEZ, J. A. & VENDRELL, J. 2012. Evaluation of Health-Related Quality of Life according to Carbohydrate Metabolism Status: A Spanish Population-Based Study (Di@bet.es Study). *International Journal of Endocrinology,* 2012**,** 6.

MARDILOVICH, K., PANKRATZ, S. L. & SHAW, L. M. 2009. Expression and function of the insulin receptor substrate proteins in cancer. *Cell Commun Signal,* 7**,** 14.

MAURIEGE, P., DESPRES, J., MARCOTTE, M., FERLAND, M., TREMBLAY, A., NADEAU, A., MOORJANI, S., LUPIEN, P., THERIAULT, G. & BOUCHARD, C. 1990. Abdominal fat cell lipolysis, body fat distribution, and metabolic variables in premenopausal women. *Journal of Clinical Endocrinology & Metabolism,* 71**,** 1028-1035.

MAZZALI, M., KIPARI, T., OPHASCHAROENSUK, V., WESSON, J. A., JOHNSON, R. & HUGHES, J. 2002. Osteopontin a molecule for all seasons. *QJM,* 95**,** 3-13.

MENDEZ, M. A., MONTEIRO, C. A. & POPKIN, B. M. 2005. Overweight exceeds underweight among women in most developing countries. *The American journal of clinical nutrition,* 81**,** 714-721.

MERRY, K., DODDS, R., LITTLEWOOD, A. & GOWEN, M. 1993. Expression of osteopontin mRNA by osteoclasts and osteoblasts in modelling adult human bone. *Journal of cell science,* 104**,** 1013-1020.

MOHAMED-ALI, V., PINKNEY, J. & COPPACK, S. 1998. Adipose tissue as an endocrine and paracrine organ. *International*

journal of obesity and related metabolic disorders: journal of the International Association for the Study of Obesity, 22**,** 1145.

MONTAGUE, C. T., PRINS, J. B., SANDERS, L., DIGBY, J. E. & O'RAHILLY, S. 1997. Depot-and sex-specific differences in human leptin mRNA expression: implications for the control of regional fat distribution. *Diabetes,* 46**,** 342-347.

MORAS, D. & GRONEMEYER, H. 1998. The nuclear receptor ligand-binding domain: structure and function. *Current opinion in cell biology,* 10**,** 384-391.

MYERS JR, M. G. & WHITE, M. F. 1996. Insulin signal transduction and the IRS proteins. *Annual review of pharmacology and toxicology,* 36**,** 615-658.

MYERS, M. G., MENDEZ, R., SHI, P., PIERCE, J. H., RHOADS, R. & WHITE, M. F. 1998. The COOH-terminal tyrosine phosphorylation sites on IRS-1 bind SHP-2 and negatively regulate insulin signaling. *Journal of Biological Chemistry,* 273**,** 26908-26914.

NEGANOVA, I., AL-QASSAB, H., HEFFRON, H., SELMAN, C., CHOUDHURY, A. I., LINGARD, S. J., DIAKONOV, I., PATTERSON, M., GHATEI, M., BLOOM, S. R., FRANKS, S., HUHTANIEMI, I., HARDY, K. & WITHERS, D. J. 2007. Role of central nervous system and ovarian insulin receptor substrate 2 signaling in female reproductive function in the mouse. *Biol Reprod,* 76**,** 1045-53.

NELMS, K., O'NEILL, T. J., LI, S., HUBBARD, S. R., GUSTAFSON, T. A. & PAUL, W. E. 1999. Alternative splicing, gene localization, and binding of SH2-B to the insulin receptor kinase domain. *Mammalian genome,* 10**,** 1160-1167.

NICHOLLS, D. G. & LOCKE, R. M. 1984. Thermogenic mechanisms in brown fat. *Physiological reviews,* 64**,** 1-64.

NOMIYAMA, T., PEREZ-TILVE, D., OGAWA, D., GIZARD, F., ZHAO, Y., HEYWOOD, E. B., JONES, K. L., KAWAMORI, R., CASSIS, L. A. & TSCHOP, M. 2007. Osteopontin mediates obesity-induced adipose tissue macrophage infiltration and insulin resistance in mice. *Journal of Clinical Investigation,* 117**,** 2877.

NUSSEY S, W. S. 2001. Endocrinology: An Integrated Approach. *Oxford: BIOS Scientific Publishers*.

O'CONNELL, J., LYNCH, L., CAWOOD, T. J., KWASNIK, A., NOLAN, N., GEOGHEGAN, J., MCCORMICK, A., O'FARRELLY, C. & O'SHEA, D. 2010. The relationship of omental and subcutaneous adipocyte size to metabolic disease in severe obesity. *PloS one,* 5**,** e9997.

O'REGAN, A. W., HAYDEN, J. M. & BERMAN, J. S. 2000. Osteopontin augments CD3-mediated interferon-γ and CD40

ligand expression by T cells, which results in IL-12 production from peripheral blood mononuclear cells. *Journal of leukocyte biology,* 68**,** 495-502.

OBSTFELD, A. E., SUGARU, E., THEARLE, M., FRANCISCO, A.-M., GAYET, C., GINSBERG, H. N., ABLES, E. V. & FERRANTE, A. W. 2010. CC chemokine receptor 2 (CCR2) regulates the hepatic recruitment of myeloid cells that promote obesity-induced hepatic steatosis. *Diabetes,* 59**,** 916-925.

OFEI, F., HUREL, S., NEWKIRK, J., SOPWITH, M. & TAYLOR, R. 1996. Effects of an engineered human anti–TNF-α antibody (CDP571) on insulin sensitivity and glycemic control in patients with NIDDM. *Diabetes,* 45**,** 881-885.

ORGANIZATION, W. H. 2010. Obesity and overweight. Fact Sheet No 311. September 2006. *Online document at: www. who. int/mediacentre/factsheets/fs311/en/index. html Accessed September,* 13.

ORGANIZATION, W. H. 2011. Obesity and overweight. 2011. *URL http://www. who. int/mediacentre/factsheets/fs311/en/index. html (accessed June 2011)*.

ORGANIZATION, W. H. 2012. *Obesity and overweight* [Online]. Available: http://www.who.int/mediacentre/factsheets/fs311/en/index.html [Accessed Fact sheet N°311].

PASARICA, M., SEREDA, O. R., REDMAN, L. M., ALBARADO, D. C., HYMEL, D. T., ROAN, L. E., ROOD, J. C., BURK, D. H. & SMITH, S. R. 2009. Reduced adipose tissue oxygenation in human obesity evidence for rarefaction, macrophage chemotaxis, and inflammation without an angiogenic response. *Diabetes,* 58**,** 718-725.

PATTI, M.-E., SUN, X.-J., BRUENING, J. C., ARAKI, E., LIPES, M. A., WHITE, M. F. & KAHN, C. R. 1995. 4PS/insulin receptor substrate (IRS)-2 is the alternative substrate of the insulin receptor in IRS-1-deficient mice. *Journal of Biological Chemistry,* 270**,** 24670-24673.

PAWSON, T. & SCOTT, J. D. 1997. Signaling through scaffold, anchoring, and adaptor proteins. *Science,* 278**,** 2075-2080.

PERMANA, P. A., NAIR, S., LEE, Y. H., LUCZY-BACHMAN, G., DE COURTEN, B. V. & TATARANNI, P. A. 2004. Subcutaneous abdominal preadipocyte differentiation in vitro inversely correlates with central obesity. *American Journal of Physiology-Endocrinology And Metabolism,* 286**,** E958-E962.

PESSIN, J. E. & SALTIEL, A. R. 2000. Signaling pathways in insulin action: molecular targets of insulin resistance. *The Journal of Clinical Investigation,* 106**,** 165-169.

PHILIP, S. & KUNDU, G. C. 2003. Osteopontin induces nuclear factor κB-mediated promatrix metalloproteinase-2 activation through

IκBα/IKK signaling pathways, and curcumin (diferulolylmethane) down-regulates these pathways. *Journal of Biological Chemistry,* 278**,** 14487-14497.

PHILIPPE, J. 1991. Structure and Pancreatic Expression of the Insulin and Glucagon Genes. *Endocrine reviews,* 12**,** 252-271.

PICKUP, J., MATTOCK, M., CHUSNEY, G. & BURT, D. 1997. NIDDM as a disease of the innate immune system: association of acute-phase reactants and interleukin-6 with metabolic syndrome X. *Diabetologia,* 40**,** 1286-1292.

PITTAS, A. G., JOSEPH, N. A. & GREENBERG, A. S. 2004. Adipocytokines and insulin resistance. *Journal of Clinical Endocrinology & Metabolism,* 89**,** 447-452.

PITTENGER, M. F., MACKAY, A. M., BECK, S. C., JAISWAL, R. K., DOUGLAS, R., MOSCA, J. D., MOORMAN, M. A., SIMONETTI, D. W., CRAIG, S. & MARSHAK, D. R. 1999. Multilineage potential of adult human mesenchymal stem cells. *Science,* 284**,** 143-147.

POPKIN, B. M. & GORDON-LARSEN, P. 2004. The nutrition transition: worldwide obesity dynamics and their determinants. *International journal of obesity,* 28**,** S2-S9.

POWELKA, A. M., SETH, A., VIRBASIUS, J. V., KISKINIS, E., NICOLORO, S. M., GUILHERME, A., TANG, X., STRAUBHAAR, J., CHERNIACK, A. D. & PARKER, M. G. 2006. Suppression of oxidative metabolism and mitochondrial biogenesis by the transcriptional corepressor RIP140 in mouse adipocytes. *Journal of Clinical Investigation,* 116**,** 125-136.

PREVIS, S. F., WITHERS, D. J., REN, J.-M., WHITE, M. F. & SHULMAN, G. I. 2000. Contrasting Effects of IRS-1 Versus IRS-2 Gene Disruption on Carbohydrate and Lipid Metabolism in Vivo. *Journal of Biological Chemistry,* 275**,** 38990-38994.

PUIGSERVER, P. & SPIEGELMAN, B. M. 2003. Peroxisome proliferator-activated receptor-γ coactivator 1α (PGC-1α): transcriptional coactivator and metabolic regulator. *Endocrine reviews,* 24**,** 78-90.

QIN YANG, T. E. G., NIMESH MODY, FREDERIC PREITNER, ODILE D. PERONI, JANICE M. ZABOLOTNY, KO KOTANI, LOREDANA QUADRO, & BARBARA B. KAHN 2005. Serum retinol binding protein 4 contributes to insulin resistance in obesity and type 2 diabetes. *Nature* 436**,** 356-362.

RAJALA, M. W. & SCHERER, P. E. 2003. Minireview: the adipocyte—at the crossroads of energy homeostasis, inflammation, and atherosclerosis. *Endocrinology,* 144**,** 3765-3773.

RANGASWAMI, H., BULBULE, A. & KUNDU, G. C. 2006. Osteopontin: role in cell signaling and cancer progression. *Trends in cell biology,* 16**,** 79-87.

RANGWALA, S. M. & LAZAR, M. A. 2004. Peroxisome proliferator-activated receptor γ in diabetes and metabolism. *Trends in Pharmacological Sciences,* 25**,** 331-336.

REAVEN, G. 2004a. The metabolic syndrome or the insulin resistance syndrome? Different names, different concepts, and different goals. *Endocrinology and metabolism clinics of North America,* 33**,** 283-303.

REAVEN, G. M. 2004b. Insulin Resistance, Cardiovascular Disease, and the Metabolic Syndrome. *Diabetes Care,* 27**,** 1011-1012.

RESHEF, L., OLSWANG, Y., CASSUTO, H., BLUM, B., CRONIGER, C. M., KALHAN, S. C., TILGHMAN, S. M. & HANSON, R. W. 2003. Glyceroneogenesis and the triglyceride/fatty acid cycle. *Journal of Biological Chemistry,* 278**,** 30413-30416.

RINDERKNECHT, E. & HUMBEL, R. E. 1978. The amino acid sequence of human insulin-like growth factor I and its structural homology with proinsulin. *Journal of Biological Chemistry,* 253**,** 2769-2776.

RODEHEFFER, M. S., BIRSOY, K. & FRIEDMAN, J. M. 2008. Identification of white adipocyte progenitor cells in vivo. *Cell,* 135**,** 240-9.

ROSEN, E. D. & MACDOUGALD, O. A. 2006. Adipocyte differentiation from the inside out. *Nat Rev Mol Cell Biol,* 7**,** 885-96.

ROSEN, E. D. & SPIEGELMAN, B. M. 2000. Molecular regulation of adipogenesis. *Annu Rev Cell Dev Biol,* 16**,** 145-71.

RUBENSTEIN, A., BLOCK, M., STARR, J., MELANI, F. & STEINER, D. 1972. Proinsulin and C-peptide in blood. *Diabetes,* 21**,** 661.

RUI, L., AGUIRRE, V., KIM, J. K., SHULMAN, G. I., LEE, A., CORBOULD, A., DUNAIF, A. & WHITE, M. F. 2001. Insulin/IGF-1 and TNF-alpha stimulate phosphorylation of IRS-1 at inhibitory Ser^ 3^ 0^ 7 via distinct pathways. *Journal of Clinical Investigation,* 107**,** 181-189.

RUI, L. & WHITE, M. F. 2003. The role of insulin receptor substrate proteins in insulin signaling and metabolic regulation. *Diabetes Mellitus: A Fundamental and Clinical Text***,** 207.

RUI, L., YUAN, M., FRANTZ, D., SHOELSON, S. & WHITE, M. F. 2002. SOCS-1 and SOCS-3 block insulin signaling by ubiquitin-mediated degradation of IRS1 and IRS2. *Science Signalling,* 277**,** 42394.

SAHAI, A., MALLADI, P., MELIN-ALDANA, H., GREEN, R. M. & WHITINGTON, P. F. 2004a. Upregulation of osteopontin expression is involved in the development of nonalcoholic steatohepatitis in a dietary murine model. *American Journal of Physiology-Gastrointestinal and Liver Physiology,* 287**,** G264-G273.

SAHAI, A., MALLADI, P., PAN, X., PAUL, R., MELIN-ALDANA, H., GREEN, R. M. & WHITINGTON, P. F. 2004b. Obese and diabetic db/db mice develop marked liver fibrosis in a model of nonalcoholic steatohepatitis: role of short-form leptin receptors and osteopontin. *American Journal of Physiology-Gastrointestinal and Liver Physiology,* 287**,** G1035-G1043.

SAMANNA, V., WEI, H., EGO-OSUALA, D. & CHELLAIAH, M. 2006. Alpha-V-dependent outside-in signaling is required for the regulation of CD44 surface expression, MMP-2 secretion, and cell migration by osteopontin in human melanoma cells. *Experimental cell research,* 312**,** 2214-2230.

SAMBROOK, J. & RUSSELL, D. W. 1989. SDS-polyacrylamide gel electrophoresis of proteins. *Molecular cloning: a laboratory manual,* 3**,** 18.47-18.59.

SARTIPY, P. & LOSKUTOFF, D. J. 2003. Monocyte chemoattractant protein 1 in obesity and insulin resistance. *Proceedings of the National Academy of Sciences,* 100**,** 7265-7270.

SAWKA-VERHELLE, D., BARON, V., MOTHE, I., FILLOUX, C., WHITE, M. F. & VAN OBBERGHEN, E. 1997. Tyr624 and Tyr628 in insulin receptor substrate-2 mediate its association with the insulin receptor. *Journal of Biological Chemistry,* 272**,** 16414-16420.

SCHÄGGER, H. 2006. Tricine–SDS-PAGE. *Nature protocols,* 1**,** 16-22.

SCHOLZEN, T. & GERDES, J. 2000. The Ki-67 protein: From the known and the unknown. *Journal of Cellular Physiology,* 182**,** 311-322.

SCHUBERT, M., BRAZIL, D. P., BURKS, D. J., KUSHNER, J. A., YE, J., FLINT, C. L., FARHANG-FALLAH, J., DIKKES, P., WAROT, X. M. & RIO, C. 2003. Insulin receptor substrate-2 deficiency impairs brain growth and promotes tau phosphorylation. *The Journal of neuroscience,* 23**,** 7084-7092.

SCHWARTZ, D. R. & LAZAR, M. A. 2011. Human resistin: found in translation from mouse to man. *Trends in Endocrinology & Metabolism,* 22**,** 259-265.

SCHWARTZ, M., SIPOLS, A., MARKS, J., SANACORA, G., WHITE, J., SCHEURINK, A., KAHN, S., BASKIN, D., WOODS, S. & FIGLEWICZ, D. 1992. Inhibition of hypothalamic neuropeptide Y gene expression by insulin. *Endocrinology,* 130**,** 3608-3616.

SEALE, P., BJORK, B., YANG, W., KAJIMURA, S., CHIN, S., KUANG, S., SCIME, A., DEVARAKONDA, S., CONROE, H. M., ERDJUMENT-BROMAGE, H., TEMPST, P., RUDNICKI, M. A., BEIER, D. R. & SPIEGELMAN, B. M. 2008. PRDM16 controls a brown fat/skeletal muscle switch. *Nature* 454**,** 961-967.

SEALE, P., KAJIMURA, S., YANG, W., CHIN, S., ROHAS, L. M., ULDRY, M., TAVERNIER, G., LANGIN, D. & SPIEGELMAN, B. M. 2007. Transcriptional control of brown fat determination by PRDM16. *Cell metabolism,* 6**,** 38-54.

SEMENZA, G. L. 2000. HIF-1 and human disease: one highly involved factor. *Genes & development,* 14**,** 1983-1991.

SENGER, D. R., ASCH, B. B., SMITH, B. D., PERRUZZI, C. A. & DVORAK, H. F. 1983. A secreted phosphoprotein marker for neoplastic transformation of both epithelial and fibroblastic cells.

SERRERO, G. & LEPAK, N. 1996. Endocrine and paracrine negative regulators of adipose differentiation. *International journal of obesity,* 20**,** S58-S64.

SHAPSES, S., CIFUENTES, M., SPEVAK, L., CHOWDHURY, H., BRITTINGHAM, J., BOSKEY, A. & DENHARDT, D. 2003. Osteopontin facilitates bone resorption, decreasing bone mineral crystallinity and content during calcium deficiency. *Calcified tissue international,* 73**,** 86-92.

SHARFI, H. & ELDAR-FINKELMAN, H. 2008. Sequential phosphorylation of insulin receptor substrate-2 by glycogen synthase kinase-3 and c-Jun NH2-terminal kinase plays a role in hepatic insulin signaling. *American Journal of Physiology-Endocrinology And Metabolism,* 294**,** E307-E315.

SHAW, J. E., SICREE, R. A. & ZIMMET, P. Z. 2010. Global estimates of the prevalence of diabetes for 2010 and 2030. *Diabetes Research and Clinical Practice,* 87**,** 4-14.

SHIMOMURA, I., MATSUDA, M., HAMMER, R. E., BASHMAKOV, Y., BROWN, M. S. & GOLDSTEIN, J. L. 2000. Decreased IRS-2 and Increased SREBP-1c Lead to Mixed Insulin Resistance and Sensitivity in Livers of Lipodystrophic and ob/ob Mice. *Molecular cell,* 6**,** 77-86.

SIMON, G. 1965. Histogenesis. *Handbook of physiology. Section,* 5**,** 101-107.

SØRENSEN, E. S., PETERSEN, T. E. & HØJRUP, P. 1995. Posttranslational modifications of bovine osteopontin: Identification of twenty-eight phosphorylation and three O-glycosylation sites. *Protein Science,* 4**,** 2040-2049.

SORIGUER, F., GODAY, A., BOSCH-COMAS, A., BORDIÚ, E., CALLE-PASCUAL, A., CARMENA, R., CASAMITJANA, R., CASTAÑO, L., CASTELL, C., CATALÁ, M., DELGADO, E., FRANCH, J., GAZTAMBIDE, S., GIRBÉS, J., GOMIS, R., GUTIÉRREZ, G., LÓPEZ-ALBA, A., MARTÍNEZ-LARRAD, M. T., MENÉNDEZ, E., MORA-PECES, I., ORTEGA, E., PASCUAL-MANICH, G., ROJO-MARTÍNEZ, G., SERRANO-RIOS, M., VALDÉS, S., VÁZQUEZ, J. A. & VENDRELL, J. 2012. Prevalence of diabetes mellitus and impaired glucose

regulation in Spain: the Di@bet.es Study. *Diabetologia,* 55**,** 88-93.
SPALDING, K. L., ARNER, E., WESTERMARK, P. O., BERNARD, S., BUCHHOLZ, B. A., BERGMANN, O., BLOMQVIST, L., HOFFSTEDT, J., NÄSLUND, E. & BRITTON, T. 2008. Dynamics of fat cell turnover in humans. *Nature,* 453**,** 783-787.
SPANGRUDE, G., HEIMFELD, S. & WEISSMAN, I. 1988. Purification and characterization of mouse hematopoietic stem cells. *Science,* 241**,** 58-62.
SPIEGELMAN, B. 1998. PPAR-gamma: adipogenic regulator and thiazolidinedione receptor. *Diabetes,* 47**,** 507-514.
SPIEGELMAN, B., CHOY, L., HOTAMISLIGIL, G., GRAVES, R., TONTONOZ, P., PUTKEY, J., DOTSON, D., MOUAWAD, P., JONES, G. & TAN, X. 1993. Regulation of adipocyte gene expression in differantiation and syndromes of obesity/diabetes. *J Biol Chem.,* 268.
SPIEGELMAN, B. M. & FLIER, J. S. 1996. Adipogenesis and Obesity: Rounding Out the Big Picture. *Cell,* 87**,** 377-389.
SPIEGELMAN, B. M. & FLIER, J. S. 2001. Obesity and the Regulation of Energy Balance. *Cell,* 104**,** 531-543.
STAHL, A. 2004. A current review of fatty acid transport proteins (SLC27). *Pflügers Archiv,* 447**,** 722-727.
STANDAL, T., BORSET, M. & SUNDAN, A. 2004. Role of osteopontin in adhesion, migration, cell survival and bone remodeling. *Exp Oncol,* 26**,** 179-84.
STARR, R., WILLSON, T. A., VINEY, E. M., MURRAY, L., RAYNER, J. R., JENKINS, B. J., GONDA, T. J., ALEXANDER, W. S., METCALF, D. & NICOLA, N. A. 1997. A family of cytokine-inducible inhibitors of signalling. *Nature,* 387**,** 917-921.
STEPPAN, C. M., BAILEY, S. T., BHAT, S., BROWN, E. J., BANERJEE, R., WRIGHT, C. M., PATEL, H. R., AHIMA, R. S. & LAZAR, M. A. 2001. The hormone resistin links obesity to diabetes. *Nature,* 409**,** 307-312.
STEPPAN, C. M., WANG, J., WHITEMAN, E. L., BIRNBAUM, M. J. & LAZAR, M. A. 2005. Activation of SOCS-3 by Resistin. *Molecular and cellular biology,* 25**,** 1569-1575.
SUGII, S., OLSON, P., SEARS, D. D., SABERI, M., ATKINS, A. R., BARISH, G. D., HONG, S.-H., CASTRO, G. L., YIN, Y.-Q. & NELSON, M. C. 2009. PPARγ activation in adipocytes is sufficient for systemic insulin sensitization. *Proceedings of the National Academy of Sciences,* 106**,** 22504-22509.
SUN, X. J., WANG, L.-M. & ZHANG, Y. 1995. Role of IRS-2 in insulin and cytokine signalling. *Nature,* 377**,** 173.
SUZUKI, K. & KONO, T. 1980. Evidence that insulin causes translocation of glucose transport activity to the plasma

membrane from an intracellular storage site. *Proceedings of the National Academy of Sciences,* 77**,** 2542-2545.

TAGUCHI, A., WARTSCHOW, L. M. & WHITE, M. F. 2007. Brain IRS2 signaling coordinates life span and nutrient homeostasis. *Science Signaling,* 317**,** 369.

TANG, W., ZEVE, D., SUH, J. M., BOSNAKOVSKI, D., KYBA, M., HAMMER, R. E., TALLQUIST, M. D. & GRAFF, J. M. 2008. White fat progenitor cells reside in the adipose vasculature. *Science,* 322**,** 583-586.

TANIGUCHI, C. M., EMANUELLI, B. & KAHN, C. R. 2006. Critical nodes in signalling pathways: insights into insulin action. *Nat Rev Mol Cell Biol,* 7**,** 85-96.

TANSEY, J., SZTALRYD, C., HLAVIN, E., KIMMEL, A. & LONDOS, C. 2004. The central role of perilipin a in lipid metabolism and adipocyte lipolysis. *IUBMB life,* 56**,** 379-385.

TAYLOR, S. I. 1992. Lilly Lecture: molecular mechanisms of insulin resistance: lessons from patients with mutations in the insulin-receptor gene. *Diabetes,* 41**,** 1473-1490.

TCHKONIA, T., GIORGADZE, N., PIRTSKHALAVA, T., TCHOUKALOVA, Y., KARAGIANNIDES, I., FORSE, R. A., DEPONTE, M., STEVENSON, M., GUO, W., HAN, J., WALOGA, G., LASH, T. L., JENSEN, M. D. & KIRKLAND, J. L. 2002. Fat depot origin affects adipogenesis in primary cultured and cloned human preadipocytes. *Am J Physiol Regul Integr Comp Physiol,* 282**,** R1286-96.

TCHKONIA, T., GIORGADZE, N., PIRTSKHALAVA, T., THOMOU, T., DEPONTE, M., KOO, A., FORSE, R. A., CHINNAPPAN, D., MARTIN-RUIZ, C., VON ZGLINICKI, T. & KIRKLAND, J. L. 2006. Fat depot-specific characteristics are retained in strains derived from single human preadipocytes. *Diabetes,* 55**,** 2571-8.

TCHKONIA, T., LENBURG, M., THOMOU, T., GIORGADZE, N., FRAMPTON, G., PIRTSKHALAVA, T., CARTWRIGHT, A., CARTWRIGHT, M., FLANAGAN, J., KARAGIANNIDES, I., GERRY, N., FORSE, R. A., TCHOUKALOVA, Y., JENSEN, M. D., POTHOULAKIS, C. & KIRKLAND, J. L. 2007. Identification of depot-specific human fat cell progenitors through distinct expression profiles and developmental gene patterns. *Am J Physiol Endocrinol Metab,* 292**,** E298-307.

TCHKONIA, T., TCHOUKALOVA, Y. D., GIORGADZE, N., PIRTSKHALAVA, T., KARAGIANNIDES, I., FORSE, R. A., KOO, A., STEVENSON, M., CHINNAPPAN, D., CARTWRIGHT, A., JENSEN, M. D. & KIRKLAND, J. L. 2005. Abundance of two human preadipocyte subtypes with distinct capacities for replication, adipogenesis, and apoptosis varies

among fat depots. *American Journal of Physiology - Endocrinology And Metabolism,* 288**,** E267-E277.
TONTONOZ, P., HU, E., GRAVES, R. A., BUDAVARI, A. I. & SPIEGELMAN, B. M. 1994a. mPPAR gamma 2: tissue-specific regulator of an adipocyte enhancer. *Genes & development,* 8**,** 1224-1234.
TONTONOZ, P., HU, E. & SPIEGELMAN, B. M. 1994b. Stimulation of adipogenesis in fibroblasts by PPARγ2, a lipid-activated transcription factor. *Cell,* 79**,** 1147-1156.
TONTONOZ, P., KIM, J., GRAVES, R. & SPIEGELMAN, B. 1993. ADD1: a novel helix-loop-helix transcription factor associated with adipocyte determination and differentiation. *Molecular and cellular biology,* 13**,** 4753-4759.
TSENG, Y.-H., KRIAUCIUNAS, K. M., KOKKOTOU, E. & KAHN, C. R. 2004. Differential roles of insulin receptor substrates in brown adipocyte differentiation. *Molecular and cellular biology,* 24**,** 1918-1929.
ULDRY, M. & THORENS, B. 2004. The SLC2 family of facilitated hexose and polyol transporters. *Pflügers Archiv,* 447**,** 480-489.
ULLRICH, A. & SCHLESSINGER, J. 1990. Signal transduction by receptors with tyrosine kinase activity. *Cell,* 61**,** 203.
VAISSE, C., HALAAS, J. L., HORVATH, C. M., DARNELL, J. E., STOFFEL, M. & FRIEDMAN, J. M. 1996. Leptin activation of Stat3 in the hypothalamus of wild–type and ob/ob mice but not db/db mice. *Nature genetics,* 14**,** 95-97.
VALVERDE, A. M., FABREGAT, I., BURKS, D. J., WHITE, M. F. & BENITO, M. 2004. IRS-2 mediates the antiapoptotic effect of insulin in neonatal hepatocytes. *Hepatology,* 40**,** 1285-1294.
VAN HARMELEN, V., RÃ¶HRIG, K. & HAUNER, H. 2004. Comparison of proliferation and differentiation capacity of human adipocyte precursor cells from the omental and subcutaneous adipose tissue depot of obese subjects. *Metabolism,* 53**,** 632-637.
VÁZQUEZ-VELA, M. E. F., TORRES, N. & TOVAR, A. R. 2008. White Adipose Tissue as Endocrine Organ and Its Role in Obesity. *Archives of Medical Research,* 39**,** 715-728.
VEGA, G. L. & GRUNDY, S. M. 2013. Metabolic Risk Susceptibility in Men Is Partially Related to Adiponectin/Leptin Ratio. *Journal of Obesity,* 2013**,** 9.
VOLIOVITCH, H., SCHINDLER, D. G., HADARI, Y. R., TAYLOR, S. I., ACCILI, D. & ZICK, Y. 1995. Tyrosine phosphorylation of insulin receptor substrate-1 in vivo depends upon the presence of its pleckstrin homology region. *J Biol Chem,* 270**,** 18083-7.

VYKOUKAL, D. & DAVIES, M. G. 2011. Vascular biology of metabolic syndrome. *Journal of Vascular Surgery,* 54**,** 819-831.

WALKEY, C. J. & SPIEGELMAN, B. M. 2008. A Functional Peroxisome Proliferator-activated Receptor-γ Ligand-binding Domain Is Not Required for Adipogenesis. *Journal of Biological Chemistry,* 283**,** 24290-24294.

WANG, B., JENKINS, J. R. & TRAYHURN, P. 2005. Expression and secretion of inflammation-related adipokines by human adipocytes differentiated in culture: integrated response to TNF-alpha. *Am J Physiol Endocrinol Metab,* 288**,** E731-40.

WANG, K. X. & DENHARDT, D. T. 2008. Osteopontin: Role in immune regulation and stress responses. *Cytokine & Growth Factor Reviews,* 19**,** 333-345.

WANG, Y., BEYDOUN, M. A., LIANG, L., CABALLERO, B. & KUMANYIKA, S. K. 2008. Will all Americans become overweight or obese? Estimating the progression and cost of the US obesity epidemic. *Obesity,* 16**,** 2323-2330.

WANG, Y., MONTEIRO, C. & POPKIN, B. M. 2002. Trends of obesity and underweight in older children and adolescents in the United States, Brazil, China, and Russia. *The American journal of clinical nutrition,* 75**,** 971-977.

WASSERMANN, F. 1965. The development of adipose tissue. *Comprehensive Physiology*.

WEISBERG, S. P., MCCANN, D., DESAI, M., ROSENBAUM, M., LEIBEL, R. L. & FERRANTE, A. W. 2003. Obesity is associated with macrophage accumulation in adipose tissue. *Journal of Clinical Investigation,* 112**,** 1796-1808.

WHITE, M. F. 1997. The insulin signalling system and the IRS proteins. *Diabetologia,* 40**,** S2-S17.

WHITE, M. F. 2002. IRS proteins and the common path to diabetes. *American Journal of Physiology - Endocrinology And Metabolism,* 283**,** E413-E422.

WHITE, M. F. 2003. Insulin Signaling in Health and Disease. *Science,* 302**,** 1710-1711.

WHITE, M. F. 2006. Regulating insulin signaling and beta-cell function through IRS proteins. *Can J Physiol Pharmacol,* 84**,** 725-37.

WHITE, M. F., MARON, R. & KAHN, C. R. 1985. Insulin rapidly stimulates tyrosine phosphorylation of a Mr-185,000 protein in intact cells.

WHITE, M. F. & YENUSH, L. 1998. The IRS-signaling system: a network of docking proteins that mediate insulin and cytokine action. *Protein modules in signal transduction.* Springer.

WITHERS, D. J. 2001. Insulin receptor substrate proteins and neuroendocrine function. *Biochem Soc Trans,* 29**,** 525-9.

WITHERS, D. J., GUTIERREZ, J. S., TOWERY, H., BURKS, D. J., REN, J. M., PREVIS, S., ZHANG, Y., BERNAL, D., PONS, S.,

SHULMAN, G. I., BONNER-WEIR, S. & WHITE, M. F. 1998. Disruption of IRS-2 causes type 2 diabetes in mice. *Nature,* 391**,** 900-4.
WON PARK, K., HALPERIN, D. S. & TONTONOZ, P. 2008. Before They Were Fat: Adipocyte Progenitors. *Cell Metabolism,* 8**,** 454-457.
WOOD, I. S., DE HEREDIA, F. P., WANG, B. & TRAYHURN, P. 2009. Cellular hypoxia and adipose tissue dysfunction in obesity. *Proceedings of the Nutrition Society,* 68**,** 370-377.
WOODS, S. C., LOTTER, E. C., MCKAY, L. D. & PORTE, D. 1979. Chronic intracerebroventricular infusion of insulin reduces food intake and body weight of baboons.
WU, Z., BUCHER, N. & FARMER, S. R. 1996. Induction of peroxisome proliferator-activated receptor gamma during the conversion of 3T3 fibroblasts into adipocytes is mediated by C/EBPbeta, C/EBPdelta, and glucocorticoids. *Molecular and cellular biology,* 16**,** 4128-4136.
WU, Z., PUIGSERVER, P. & SPIEGELMAN, B. M. 1999. Transcriptional activation of adipogenesis. *Current Opinion in Cell Biology,* 11**,** 689-694.
XIE, Y., SAKATSUME, M., NISHI, S., NARITA, I., ARAKAWA, M. & GEJYO, F. 2001. Expression, roles, receptors, and regulation of osteopontin in the kidney. *Kidney international,* 60**,** 1645-1657.
YASUKAWA, H., SASAKI, A. & YOSHIMURA, A. 2000. Negative regulation of cytokine signaling pathways. *Annual review of immunology,* 18**,** 143-164.
YEAMAN, S. J. 2004. Hormone-sensitive lipase--new roles for an old enzyme. *Biochemical Journal,* 379**,** 11.
YENUSH, L., MAKATI, K. J., SMITH-HALL, J., ISHIBASHI, O., MYERS, M. G. & WHITE, M. F. 1996. The pleckstrin homology domain is the principle link between the insulin receptor and IRS-1. *Journal of Biological Chemistry,* 271**,** 24300-24306.
YKI-JÄRVINEN, H. 2004. Thiazolidinediones. *New England Journal of Medicine,* 351**,** 1106-1118.
YOKOMORI, N., TAWATA, M. & ONAYA, T. 1999. A transcriptional repressor regulates mouse GLUT4 gene expression during the differentiation of 3T3-L1 cells. *Diabetes,* 48**,** 2471-2474.
YUAN, M., KONSTANTOPOULOS, N., LEE, J., HANSEN, L., LI, Z.-W., KARIN, M. & SHOELSON, S. E. 2001. Reversal of obesity-and diet-induced insulin resistance with salicylates or targeted disruption of Ikkbeta. *Science Signaling,* 293**,** 1673.
ZEYDA, M., GOLLINGER, K., TODORIC, J., KIEFER, F. W., KECK, M., ASZMANN, O., PRAGER, G., ZLABINGER, G. J., PETZELBAUER, P. & STULNIG, T. M. 2011. Osteopontin Is

an Activator of Human Adipose Tissue Macrophages and Directly Affects Adipocyte Function. *Endocrinology,* 152**,** 2219-2227.

ZHANG, G., GURTU, V., KAIN, S. R. & YAN, G. 1997. Early detection of apoptosis using a fluorescent conjugate of annexin V. *Biotechniques,* 23**,** 525-531.

ZHANG, Y., PROENCA, R., MAFFEI, M., BARONE, M., LEOPOLD, L. & FRIEDMAN, J. M. 1994. Positional cloning of the mouse obese gene and its human homologue. *Nature,* 372**,** 425-432.

ZHU, Y., QI, C., KORENBERG, J. R., CHEN, X.-N., NOYA, D., RAO, M. S. & REDDY, J. K. 1995. Structural organization of mouse peroxisome proliferator-activated receptor gamma (mPPAR gamma) gene: alternative promoter use and different splicing yield two mPPAR gamma isoforms. *Proceedings of the National Academy of Sciences,* 92**,** 7921-7925.

ZUK, P. A., ZHU, M., ASHJIAN, P., DE UGARTE, D. A., HUANG, J. I., MIZUNO, H., ALFONSO, Z. C., FRASER, J. K., BENHAIM, P. & HEDRICK, M. H. 2002. Human adipose tissue is a source of multipotent stem cells. *Mol Biol Cell,* 13**,** 4279-95.

ZUK, P. A., ZHU, M., MIZUNO, H., HUANG, J., FUTRELL, J. W., KATZ, A. J., BENHAIM, P., LORENZ, H. P. & HEDRICK, M. H. 2001. Multilineage Cells from Human Adipose Tissue: Implications for Cell-Based Therapies. *Tissue Engineering,* 7**,** 211-228.

ZULET, M. A., MORENO-ALIAGA, M. J. & MARTÍNEZ, J. A. 2012. Dietary Determinants of Fat Mass and Body Composition

Adipose Tissue Biology. *In:* SYMONDS, M. E. E. (ed.). Springer New York.